Response of *Bacillus subtilis* to Antimicrobial Peptide Stress

Dissertation

zur Erlangung des Doktorgrades
der Fakultät für Biologie
der Ludwig-Maximilians-Universität München

vorgelegt von

Carolin Höfler

aus Heidelberg

München
2015

Erstgutachter:	Prof. Dr. Thorsten Mascher
Zweitgutachter:	Prof. Dr. Marc Bramkamp
Tag der Abgabe:	24.09.2015
Tag der mündlichen Prüfung:	15.01.2016

Eidesstattliche Versicherung und Erklärung

Hiermit versichere ich an Eides statt, dass die vorliegende Dissertation von mir selbstständig und ohne unerlaubte Hilfe angefertigt wurde. Zudem wurden keine anderen als die angegebenen Quellen verwendet.

Außerdem versichere ich, dass die Dissertation keiner anderen Prüfungskommission vorgelegt wurde und ich mich nicht anderweitig einer Doktorprüfung ohne Erfolg unterzogen habe.

München, 24.09.2015

Carolin Höfler

Contents

EIDESSTATTLICHE VERSICHERUNG UND ERKLÄRUNG I

LIST OF PUBLICATIONS IV

CONTRIBUTIONS TO PUBLICATIONS V

SUMMARY VI

ZUSAMMENFASSUNG VIII

CHAPTER I 1

1 INTRODUCTION 2

1.1 THE BACTERIAL CELL ENVELOPE AND CELL WALL BIOSYNTHESIS 2

1.2 CELL WALL ACTIVE ANTIMICROBIAL PEPTIDES 4

1.3 RESISTANCE MECHANISMS AGAINST ANTIMICROBIAL PEPTIDES 8

1.4 CELL ENVELOPE STRESS RESPONSE IN *B. SUBTILIS* 9

1.4.1 The LiaSR two-component system 11

1.4.2 Bce-like two-component systems of B. subtilis 13

1.4.3 ECF σ factors σ^M, σ^X and σ^W – a short overview 14

1.5 SPORULATION – TAKING THE LAST EXIT 16

1.6 CANNIBALISM – A STRATEGY TO DELAY SPORULATION 18

1.7 AIMS OF THIS THESIS 19

CHAPTER II 21

IMMEDIATE AND HETEROGENEOUS RESPONSE OF THE LIAFSR TWO-COMPONENT SYSTEM OF *BACILLUS SUBTILIS* TO THE PEPTIDE ANTIBIOTIC BACITRACIN

CHAPTER III 34

SUBCELLULAR LOCALIZATION, INTERACTIONS AND DYNAMICS OF THE PHAGE-SHOCK PROTEIN-LIKE LIA RESPONSE IN *BACILLUS SUBTILIS*

CHAPTER IV 52

CANNIBALISM STRESS RESPONSE IN *BACILLUS SUBTILIS*

4.1 ABSTRACT 54

4.2 INTRODUCTION 54

4.3 METHODS 55

4.3.1 Media and growth conditions 55

4.3.2 Bacterial strains and plasmids 56

4.3.3 DNA manipulations 56

4.3.4 Allelic replacement mutagenesis of sdpAB, sdpC, sdpI, skfA-H, skfA, skfBC, skfEF, skfGH, skfH, sunA and yydF-J using LFH-PCR ... *56*

4.3.5 Luminescence Assay ... *56*

4.4 RESULTS AND DISCUSSION ... 60

4.4.1 Intrinsic induction of CESR target promoters during stationary phase growth ... *60*

4.4.2 AMPs and cannibalism toxins induce CESR systems ... *61*

4.4.3 Toxin production correlates with P_{bceA} induction ... *63*

4.4.4 The BceRS system does not mediate resistance against cannibalism toxins ... *64*

4.4.5 Mature SKF toxin strongly acts as inducer ... *66*

4.4.6 Mature SDP toxin acts as inducer ... *67*

4.5 CONCLUSION ... 69

4.6 ACKNOWLEDGEMENTS ... 70

4.7 REFERENCES OF CHAPTER IV ... 71

CHAPTER V ... 73

5 DISCUSSION ... 74

5.1 HETEROGENEOUS ACTIVATION OF THE LIASR SYSTEM AND ITS ORIGINS ... 75

5.1.1 Heterogeneity might originate from the LiaSR system itself ... *75*

5.2 LIAIH DYNAMICS VARY UNDER STRESS AND NON-STRESS CONDITIONS ... 78

5.2.1 The PSP response of E. coli – similarities in B. subtilis ... *78*

5.2.2 LiaH and its connection to the YvlABCD interaction network ... *80*

5.2.3 The PSP response of Y. enterocolitica – similarities and differences in B. subtilis ... *81*

5.3 A NOVEL MODE OF BCERS ACTIVATION BY THE CANNIBALISM TOXINS SDP AND SKF ... 82

5.4 FUTURE PERSPECTIVES AND CONCLUDING REMARKS ... 84

REFERENCES OF CHAPTER I AND CHAPTER V ... 86

ACKNOWLEDGEMENTS ... 93

CURRICULUM VITAE ... 94

List of Publications

Publications originating from this thesis

CHAPTER II

Kesel, S., Mader, A., **Höfler, C.**, Mascher, T., Leisner, M. (2013). Immediate and heterogeneous response of the LiaFSR two-component system of *Bacillus subtilis* to the peptide antibiotic bacitracin. *PloS one* **8**: e53457

CHAPTER III

Dominguez-Escobar, J.*, Wolf, D.*, Fritz, G., **Höfler, C.**, Wedlich-Söldner, R., Mascher, T. (2014). Subcellular localization, interactions and dynamics of the phage-shock protein-like Lia response in *Bacillus subtilis*. *Molecular Microbiology* **92**: 716-732

(* shared first authorship)

CHAPTER IV

Höfler, C., Heckmann, J., Fritsch, A., Popp, P., Gebhard, S., Fritz, G., Mascher, T. (2015). Cannibalism Stress Response in *Bacillus subtilis*. *Microbiology*, published ahead of print, doi: 10.1099/mic.0.000176

Contributions to Publications

CHAPTER II

Kesel, S., Mader, A., **Höfler, C.**, Mascher, T., Leisner, M. (2013). *PloS one* **8**: e53457

Sara Kesel and Andreas Mader performed the experiments. Carolin Höfler was involved in strain constructions. Sara Kesel and Madeleine Leisner analyzed the data obtained from the microscopy experiments. Thorsten Mascher and Madeleine Leisner conceived and designed the experiments and wrote the manuscript.

CHAPTER III

Dominguez-Escobar, J.*, Wolf, D.*, Fritz, G., **Höfler, C.**, Wedlich-Söldner, R., Mascher, T. (2014). *Molecular Microbiology* **92**: 716-732

Julia Dominguez-Escobar, Diana Wolf and Carolin Höfler carried out the experiments, drew the figures and constructed the tables. Julia Dominguez-Escobar, Diana Wolf and Georg Fritz analyzed the data. Roland Wedlich-Söldner and Thorsten Mascher designed the experiments. Julia Dominguez-Escobar, Diana Wolf, Roland Wedlich-Söldner and Thorsten Mascher wrote the manuscript.

CHAPTER IV

Höfler, C., Heckmann, J., Fritsch, A., Popp, P., Gebhard, S., Fritz, G., Mascher, T. (2015). *Microbiology*, published ahead of print, doi: 10.1099/mic.0.000176

Carolin Höfler performed the majority of the experiments, drew the figures and tables and supervised the students Judith Heckmann, Anne Fritsch and Philipp Popp, who constructed some strains and performed some experiments. Susanne Gebhard, Georg Fritz and Thorsten Mascher designed the experiments. Carolin Höfler, Susanne Gebhard, Georg Fritz and Thorsten Mascher wrote the manuscript.

We hereby confirm the above mentioned declaration.

Carolin Höfler	Prof. Dr. Thorsten Mascher

Summary

Bacteria share their often complex habitats with many different microorganisms with whom they must constantly compete for nutrients. Thus, they have evolved various mechanisms to attack rivaling species and defend themselves accordingly. The Gram-positive spore-forming soil organism *Bacillus subtilis* is a member of the Firmicutes phylum and is able to produce and secrete many antimicrobial peptides (AMPs) to kill its competitors. These peptides are usually produced in stationary growth phase when nutrient availability is limited. Their main target is the bacterial cell envelope, which is the first structural barrier for defense. Therefore, close monitoring of cell envelope integrity is pivotal for survival. In addition to extracytoplasmic function sigma factors (ECF σ factors), *B. subtilis* employs four different two-component systems (2CSs) to counteract cell envelope stress (LiaSR, BceRS, PsdRS and YxdJK).

The first part of this thesis deals with the LiaSR 2CS of *B. subtilis*. It consists of a histidine kinase LiaS and its cytosolic response regulator LiaR. Additionally, there is an accessory inhibitor protein LiaF located in the membrane, which keeps LiaS in its OFF-state under non-inducing conditions. The LiaSR system is encoded within two adjacent operons regulated by two promoters and harboring six genes (*liaIH-liaGFSR*). The first operon, *liaIH*, is under control of the LiaR-dependent target promoter P_{liaI}. It is tightly regulated and has very low basal activity under non-inducing conditions. In contrast, the second promoter P_{liaG} controlling expression of the adjacent operon *liaGFSR* is relatively strong and constitutive.
The LiaSR system responds to a great variety of envelope-targeting AMPs, e.g. the cyclic AMP bacitracin. Upon its addition, P_{liaI} and hence, expression of *liaIH* is strongly induced. The LiaSR system responds to AMP damage, rather than the compound itself and mounts a secondary layer of defense against envelope perturbations. We could demonstrate that the system responds not only fast and strongly to different external bacitracin concentrations but also shows a heterogeneous response: At low bacitracin concentrations the majority of the population remains in its OFF-state while only few cells activate the LiaSR system.

The second part of this thesis deals with the subcellular localization, interactions and dynamics of the phage-shock protein-like Lia response in *B. subtilis*. Despite extensive studies on the LiaSR system over the last decade, its physiological role remains unclear. In this study, we used fluorescence and time-lapse microscopy to study the subcellular localization and interaction of the small membrane protein LiaI and phage-shock protein A homolog LiaH under inducing and non-inducing conditions. LiaI localizes into few distinct foci at the membrane which are highly dynamic under non-inducing conditions, while LiaH exhibited disperse cytosolic localization. Upon bacitracin induction, the number of LiaI foci increase, they become static at the membrane and recruit LiaH into these protein complexes. Our data indicated that LiaI scans the membrane for envelope damage and stops at sites of AMP-generated damage. Once recruited to these spots, LiaH is hypothesized to serve as a “patch” from the inside to shield against AMP-induced damage.

The LiaSR system is not only triggered by the external addition of cell wall antibiotics. It is also intrinsically activated during transition from exponential to stationary growth phase. The induction was previously shown to be at least partially due to Spo0A-mediated de-repression of P_{liaI}: The LiaSR system is kept inactive during logarithmic growth phase by the transcriptional regulator AbrB, which itself is negatively regulated by Spo0A, the master regulator of sporulation at the onset of stationary phase. Since Spo0A-mediated de-repression alone is not sufficient for the transition phase induction of the LiaSR system, we sought to identify other potential inducers, i.e. AMPs produced by *B. subtilis* itself during this growth stage. In the course of studying this intrinsic transition phase induction of the LiaSR system, we observed that other 2CSs, the BceRS and PsdRS, as well as the ECF σ factors σ^M, σ^X and σ^W are also induced in stationary phase by an unknown stimulus.

The third part of this thesis deals with the identification of the stimuli leading to this intrinsic activation of the different systems. Using a *lux*-reporter system to monitor target promoter activity of each system, we searched for AMPs produced by *B. subtilis* W168 itself. As previously reported, the YydF peptide was shown to be an inducer of the LiaSR system responsible for its heterogeneous activation. In this study, we found that the BceRS and PsdRS 2CSs, as well as the ECF σ factors σ^M, σ^X and σ^W, are activated by the two cannibalism toxins, SDP and SKF, in stationary phase. The most prominent effect was observed for the BceRS system. Therefore, we focused on this system in the last part of this thesis to gain deeper insight into the physiological relevance of this process. While the BceRS response is stronger for SKF compared to SDP, we found no evidence that the BceRS system is involved in mediating resistance against the two toxins. Surprisingly, their own membrane immunity determinants, SkfEF and SdpI, respectively, seem to be important for BceRS activation since induction is lost in the corresponding deletion strains. This observation suggests that the AMPs have to be bound to a membrane target in order to be perceived by the BceRS system.

Zusammenfassung

Bakterien teilen sich ihre oft komplexen Habitate mit vielen verschiedenen Mikroorganismen, mit denen sie stetig um Nährstoffe konkurrieren müssen. Deswegen entwickelten sie diverse Mechanismen um rivalisierende Spezies zu bekämpfen und sich entsprechend selbst zu verteidigen. Das Gram-positive, sporenbildende Bodenbakterium *Bacillus subtilis* gehört zum Stamm der Firmicuten und produziert und sekretiert viele verschiedene antimikrobielle Peptide um seine Konkurrenten zu töten. Diese Peptide werden üblicherweise in der stationären Wachstumsphase produziert, in welcher die Nährstoffverfügbarkeit begrenzt ist. Ihr Hauptangriffspunkt ist die bakterielle Zellhülle, die die erste mechanische Barriere der Verteidigung darstellt. Aus diesem Grund ist die strikte Überwachung der Zellhüllintegrität entscheidend für das Überleben. Zusätzlich zu den ECF (*extracytoplasmic function*) Sigma Faktoren, nutzt *B. subtilis* vier verschiedene Zweikomponentensysteme um Zellhüllstress entgegen zu wirken (das LiaSR, BceRS, PsdRS und YxdJK System).

Der erste Teil dieser Arbeit behandelt das LiaSR Zweikomponentensystem in *B. subtilis*. Es besteht aus einer Histidinkinase LiaS und ihrem cytosolischen Antwortregulator LiaR. Weiterhin gibt es noch ein zusätzliches Inhibitorprotein LiaF, das in der Membran lokalisiert ist und LiaS unter nicht-induzierenden Bedingungen im AUS-Zustand hält. Das LiaSR System ist innerhalb von zwei aneinandergrenzenden Operons kodiert, die wiederum von zwei Promotoren reguliert werden und insgesamt sechs Gene beinhalten (*liaIH-liaGFSR*). Das erste Operon, *liaIH*, wird vom LiaR-abhängigen Zielpromotor P_{liaI} kontrolliert. Dieser wird strikt reguliert und hat unter nicht-induzierenden Bedingungen eine sehr geringe Basalaktivität. Im Gegenzug dazu ist der zweite Promotor P_{liaG}, der die Expression des an *liaIH* angrenzenden Operons *liaGFSR* kontrolliert, vergleichsweise stark und konstitutiv.
Das LiaSR System reagiert auf eine große Zahl von antimikrobiellen Peptiden, die die Zellhülle angreifen, wie z.B. das zyklische antimikrobielle Peptid Bacitracin. Nach seiner Zugabe wird P_{liaI} und damit die Expression von *liaIH* stark induziert. Das LiaSR System reagiert auf Schäden, die durch antimikrobielle Peptide hervorgerufen werden anstatt auf die eigentliche Substanz selbst und errichtet damit eine zweite Verteidigungslinie gegen die Zellhüllrisse. Wir fanden wir heraus, dass das System nicht nur schnell und stark auf unterschiedliche externe Bacitracin-Konzentrationen reagiert sondern auch eine sehr heterogene Antwort zeigt: Bei geringen Bacitracin-Konzentrationen verbleibt die Mehrheit der Population im AUS-Zustand, während nur wenige Zellen das LiaSR System aktivieren.

Im zweiten Teil dieser Arbeit geht es um die subzelluläre Lokalisation, Interaktionen und Dynamiken der Phagenschockprotein-ähnlichen Lia Antwort in *B. subtilis*. Trotz umfassender Studien zum LiaSR System in den vergangenen 10 Jahren ist seine physiologische Rolle bisher unklar. In dieser Arbeit wandten wir Fluoreszenz- und Time-lapse Mikroskopietechniken an um die subzelluläre Lokalisation und Interaktion vom kleinen Membranprotein LiaI und dem Phagenschockprotein A Homolog LiaH unter induzierenden und nicht-induzierenden Bedingungen

zu untersuchen. LiaI bildet wenige aber dennoch distinkte Foci an der Membran, die unter nicht-induzierenden Bedingungen hochdynamisch sind, während LiaH dispers im Cytosol lokalisiert. Nach Bacitracin-Induktion erhöht sich die Anzahl an LiaI Foci, welche an der Membran statisch werden und welche LiaH in diese Proteinkomplexe rekrutieren. Unsere Daten deuten darauf hin, dass LiaI die Membran „abscannt" um Membranschäden zu detektieren und an den Stellen stoppt, die durch ein antimikrobielles Peptid geschädigt wurden. Sobald LiaH an diese Stellen rekrutiert wurde, könnte LiaH als eine Art „Flicken" von innen heraus dienen, um die beschädigte Stelle abzudecken.

Das LiaSR System wird nicht nur durch externe Zugabe von Zellwandantibiotika induziert. Es zeigt auch eine intrinsische Aktivierung beim Übergang von der exponentiellen in die stationäre Wachstumsphase. Vor einiger Zeit wurde gezeigt, dass der Induktion zumindest teilweise eine Spo0A-vermittelte De-Repression von P_{lial} zugrunde liegt: Das LiaSR System wird während der logarithmischen Wachstumsphase durch den transkriptionellen Regulator AbrB inaktiv gehalten, welcher selbst negativ reguliert wird vom Masterregulator der Sporulation, Spo0A, zu Beginn der stationären Phase. Da die Spo0A-vermittelte De-Repression allein für die Übergangsphase-Induktion des LiaSR Systems nicht ausreichend ist, strebten wir danach weitere potenzielle Induktoren zu identifizieren, nämlich antimikrobielle Peptide, die von *B. subtilis* selbst in dieser Wachstumsphase produziert werden. Während wir die intrinsische Übergangsphase-Induktion im LiaSR System untersuchten, stellten wir fest, dass sowohl andere Zweikomponentensysteme, wie das BceRS und PsdRS System, als auch die ECF Sigma Faktoren σ^M, σ^X und σ^W ebenso in der stationären Phase von einem bislang unbekannten Stimulus aktiviert werden.
Im dritten Teil dieser Arbeit geht es nun um die Identifizierung der Stimuli, die zur intrinsischen Aktivierung der unterschiedlichen Systeme führen. Wir benutzten ein *lux*-Reporter System um die Zielpromotoraktivität jedes Systems zu messen und suchten nach antimikrobiellen Peptiden, die von *B. subtilis* W168 produziert werden. Schon vor einiger Zeit wurde das YydF Peptid als ein Induktor des LiaSR System identifiziert, der für die heterogene Aktivierung verantwortlich ist. Sowohl das BceRS und PsdRS System als auch die ECF Sigma Faktoren σ^M, σ^X und σ^W werden in der stationären Phase von den zwei Kannibalismus-Toxinen SDP und SKF induziert. Der markanteste Effekt wurde für das BceRS System beobachtet. Daher fokussierten wir uns im letzten Teil der Arbeit auf dieses System um tiefere Einblicke in die physiologische Relevanz dieses Prozesses zu bekommen. Obwohl die durch SKF hervorgerufene BceRS Reaktion stärker ist als die durch SDP, fanden wir keinen Hinweis darauf, dass das BceRS System Resistenz gegen die beiden Toxine vermittelt. Erstaunlicherweise scheinen die jeweiligen Eigenimmunitätskomponenten, SkfEF und SdpI, für die BceRS Aktivierung wichtig zu sein, da in den entsprechenden Deletionsstämmen die Induktion fehlt. Diese Beobachtung deutet darauf hin, dass antimikrobielle Peptide an ein Membranprotein gebunden sein müssen, um vom BceRS System wahrgenommen zu werden.

CHAPTER I

Introduction

Aims

1 Introduction

The soil is a complex habitat for many different microorganisms such as the Gram-positive organism *Bacillus subtilis*, a member of the Firmicutes phylum, and others such as Actinobacteria. Bacteria have to adapt quickly to changing environmental conditions such as heat, moisture or oxygen. Additionally, they compete for limited nutrients in order to survive. Therefore, they have evolved a variety of antimicrobial peptides (AMPs) which often target the bacterial cell envelope. In response to suppress the growth of competitors, bacteria have developed signal transducing systems to monitor such extrinsic substances and to counteract these severe stress conditions accordingly (Msadek, 1999).

1.1 The bacterial cell envelope and cell wall biosynthesis

The envelope is an essential structure for the cell. It determines the shape, protects the cell from environmental stresses and counteracts the internal osmotic pressure (Höltje, 1998, Delcour *et al.*, 1999). The cell envelope of Gram-positive and Gram-negative bacteria differs significantly (Fig. 1.1). While Gram-positive bacteria have, in addition to their cytoplasmic membrane, a rather thick peptidoglycan layer with teichoic acids (Foster & Popham, 2002) resulting in an overall negative charge of the cell wall, Gram-negative bacteria harbor only a thin peptidoglycan layer lacking teichoic acids. But in contrast to Gram-positives, Gram-negatives possess a periplasmic space and an additional outer membrane (Silhavy *et al.*, 2010). Here, I will focus on Gram-positive bacteria since all the work presented in this thesis was performed in *B. subtilis*.

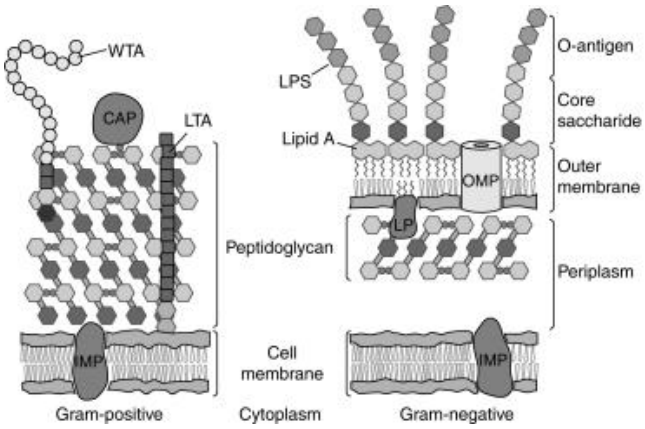

Fig. 1.1: Comparison of the Gram-positive and Gram-negative cell envelope composition. CAP, covalently attached protein; IMP, integral membrane protein; LP, lipoprotein; LPS, lipopolysaccharide; LTA, lipoteichoic acid; OMP, outer membrane protein; WTA, wall teichoic acid. This figure is taken from (Silhavy *et al.*, 2010).

Although the composition of the peptidoglycan layer differs between species, the overall structure is identical. The cell wall forms a polymer consisting of sugars and amino acids building up a net-like structure outside the cytoplasmic membrane. The sugars are composed of alternating residues of β-(1,4) linked *N*-acetylglucosamine (Glc*N*Ac) and *N*-acetylmuramic acid (Mur*N*Ac). The Mur*N*Ac molecules are connected pentapeptide bridges leading to the characteristic 3D mesh-like strong and rigid layer (Vollmer *et al.*, 2008).

The peptidoglycan biosynthesis starts in the cytoplasm where the peptidoglycan building blocks are synthesized and then covalently attached to a carrier molecule, bactoprenol (undecaprenol-monophosphate). Bactoprenol transports the peptidoglycan monomers across the membrane to the extracellular space where they are inserted into the growing cell wall (Fig. 1.2). The first step of peptidoglycan biosynthesis is the conversion of fructose-6-phosphate to Glc*N*Ac in the cytoplasm. Next, Glc*N*Ac is activated by the addition of uridine diphosphate (UDP) resulting in UDP-Glc*N*Ac, which is further converted to UDP-Mur*N*Ac. Then, the pentapeptide chain including a D-alanyl-D-alanine dipeptide (D-Ala-D-Ala) is attached to UDP-Mur*N*Ac followed by its connection to the lipid carrier molecule, bactoprenol, at the inner surface of the membrane (Bouhss *et al.*, 2008). This complex is called lipid I. Another Glc*N*Ac molecule is coupled to the Mur*N*Ac residue of lipid I resulting in lipid II. The following steps all involving bactoprenol are called the lipid II cycle (Delcour *et al.*, 1999, Foster & Popham, 2002). The complete peptidoglycan subunit linked by a pyrophosphate to the lipid carrier bactoprenol is then flipped to the outer surface of the membrane where it is incorporated into the nascent peptidoglycan net through transglycosylation and transpeptidation to produce new glycan strands (Barrett *et al.*, 2007, Sauvage *et al.*, 2008). The remaining undecaprenol-pyrophosphate (UPP) is dephosphorylated and transferred back to the inner surface of the membrane. Thus, the lipid carrier is recycled and ready for the next round of coupling and transfer of a new peptidoglycan subunit (Chang *et al.*, 2014).

Because of its essential nature, cell wall biosynthesis is the target for many AMPs (Fig. 1.2), as described in the next section.

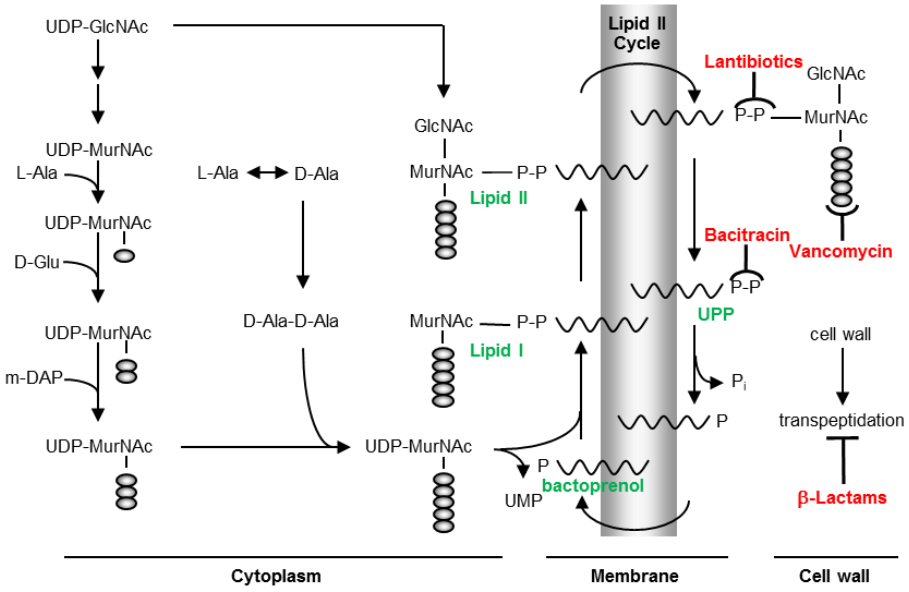

Fig. 1.2: Cell wall biosynthesis of Gram-positive bacteria and inhibition by selected antibiotics. Important steps of cell wall biosynthesis at their specific cellular level are schematically indicated. Glc*N*Ac, *N*-acetylglucosamine; Mur*N*Ac, *N*-acetylmuramic acid; UDP, uridine diphosphate; UMP, uridine monophosphate; UPP (undecaprenol pyrophosphate); P, phosphoryl group; P_i, inorganic phosphate. Amino acids are depicted as small grey circles; bactoprenol (undecaprenol monophosphate) is indicated by the waved line. Antibiotics targeting essential steps are highlighted in red and their site of action is shown. Lantibiotics comprise a group of several antibiotics (nisin, subtilin, gallidermin, actagardine and mersacidin). Amino acids are depicted as three-letter code. This figure is taken from (Jordan *et al.*, 2008) with modifications.

1.2 Cell wall active antimicrobial peptides

Nearly all stages of cell wall biosynthesis are prone to AMP attacks (Fig. 1.2) (Schneider & Sahl, 2010). Production of AMPs, though, is not restricted to bacteria but has been reported in basically all groups of organisms including fungi, plants and animals (Peschel & Sahl, 2006). They are active against other bacteria of the same species or across genera (Cotter *et al.*, 2005). Noteworthy, producers simultaneously express dedicated immunity proteins in order to avoid self-killing (Gonzalez-Pastor *et al.*, 2003, Ellermeier *et al.*, 2006, Dubois *et al.*, 2009). AMPs often have a cationic and amphipathic nature but vary in size, secondary structure and sequence (Peschel & Sahl, 2006). AMPs produced by bacteria can be ribosomally or non-ribosomally synthesized. In the following paragraphs, I would like to describe selected AMPs that are relevant for this thesis.

Non-ribosomally synthesized AMPs are assembled within protein complexes which modify and release the active peptide (Stein, 2005). One relevant example is **bacitracin**, a cyclic lipopeptide antibiotic produced by *B. subtilis and B. licheniformis*. It is primarily active against Gram-positive bacteria and requires a divalent metal ion, usually zinc, to exhibit its full activity (Ming & Epperson, 2002). It inhibits cell wall biosynthesis by tightly binding to UPP (Fig. 1.2) (Stone & Strominger, 1971). It encloses the pyrophosphate group entirely and prevents accessibility for phosphatases and thus, recycling of the lipid carrier is restricted, ultimately leading to cell death (Stone & Strominger, 1971, Storm & Strominger, 1973, Economou *et al.*, 2013). To counteract its damage, resistance mechanisms have been developed to remove bacitracin from its site of action. The major resistance determinant in *B. subtilis* is composed of the BceRS two-component system (2CS) regulating the adenosine triphosphate-binding cassette (ABC) transporter BceAB (Mascher *et al.*, 2003, Ohki *et al.*, 2003) (see sections 1.3 and 1.4.2 for details). A secondary mechanism for bacitracin resistance is the upregulation of BcrC, an alternative phosphatase that dephosphorylates UPP on the extracellular side of the membrane (Cao & Helmann, 2002, Bernard *et al.*, 2005). Subsequent lipid carrier recycling ensures successful completion of cell wall biosynthesis and survival of the cell.

Ribosomally synthesized AMPs are gene-encoded peptides that usually require posttranslational modifications to become fully active (Papagianni, 2003). They vary broadly in structure and can form linear or cyclic peptides. They often have a cationic and amphiphilic nature, which facilitates contact with the negatively charged bacterial envelope and enables membrane permeabilization (Papagianni, 2003). Examples of this class are the heavily modified **lantibiotics**. Their characteristic feature is the presence of lanthionine or methyllanthionine residues. They are structurally diverse, forming elongated, flexible molecules such as nisin, or more globular shapes like mersacidin (Sahl *et al.*, 1995, Bierbaum & Sahl, 2009). Another set of ribosomally synthesized AMPs are the two cannibalism toxins **SDP** (**s**porulation **d**elaying **p**rotein) and **SKF** (**s**porulation **k**illing **f**actor) which will be described in detail later (see below).

One previously reported lantibiotic peptide produced by *B. subtilis* 168 is **sublancin**, encoded within the SPβ-prophage. Its structure contains a characteristic dehydroalanine residue and a methyllanthionine bridge (Paik *et al.*, 1998). Usually, lantibiotics and other ribosomally

synthesized AMPs harbor an N-terminal leader peptide sequence for export and a C-terminal core which finally constitutes the mature peptide (Willey & van der Donk, 2007). This initial precursor peptide is then posttranslationally modified by enzymes to release the mature and active peptide. However, the *B. subtilis* 168 genome does not harbor such enzyme loci for lantibiotics (Oman *et al.*, 2011). Oman and coworkers studied sublancin biosynthesis and postulated that it is not a lantibiotic but rather a very uncommon S-linked glycopeptide (Oman *et al.*, 2011). The biosynthetic loci for sublancin contain the gene *sunA* and two genes, *bdbA* and *bdbB*, encoding two thiol-disulfide oxidoreductases. Additionally, the immunity protein SunI (formerly YolF) is encoded within the same locus. Furthermore, it has been proposed that SunS (formerly YolJ) is a glycosyltransferase mediating addition of glucose to the cysteine residue at position 22 (Oman *et al.*, 2011). The active and mature peptide is then transported across the membrane by the ABC transporter SunT. Expression of *sunA* is known to be repressed during exponential growth phase by the transcriptional regulators AbrB and Rok (Albano *et al.*, 2005, Strauch *et al.*, 2007). Transcription of *sunA* is initiated due to AbrB inhibition at the onset of stationary phase by the master regulator of sporulation, Spo0A (see also section 1.5, Fig. 1.9).

Subtilosin A is another bacteriocin produced by *B. subtilis* 168. It is also known to be repressed by AbrB and Rok during logarithmic growth but transcription is additionally dependent on the two-component regulatory proteins ResDE (Nakano *et al.*, 2000, Albano *et al.*, 2005). Thus, it is induced under stress conditions like nutrient or oxygen depletion in stationary phase (Nakano *et al.*, 2000). Subtilosin A (SboA) is encoded within the *sbo-alb* operon overlapping with *sboX*, which constitutes another bacteriocin-like product and the *albABCDEFG* genes required for processing, export and immunity of the circular peptide. AlbA and AlbF have been shown to be essential for SboA biosynthesis and probably processing and maturation of the linear SboA precursor into a cyclic thioether-bridged peptide (Zheng *et al.*, 2000). AlbB, AlbC and AlbD have been reported to be involved in mediating immunity, while the functions of SboX and AlbG still remain elusive (Zheng *et al.*, 2000). Due to their homology to zinc-dependent proteases, AlbE and AlbF represent putative peptidases and a role in leader-peptide cleavage has been proposed (Flühe *et al.*, 2012).

The **YydF peptide** encoded in the *yydFGHIJ* operon represents another peptide which is produced by *B. subtilis* 168 at the onset of stationary phase. Its production is again repressed by AbrB during exponential growth. At the transition from logarithmic to stationary phase, AbrB repression is released and transcription of the *yydFGHIJ* operon is initiated (Butcher *et al.*, 2007). It has been debated whether Rok is a regulator of *yydFGHIJ* expression or not (Albano *et al.*, 2005, Butcher *et al.*, 2007). Based on sequence homology studies, the YydF precursor is proposed to be modified by YydG, a predicted Fe-S oxidoreductase and to be proteolytically cleaved by the peptidase YydH. Export and immunity are hypothesized to be mediated by the predicted ABC transporter YydIJ (Butcher *et al.*, 2007). It could be demonstrated that in the absence of YydIJ, the LiaSR system is highly induced probably due to accumulation of the YydF peptide causing cell envelope damage (Butcher *et al.*, 2007).

One very remarkable AMP causing envelope damage by collapsing the proton motive force is the cannibalism toxin **SdpC** (for simplicity reasons the mature form will be called **SDP** hereafter) (Lamsa *et al.*, 2012). SDP is a 42-amino acid linear AMP that is ribosomally synthesized and first

transcribed as an inactive precursor, pro-SdpC (Liu *et al.*, 2010, Perez Morales *et al.*, 2013). Pro-SdpC contains an N-terminal extension including its signal peptide sequence required for export which is proteolytically cleaved during export via the general secretory pathway (Linde *et al.*, 2003, Perez Morales *et al.*, 2013). Subsequent disulfide bond formation is needed for the full activity of the peptide but is not essential. Further N- and C-terminal processing of the precursor peptide requires two extra proteins, SdpA and SdpB, encoded within the same operon (Fig. 1.3A).

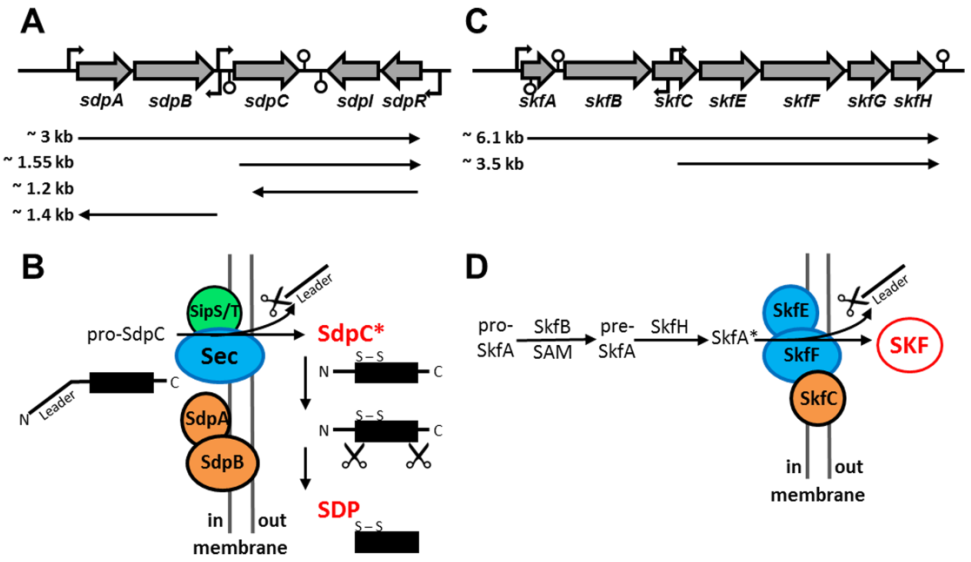

Fig. 1.3: Schematic representation of the genomic context of the *sdpABC-sdpRI* (A) and *skfABCEFGH* (C) operon and processing of the SdpC (B) and SkfA (D) precursor into mature SDP and SKF. Genomic context of the *sdpABC-sdpRI* and *skfABCEFGH* operon including all mapped promoters and terminators as well as the main transcripts are shown (A, C). Steps of SDP/SKF processing are indicated in (B, D). See text for details. This figure is based on (Liu *et al.*, 2010, Nicolas *et al.*, 2012, Perez Morales *et al.*, 2013) and taken from (Höfler *et al.*, 2015).

SdpA is a cytosolic protein which also localizes to the membrane in a SDP-dependent manner. SdpB is predicted to constitute a membrane protein harboring six transmembrane helices (Perez Morales *et al.*, 2013). Together, they are hypothesized to mediate the final processing of the SDP precursor peptide, thereby releasing the active and mature SDP toxin to the environment (Perez Morales *et al.*, 2013). The gene *sdpC* is encoded in the *sdpABC* operon and is regulated by two promoters, P_{sdpA} and P_{sdpC} (Fig. 1.3A). Its dedicated immunity protein, SdpI, is expressed from an opposing operon, *sdpRI*, under control of P_{sdpR} (Fig. 1.3A). SdpI is a membrane protein proposed to be involved both in immunity and signal transduction. Although the mechanism of how SdpI provides immunity remains elusive, it was shown to be an important resistance determinant (Ellermeier *et al.*, 2006). Its signaling properties come into play, when SDP is produced. SDP is proposed to bind to SdpI at the membrane and this complex then sequesters SdpR away from the DNA thereby inducing transcription of *sdpRI* (Ellermeier *et al.*, 2006). SdpR is a negative regulator of its own promoter in the absence of SDP (Ellermeier *et al.*, 2006). This repression is then relieved in the presence of SDP. Expression of the *sdpABC* and *sdpRI* operons is induced at the onset of stationary phase by indirect activation through the master regulator of sporulation, Spo0A (see also section 1.5, Fig. 1.9) (Gonzalez-Pastor *et al.*, 2003). During exponential growth phase, transcription

is blocked by the transition state regulator AbrB. This inhibition is then released by increasing concentrations of active Spo0A (Spo0A~P), thereby repressing AbrB activity (see also section 1.5, Fig. 1.9) (Fujita *et al.*, 2005, Chen *et al.*, 2006). Importantly, a broadly heterogeneous activation of Spo0A is the trigger for this transcription initiation (Chung *et al.*, 1994). SDP is a cannibalism toxin able to lyse sensitive siblings. Cannibalism and its contribution to survival under stress conditions will be explained further in section 1.6.

In contrast to the *sdpABC-sdpRI* operon, information about the second cannibalism toxin, **SkfA**, is still limited (for simplicity reasons called **SKF** hereafter). SKF is encoded within the *skfABCEFGH* operon (Fig. 1.3C) and is a ribosomally assembled AMP which needs posttranslational modifications in order to become fully active (Fig. 1.3D) (Gonzalez-Pastor *et al.*, 2003). SKF was first described to be able to kill the Gram-positive plant pathogen *Xanthomonas oryzae* (Lin *et al.*, 2001). SKF is a 26-amino acid cyclic sactipeptide harboring disulfide and thioether bonds (Liu *et al.*, 2010, Arnison *et al.*, 2013). The gene products of the *skfABCEFGH* operon have been postulated to be involved in SKF maturation. SkfB is a radical S-adenosylmethionine (SAM) enzyme containing a 4Fe-4S cluster, which is needed for an unusual thioether bond formation in SKF between the cysteine residue Cys4 and the α-carbon of the methionine residue Met12 (Liu *et al.*, 2010). SkfC is a member of the CAAX protease family and is assumed to be responsible for leader peptide cleavage and the cyclization reaction of the peptide. SkfE and SkfF are hypothesized to constitute an ABC transporter for export of and immunity against SKF. SkfE is a predicted ATPase while SkfF constitutes a permease. While the role of SkfG remains elusive so far, SkfH is a thioredoxin-oxidoreductase-like protein which is assumed to be involved in disulfide bond formation (Liu *et al.*, 2010). The *skfABCEFGH* operon is expressed in a growth phase-dependent manner and induced at the beginning of stationary phase and/or under nutrient limiting conditions. Like SDP, it is negatively regulated by AbrB and activated by increasing levels of phosphorylated Spo0A (see also Fig. 1.9) (Burbulys *et al.*, 1991, Gonzalez-Pastor *et al.*, 2003, Molle *et al.*, 2003). Expression of SKF is regulated by one main promoter, P_{skfA}, and a second one within *skfC*, as determined by a recent genome-wide transcriptome study (Nicolas *et al.*, 2012).

All the above mentioned peptides share some characteristic features: They are encoded in operons with genes associated with their posttranslational modification and processing, export and immunity. Their promoters are regulated by transcriptional regulators (Rok, AbrB and Spo0A) usually in a growth phase- and nutrient-dependent manner. Dedicated immunity proteins ensure that toxin producers are resistant against their own peptides and only sensitive siblings are lysed. However, the spectrum of resistance mechanisms, which bacteria have evolved against AMPs, is large and is explained in more detail in the following section.

1.3 Resistance mechanisms against antimicrobial peptides

AMPs often lead to the induction of stress response countermeasures, which are specifically induced upon stress signal occurrence. There are several mechanisms bacteria employ to counteract such stresses.

One mechanism describes the destruction or modification of the antibiotic, thereby rendering it inactive (Breukink & de Kruijff, 2006). For instance, the β-lactam ring of β-lactam antibiotics structurally resembles the D-Ala-D-Ala moiety of the UDP-Mur*N*Ac pentapeptide of the peptidoglycan units. As a consequence, they are recognized by transpeptidases and block crosslinking of the glycan chains (Fig. 1.2) (Strominger & Tipper, 1965). Resistance is achieved by β-lactamases, which hydrolyze the β-lactam rings (Ghuysen, 1991).

Another mechanism many bacteria use is to shield the target of the antibiotic such that the antimicrobial substances cannot access the target. Bacteria are able to reduce the accessibility of lipid II by changing the cell wall composition (Davies *et al.*, 1996, Maisnier-Patin & Richard, 1996, Verheul *et al.*, 1997, Crandall & Montville, 1998, Mantovani & Russell, 2001, Kramer *et al.*, 2004). Usually, the cell wall of Gram-positive bacteria is negatively charged due to the phosphate groups of the teichoic acids. AMPs are cationic and amphipathic molecules with positive charges that facilitate contact with their targets at the cell surface. Therefore, one possible resistance mechanism for the cell is to incorporate positive charges into the growing cell wall. This leads to an electrostatic repulsion between cationic AMPs (CAMPs) and the bacterial cell envelope (Peschel & Sahl, 2006). Incorporation of positive charges is achieved by coupling D-alanine residues to teichoic acids resulting in an overall positive charge (Neuhaus & Baddiley, 2003). For example, *B. subtilis* regulates its cell wall charge via upregulation of the *dltABCDE* operon resulting in D-alanylation of teichoic acids (Perego *et al.*, 1995, Neuhaus & Baddiley, 2003, Reichmann *et al.*, 2013). These positive charges of the cell wall repel the positively charged antimicrobial substances and as a consequence, access to the antibiotic target structures is denied.

A second mode of action involving the *dlt* system is based on steric hindrance of CAMPs. Through D-alanylation of the teichoic acids, the cell wall becomes more compact and dense, leading to impermeability of the CAMPs to the membrane (Revilla-Guarinos *et al.*, 2014).

The next possible resistance mechanism bacteria have evolved to cope with antibiotic stress is the presence of resistance pumps. Usually, these pumps constitute ABC transporters which can be coupled to a 2CS for signal transmission. Such ABC transporters can also be found within the cell envelope stress response network of *B. subtilis*, which will be described in more detail in the following sections. ABC transporters can also function as exporters for the synthesized AMP, in addition to being immunity determinants. One example is YydIJ, which is postulated to be an ABC transporter/immunity determinant of the YydF peptide (Butcher *et al.*, 2007). Another example is SkfEF constituting a possible exporter/immunity protein of the cannibalism toxin SKF.

1.4 Cell envelope stress response in *B. subtilis*

As mentioned above, the cell envelope of a microbial cell constitutes a key target for many AMPs produced and secreted by other species. In order to survive in competitive, AMP-rich environments, bacteria need to sense cell wall/membrane damage and the respective cell wall active compounds to protect themselves from irreversible damage. For this, they have evolved a set of cell envelope stress response (CESR) systems to cope with stress signals from the environment. These signals provoke a stimulus-specific response within the cell typically through differential gene expression to mediate resistance by mounting protective countermeasures.

Bacteria employ three major routes of transmembrane signaling: one-component systems (1CSs), two-component systems (2CSs) and alternative extracytoplasmic function sigma factors (ECF σ factors) (Staroń & Mascher, 2010). In 1CSs, the input and output domains are located on a single polypeptide chain. Signal perception by the input domain modulates the activity of the output domain which then acts as a transcriptional regulator binding to its target genes to repress or activate transcription (Ulrich *et al.*, 2005). 1CSs usually play a minor role in transmembrane signaling due to their restricted protein architecture. In contrast, input and output domains of 2CSs and ECF σ factors are not encoded by a single polypeptide chain. Instead, they are separated on two proteins which facilitate signal transduction derived from the extracellular environment (Mascher *et al.*, 2006, Staroń *et al.*, 2009).

Typical 2CSs consist of a membrane-spanning histidine kinase (HK) and a cognate cytoplasmic response regulator (RR). The HK acts as a sensor protein which is able to detect specific stimuli from the environment via its extracellular N-terminal input domain. Subsequently, it undergoes a conformational change leading to autophosphorylation of a conserved histidine residue in its C-terminal transmitter domain. The phosphoryl group is then transferred to the RR resulting in phosphorylation of a conserved aspartate residue in the receiver domain. In its phosphorylated (activated) state, the RR binds to specific target promoters and can modulate the transcription of target genes. In order to set the system back to the pre-stimulus state, dephosphorylation of the RR can be accomplished by the phosphatase activity of the HK, by the RR itself or by external phosphatases (Stock *et al.*, 2000, Mascher *et al.*, 2006).

ECF σ factors are controlled by their cognate anti-σ factor consisting of a cytoplasmic and an extracellular domain linked by one transmembrane helix. In the absence of stress signals, the anti-σ factor solidly binds to its ECF σ factor and keeps it inactive. However, in the presence of a specific stimulus, the anti-σ factor gets inhibited and releases the ECF σ factor which can interact with the RNA polymerase (RNAP) and activate transcription of downstream target genes (Helmann, 2002).

The CESR network of *B. subtilis* consists of seven ECF σ factors and four 2CSs. They have been well studied and characterized over the last decade both at the level of differential gene expression and protein production (Wecke & Mascher, 2011) and have been described to respond to various cell wall antibiotics (Fig. 1.4) (Jordan *et al.*, 2008). Out of the seven ECF σ factors, three appear to play important roles in the CESR, σ^M, σ^X and σ^W, each regulating a set of ~30-60 target genes with

partially overlapping specificity (Mascher *et al.*, 2007, Kingston *et al.*, 2013). Furthermore, three out of the four 2CSs, the BceRS, PsdRS and YxdJK systems, specifically respond to a variety of AMPs and mediate resistance against them (Staroń *et al.*, 2011). These three 2CSs are referred to as Bce-like 2CSs because they share the same protein architecture and mechanistic features. They are all linked to and regulate the expression of genes encoding ABC transporters which are strongly induced by specific AMPs and represent the resistance determinant of each system (Jordan *et al.*, 2008, Staroń *et al.*, 2011). Moreover, the ABC transporters are required for sensing the AMPs and for transmission of the information to the cognate 2CS (Rietkötter *et al.*, 2008, Staroń *et al.*, 2011). All 2CSs, together with their cognate ABC transporters, comprise the so-called detoxification modules of *B. subtilis* (Staroń *et al.*, 2011). The fourth 2CS, the LiaSR system, responds to a broader range of AMPs and is presumably involved in envelope damage sensing (Wolf *et al.*, 2012).

This thesis focuses mainly on the BceRS-like and LiaSR 2CSs as well as in parts on the ECF σ factors σ^M, σ^X and σ^W of *B. subtilis*. Therefore, these systems will be described in detail in the following sections.

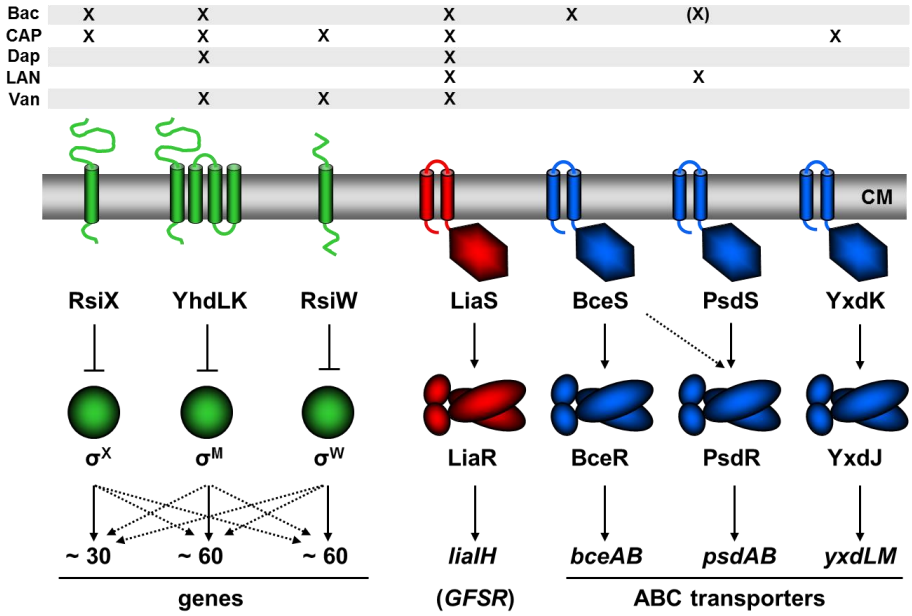

Fig. 1.4: Cell envelope stress response network of *B. subtilis*. ECF σ factors and their corresponding anti-σ factors are depicted in green. For simplicity reasons, ABC transporters and other accessory proteins or domains are omitted from this scheme and only 2CSs are depicted. Further details can be found in section 1.4.1 and 1.4.2 (Figs 1.5 and 1.7). The 2CSs coupled to ABC transporters are shown in blue, the LiaSR system in red. Membrane sensor proteins are depicted on top, regulator proteins are below. Target genes are shown at the bottom. Arrows indicate activation. T-shaped lines imply inhibition. Dotted lines illustrate cross regulation. Selected AMPs that induce the CESR systems are depicted above. Bac, bacitracin; CAP, cationic antimicrobial peptides; Dap, daptomycin; LAN, lantibiotics; Van, vancomycin; CM, cytoplasmic membrane. This figure is taken from (Jordan *et al.*, 2008) with modifications.

1.4.1 The LiaSR two-component system

LiaSR-like systems are highly conserved within the Firmicutes phylum of Gram-positive bacteria. The best characterized system until now is the LiaSR system in *B. subtilis* (Fig. 1.5). It has been originally discovered and described in the course of studying the bacitracin stimulon (Mascher *et al.*, 2003). Its name, LiaSR, derives from "**l**ipid II cycle **i**nterfering **a**ntibiotic **s**ensor and response **r**egulator" and is one of the 2CSs within the CESR network (Mascher *et al.*, 2004, Jordan *et al.*, 2006). As its name implies, it is primarily induced by AMPs interfering with the lipid II cycle of cell wall biosynthesis, e.g. bacitracin, vancomycin or cationic AMPs (CAMPs) as shown in Fig. 1.2 and 1.4 (Mascher *et al.*, 2004, Pietiäinen *et al.*, 2005). Additionally, it responds to more unspecific stimuli such as alkaline shock, detergents or organic solvents (e.g. ethanol, phenol) although to a much weaker extent (Petersohn *et al.*, 2001, Wiegert *et al.*, 2001, Mascher *et al.*, 2004, Pietiäinen *et al.*, 2005, Tam le *et al.*, 2006). Given the lack of substrate specificity of the LiaSR system, a direct role in mediating resistance against these AMPs could not be shown. However, current data indicate some level of interdependence between the different CESR systems regarding resistance to bacitracin. If the BceRS system is deleted, cells are up to 85-fold more sensitive to bacitracin compared to wild type. If *liaIH* is deleted additionally, sensitivity increases up to 512-fold although a *liaIH* single mutant is as sensitive as wild type (personal communication, Georg Fritz). Hence, double mutants reveal hidden layers of resistance of the different CESR systems. Therefore, the LiaSR system is proposed to be rather a damage sensing system and to represent a secondary resistance layer when the primary layer (BceAB) is missing (Rietkötter *et al.*, 2008, Wolf *et al.*, 2012) (personal communication, Georg Fritz).

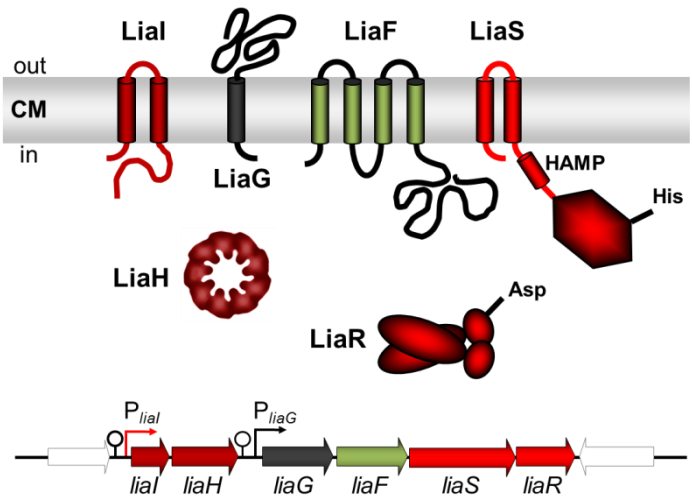

Fig. 1.5: The LiaSR system of *B. subtilis*. The 2CS consisting of LiaS and LiaR is shown in red, the accessory protein LiaF is colored in green. The membrane protein LiaI and the cytoplasmic phage-shock protein A homolog LiaH are depicted in dark red. According to sequence analysis, LiaG is a small membrane protein with one transmembrane helix shown in dark grey. The genomic context is indicated below. Promoters are marked as bent arrows and terminators are represented by vertical bars and a circle. Genes flanking the *liaIH-GFSR* operon are shown in white. Expression of *liaIH* is driven by the inducible P_{liaI} and expression of the 2CS (*liaSR*) is under control of the constitutive promoter P_{liaG}.

The HK, LiaS, constitutes an intramembrane-sensing HK with two transmembrane helices linked by a short extracellular loop (Mascher, 2006, Mascher, 2014). The second helix is connected to a cytoplasmic HAMP (short for: present in **h**istidine kinases, **a**denylate cyclases, **m**ethyl accepting proteins and **p**hosphatases) domain which is presumably involved in intramolecular signal conversion (Hulko *et al.*, 2006, Mascher, 2014). Upon activation, LiaS undergoes a conformational change leading to autophosphorylation at a conserved histidine residue. The phosphoryl group is

then transferred to an aspartate residue of its cognate RR, LiaR, within its conserved N-terminal receiver domain. This activation of LiaR leads to binding of target promoters on the DNA via its C-terminal DNA binding domain containing a characteristic helix-turn-helix motif (Jordan *et al.*, 2006).

The LiaSR 2CS is genetically and functionally associated with an accessory protein, LiaF. This membrane protein has been shown to keep LiaS inactive under non-inducing conditions. Current research implies that such accessory proteins are the actual sensor component and the transmembrane helices within the kinase serve as signal transfer regions that connect the signal perceived by the accessory protein with the phosphorylation status of the RR (Mascher, 2014).

The *lia* operon consists of six genes in total, *liaIH-GFSR*. The genes encoding the 2CS are under control of a constitutive promoter upstream of *liaG* (P_{liaG}, Fig. 1.5) (Jordan *et al.*, 2006). This ensures appropriate amounts of the respective signaling proteins, Lia(F)SR, in case of cell envelope stress stimuli. Inducing conditions then lead to a strong LiaR-dependent activation of the promoter upstream of *liaI* (P_{liaI}). Activation of P_{liaI} results in the expression of two transcripts: the first transcript covers *liaIH*, being the major transcript of 1.1 kb in size. The second one comprises the whole *lia* operon, *liaIH-GFSR* of about 4 kb. This is due to a weak terminator downstream of *liaH* leading to substantial read-through from P_{liaI} into the downstream genes (Mascher *et al.*, 2004). P_{liaI} is the only relevant target promoter of LiaR; however, the exact physiological role of LiaIH has not been characterized in detail yet. Recent studies demonstrate that the small membrane protein LiaI serves as a membrane anchor for the phage-shock protein A homolog, LiaH, upon cell envelope stress conditions (Dominguez-Escobar *et al.*, 2014). While LiaH has been shown to localize in the cytosol under non-inducing conditions and LiaI locates in highly motile foci within the cytoplasmic membrane, this pattern changes upon inducing conditions: LiaI and LiaH co-localize into distinct static foci at the membrane presumably to protect the envelope from the AMP-induced membrane damage (Dominguez-Escobar *et al.*, 2014).

The LiaSR system is not only induced upon external addition of cell wall antibiotics and other less specific stimuli. It has been shown to be also intrinsically induced in a growth phase-dependent manner (Fig. 1.6) (Jordan *et al.*, 2007). During transition from exponential to stationary growth phase, *B. subtilis* cells undergo a complex differentiation cascade in order to adapt to changing environmental conditions, e.g. nutrient limitation. This cascade is regulated by the master regulator of sporulation, Spo0A. It orchestrates the conversion from vegetative cells to highly resistant dormant endospores (see also section 1.5) (Msadek, 1999, Phillips & Strauch, 2002, Errington, 2003, McKenney *et al.*, 2013). During exponential growth phase, the transition state regulator AbrB represses P_{liaI} activity by direct binding to the *liaI* promoter region (Fig. 1.6, right). Additionally, under non-inducing conditions, LiaF inhibits LiaS and keeps it in its OFF-state. During transition from exponential to stationary phase, Spo0A becomes active (Spo0A~P) and inhibits AbrB (Fig. 1.6, left), thereby releasing AbrB on P_{liaI}. But this indirect activation of P_{liaI} is not sufficient to induce transcription of *liaIH*, since the system needs to be activated simultaneously by an intrinsic stimulus to release the LiaS inhibition by LiaF. This results in the activation of LiaR and subsequent initiation of transcription of *liaIH* (Jordan *et al.*, 2007). One previous report suggested that the YydF peptide

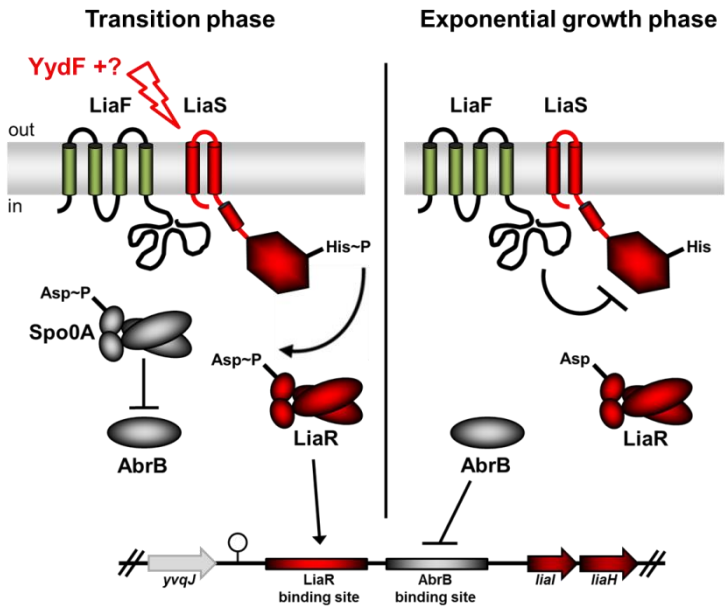

Fig. 1.6: Schematic comparison of transition phase activation and exponential growth of the LiaSR system in *B. subtilis*. The LiaSR 2CS is shown in red, the accessory protein LiaF in green. The repressor proteins Spo0A and AbrB are depicted in grey. LiaR (red) and AbrB (grey) binding sites are enlarged. Activation is indicated by a black arrow, repression by T-shaped lines. The figure is adapted from (Jordan *et al.*, 2007). See text for details.

encoded in the *yydFGHIJ* operon is able to induce the LiaSR system in the absence of its own immunity ABC transporter YydIJ (Butcher *et al.*, 2007). Expression of the YydF peptide was shown to be repressed by AbrB during vegetative growth. At the onset of stationary phase, AbrB repression is released by Spo0A and the peptide is most probably produced (Butcher *et al.*, 2007). Indeed, our own unpublished data suggest that YydF is an inducer of the LiaSR system during transition phase. However, transition phase induction is significantly weaker compared to the strong induction by cell wall antibiotics (approx. 10-15-fold vs. 100-fold) (Jordan *et al.*, 2007).

In conclusion, the LiaSR system is induced by a wide range of AMPs and some rather unspecific stimuli perturbing the cell membrane as well as during transition from exponential to stationary growth phase. This intrinsic activation can be attributed to the YydF peptide. Upon intrinsic activation of the LiaSR system, subsequent gene expression involves at least five regulatory proteins: LiaF, LiaS and LiaR as well as AbrB and Spo0A (Jordan *et al.*, 2007). The biological significance of *liaIH* induction has been investigated recently (Dominguez-Escobar *et al.*, 2014). LiaI has been suggested to scan the membrane and recruit LiaH in the presence of membrane damage to co-localize into static foci to shield against AMP-generated membrane damage.

1.4.2 Bce-like two-component systems of *B. subtilis*

The remaining three 2CSs of the cell envelope stress response in *B. subtilis*, the BceRS, PsdRS and YxdJK systems, are all genetically and functionally linked to genes encoding ABC transporters (Dintner *et al.*, 2011). They represent so-called AMP detoxification modules since they have been shown to respond to and mediate resistance against a wide range of AMPs. The best characterized module is BceRSAB, which specifically responds to bacitracin and to a lesser extent to the lantibiotics actagardine and mersacidin (Staroń *et al.*, 2011). The 2CS consists of an intramembrane-sensing HK, BceS, and its cognate cytosolic RR, BceR. Like LiaS, BceS is not the sensor component of the system. It is again an accessory protein, the ABC transporter BceAB, which comprises the sensing part of the system (Fig. 1.7). It consists of an ATPase domain (BceA) and a permease domain (BceB) harboring ten transmembrane helices and a large unique

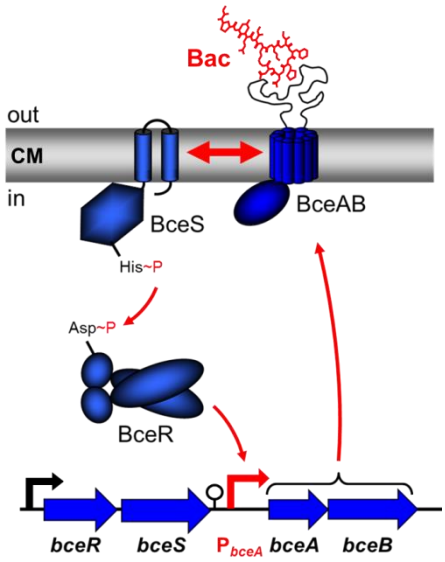

Fig. 1.7: The BceRSAB detoxification module of *B. subtilis*. The 2CS, BceR and BceS, regulate the expression of *bceAB*, encoding an ABC transporter responsible for stimulus perception, signal transduction and mediation of resistance. Phosphorylated BceR binds to P_{bceA} in order to activate transcription of *bceAB*. The signal transduction pathway is further explained in the text. This figure is adapted from (Rietkötter *et al.*, 2008).

extracellular loop structure between transmembrane helix seven and eight (Rietkötter *et al.*, 2008). Under inducing conditions, *bceAB* expression is upregulated to confer resistance to the peptide antibiotic. However, this upregulation of *bceAB* requires the BceAB ABC transporter itself for signal perception. It has been shown that BceS alone is unable to sense stimuli and therefore insufficient for signal transduction (Bernard *et al.*, 2007, Rietkötter *et al.*, 2008, Dintner *et al.*, 2014). Hence, only in presence of BceAB, BceS is able to be activated by autophosphorylation upon peptide antibiotic stress. Subsequent phosphoryl group transfer to BceR results in DNA binding to the *bceA* promoter region and initiation of *bceAB* transcription. This autoregulation of BceAB ensures that resistance to an AMP can be maintained any time. Notably, it has been shown recently that BceAB senses the transport flux of bacitracin, thereby directly monitoring its current detoxification capacity (Fritz *et al.*, 2015). This enables a cost-efficient and precise regulation of antibiotic resistance depending on the current capacity (Fritz *et al.*, 2015).

The other two Bce-like 2CSs described in *B. subtilis*, PsdRS and YxdJK, are paralogous in sequence and genomic context organization to the BceRS 2CS, but differ in their substrate specificity. The PsdRS 2CS responds primarily to lantibiotics such as nisin, subtilin, actagardine and gallidermin and to the lipopeptide enduracidin, which all interfere with the lipid II cycle (Staroń *et al.*, 2011). The PsdRS 2CS also responds to bacitracin, but to a much weaker extent. This is due to cross-activation of the PsdR RR by the paralogous BceS HK (Mascher *et al.*, 2003, Rietkötter *et al.*, 2008).

Little is known about the YxdJK 2CS and its cognate ABC transporter YxdLM. The expression of *yxdLM* is dependent on the YxdJ RR and it has been shown to respond to the human cationic antimicrobial peptide LL-37 (Joseph *et al.*, 2004, Pietiäinen *et al.*, 2005, Staroń *et al.*, 2011). The question remains why a soil-living bacterium has evolved a system that responds to a human peptide. Since LL-37 is, so far, the only inducer of the YxdJK 2CS, the biological significance remains elusive.

1.4.3 ECF σ factors σ^M, σ^X and σ^W – a short overview

The ECF σ factors σ^M, σ^X and σ^W play roles in the CESR of *B. subtilis* (Missiakas & Raina, 1998, Helmann, 2002, Mascher *et al.*, 2007, Eiamphungporn & Helmann, 2008, Kingston *et al.*, 2013).

In general, σ factors are part of the RNA polymerase (RNAP). They are able to bind to the core enzyme and direct the RNAP holoenzyme to appropriate promoters to initiate transcription. All

bacteria contain primary (or housekeeping) σ factors that are responsible for the expression of most of the genes. Additionally, many bacteria living in complex habitats, such as the soil, also contain alternative σ factors, which are only activated under specific conditions. ECF σ factors constitute a subgroup of alternative σ factors. They are able to replace primary σ factors to redirect the RNAP and activate transcription of a different set of genes from specific alternative promoters (Helmann, 2002). ECF σ factors are kept inactive under non-inducing conditions by their cognate anti-σ factor through direct protein-protein interactions (Brown & Hughes, 1995). They are usually co-expressed with their anti-σ factors (see Fig. 1.4). In the presence of a stimulus, the ECF σ factor is released from the anti-σ factor, resulting in binding to the RNAP core enzyme and activating transcription from alternative promoters (Helmann, 2002). Besides this extrinsic induction by specific compounds, intrinsic induction of the ECF σ factors, i.e. without any external stimulus, occurs in a growth phase- and growth medium-dependent manner (Huang *et al.*, 1998). While σ^M and σ^X are induced generally in late logarithmic growth phase, σ^W only becomes active in early stationary phase (Huang *et al.*, 1998, Nicolas *et al.*, 2012).

One of the best characterized ECF σ factors is σ^W regulating the activity of about 30 promoters which control expression of approx. 60 genes (see Fig. 1.4). These genes often encode proteins or peptides involved in detoxification. Thus, σ^W has been postulated to mediate intrinsic immunity against a wide range of antibiotic compounds (Cao *et al.*, 2001, Butcher & Helmann, 2006). σ^W is particularly activated by cell wall antibiotics such as vancomycin or cephalosporin C (Cao *et al.*, 2002) as well as alkaline shock (Wiegert *et al.*, 2001). However, σ^W does not seem to be required for resistance against these compounds despite its strong induction (Cao *et al.*, 2002). Nevertheless, a *sigW* mutant has been shown to be more susceptible to a broad range of AMPs produced by other *Bacillus* species (Butcher & Helmann, 2006).

The second ECF σ factor involved in the CESR is σ^M (see Fig. 1.4). It is predominantly induced by acid, heat, salt and superoxide stress conditions as well as by specific cell wall antibiotics such as bacitracin or vancomycin (Cao *et al.*, 2002, Mascher *et al.*, 2003, Thackray & Moir, 2003). Similar to σ^W, σ^M regulates the expression of about 60 genes within 30 operons upon stress conditions (Eiamphungporn & Helmann, 2008). These genes of the σ^M regulon have distinct functions varying from cell wall synthesis, shape determination, cell division, DNA damage monitoring and detoxification (Eiamphungporn & Helmann, 2008). One example is the expression of *bcrC*, which is upregulated upon bacitracin exposure. Elevated levels of BcrC contribute to resistance against bacitracin (Cao & Helmann, 2002). Its expression is dependent on σ^M, however *bcrC* has been identified to constitute an *in vitro* target of σ^X-directed transcription and was shown to be part of the σ^W-regulon as well (Cao & Helmann, 2002, Pietiäinen *et al.*, 2005).

The third ECF σ factor is σ^X (see Fig. 1.4). It controls the expression of about ten operons encoding proteins primarily involved in cell envelope composition and cell surface modification (Cao & Helmann, 2004). One of the target operons of σ^X is the *dltABCDE* operon. It is responsible for introducing positively charged amino acids (D-alanylation) into the teichoic acids, thereby reducing the overall negative charge of the cell wall (Neuhaus & Baddiley, 2003). This significantly decreases susceptibility to cationic AMPs and constitutes an important resistance mechanism. In

fact, a *sigX* mutant is prone to autolysis and more sensitive to nisin which has been shown to form pores in the membrane (van Heusden *et al.*, 2002, Cao & Helmann, 2004).

In conclusion, ECF σ factors are involved in the complex CESR of *B. subtilis* controlling an "antibiosis regulon" which counteracts cell wall stress. The ECF σ factor response is complex, since it has been shown that σ^W, σ^M and σ^X control an overlapping set of genes (see Fig. 1.4) (Mascher *et al.*, 2007, Kingston *et al.*, 2013). With this overlapping specificity it is possible to induce appropriate countermeasures against stresses although one σ factor might be missing.

1.5 Sporulation – taking the last exit

B. subtilis is a widely used Gram-positive model organism to study basic and complex cellular mechanisms. It is able to form endospores, which involves a complex sporulation cascade. Many genes and gene products are associated with sporulation and a combined interplay is necessary to coordinate the steps in the spore development. Fig. 1.8 gives an overview of the sporulation cycle.
The sporulation process starts when vegetatively growing cells suffer from nutrient exhaustion (Trach *et al.*, 1991). Formation of highly resistant and dormant endospores is the only way bacteria can overcome starvation conditions in a long-term prospective. The whole cycle is regulated by the master regulator of sporulation, Spo0A. As depicted in Fig. 1.8, the cycle starts with an asymmetric polar division into two compartments, the mother cell and the forespore (or prespore), which is orchestrated by genes regulated by Spo0A and σ^H (Levin & Losick, 1994). Within both compartments, spore development is tightly organized by an elaborate set of genes activated by a series of compartment-specific σ factors (Errington, 2003, Tan & Ramamurthi, 2014).

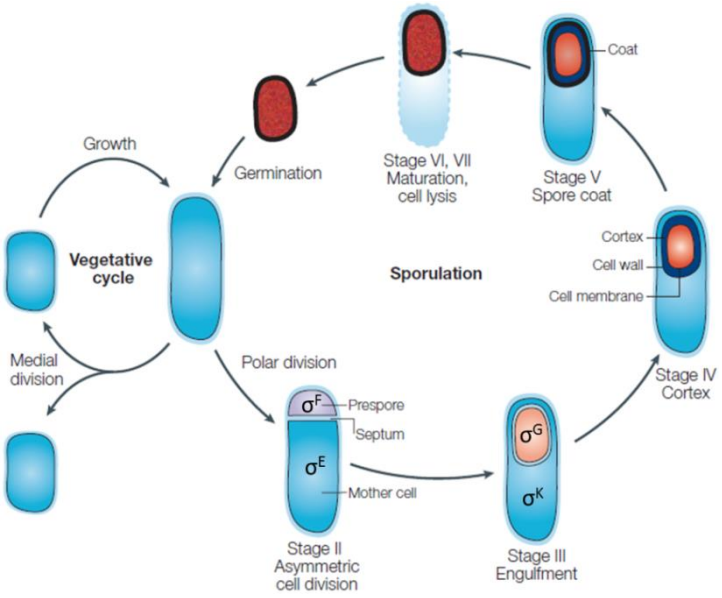

Fig. 1.8: The sporulation cycle of *B. subtilis*. Sporulation includes a complex differentiation cascade and involves different stages of forespore (prespore) formation and maturation until the final release of the spore. See text for details. This figure is taken and modified from (Errington, 2003).

Once the spore has matured and the spore coat has formed, the mother cell lyses and releases the spore to the environment (Errington, 2003, McKenney *et al.*, 2013, Tan & Ramamurthi, 2014). Outgrowth of the spore occurs under nutrient-rich conditions, upon which it can re-enter its vegetative cycle.
As already mentioned, starvation and high cell densities promote sporulation by activation of the transcriptional regulator, Spo0A.

Indeed, Spo0A as being the master regulator of sporulation is part of a well-studied phosphorelay system (Burbulys *et al.*, 1991). Several kinases (KinA, KinB, KinC, KinD and KinE) are involved in that system and activated by different stimuli. KinA and KinB primarily respond to changes in ATP levels whereas KinC and KinD are activated by unknown signals but appear to be relevant for controlling the expression of cannibalism genes and are important for biofilm formation (LeDeaux *et al.*, 1995, Eswaramoorthy *et al.*, 2010, Devi *et al.*, 2015). KinE does not play a role in sporulation (Fujita *et al.*, 2005). Upon activation of KinA and KinB, they undergo subsequent autophosphorylation and indirectly phosphorylate Spo0A. This is achieved by two intermediates Spo0F and Spo0B (Burbulys *et al.*, 1991, Higgins & Dworkin, 2012, Boguslawski *et al.*, 2015). KinA and KinB transfer the phosphoryl group to Spo0F which then, in turn, phosphorylates Spo0B. Thereupon, Spo0B~P transfers the phosphoryl group to Spo0A and sporulation is subsequently initiated.

This tight regulation of sporulation is crucial since sporulation is a very energy-demanding process and irreversible once the asymmetric septum is formed (Parker *et al.*, 1996). Additionally, different levels of Spo0A~P lead to different gene expression. High levels of Spo0A~P initiate sporulation, while low concentrations of Spo0A~P regulate a different set of genes in the cell. This includes genes for production, export and immunity to toxins or AMPs mostly indirectly via repression of the transition state regulator AbrB (Fig. 1.9). The two cannibalism toxins, SDP and SKF, are induced by this pathway. This difference in activation of different sets of genes is due to the binding affinity of Spo0A~P to different promoter regions (Fujita *et al.*, 2005). Genes which require a high level of Spo0A~P to be induced were shown to have low binding constants, while genes which need lower levels of Spo0A~P revealed high binding affinities or were indirectly activated by Spo0A-mediated relief of repression by AbrB. Cell-to-cell variations in (in)active Spo0A lead to a highly heterogeneous population at the onset of stationary growth phase where nutrients become scarce (Figs 1.9 and 1.10).

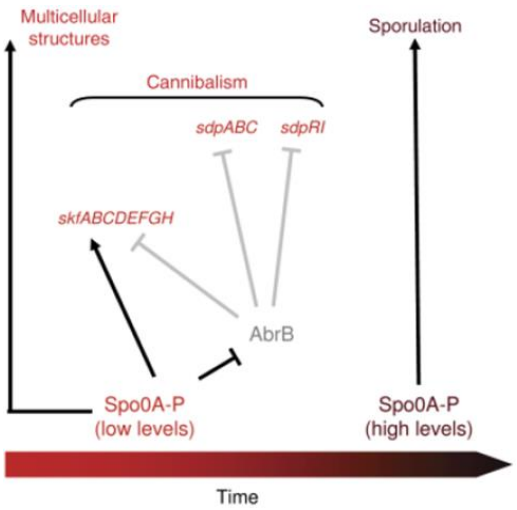

Fig. 1.9: Different levels of phosphorylated Spo0A lead to different cellular responses. Low levels of Spo0A~P induce the transcription of the two cannibalism operons, *sdpABC-sdpRI* and *skfABCEFGH*, either directly or indirectly by repression of AbrB, a negative regulator of *sdpABC-sdpRI* and *skfABCEFGH*. Low Spo0A~P levels also promote the formation of multicellular aerial structures (Fujita *et al.*, 2005). High levels of Spo0A~P trigger sporulation directly. This figure is taken from (Gonzalez-Pastor, 2011).

One important effect of Spo0A~P at the beginning of transition phase adaptation is the repression of the negative regulator AbrB (Fig. 1.9) (Perego *et al.*, 1988). AbrB is active during logarithmic growth phase and known to repress many genes involved in sporulation or AMP production (Strauch *et al.*, 1989, Albano *et al.*, 2005, Stein, 2005). When Spo0A~P levels begin to increase, *abrB* is directly repressed (Strauch *et al.*, 1990). Both cannibalism operons (*sdpABC-sdpRI* and *skfABCEFGH*) are under direct negative control of AbrB and indirectly

activated by Spo0A. Cannibalism describes a strategy that cells usually employ before they undergo sporulation. This will be described in the following section.

1.6 Cannibalism – a strategy to delay sporulation

Cannibalism is a social behavior and occurs during the early stages of sporulation of *B. subtilis*. It has been proposed to be a sporulation delay strategy to overcome temporary nutrient limitation dependent on the master regulator of sporulation, Spo0A (Gonzalez-Pastor *et al.*, 2003). Cannibalism can be particularly beneficial for the cells since the sporulation cascade is very energy-consuming and irreversible once the asymmetric septum is formed (Parker *et al.*, 1996). The basis for cannibalism is the heterogeneity of a sporulating population. It can be divided into two subpopulations: (1) sporulating cells with active Spo0A and (2) nonsporulating cells with inactive Spo0A (Fig. 1.10).

Induction of the cannibalism operons *sdpABC-sdpRI* and *skfABCEFGH* is regulated in an AbrB- and Spo0A-dependent manner (see also section 1.2) (Fujita *et al.*, 2005, Chen *et al.*, 2006). Transcription of both operons is repressed by AbrB during logarithmic growth and repression is released by rising levels of active Spo0A during early stationary phase. Hence, low levels of Spo0A~P indirectly activate expression of the *sdpABC-sdpRI* and *skfABCEFGH* operons (Strauch *et al.*, 1990, Fujita *et al.*, 2005, Chen *et al.*, 2006). Additionally, the *skf* regulatory region harbors a high-affinity binding site for Spo0A resulting in activation at low doses of Spo0A~P. This means that *skfABCEFGH* expression is not only indirectly activated by Spo0A via AbrB relief but also directly induced by Spo0A (Fujita *et al.*, 2005, Gonzalez-Pastor, 2011). On the other hand, it has been demonstrated that high levels of Spo0A~P can repress the expression of *sdpABC-sdpRI* by binding of Spo0A~P to a low affinity binding site within the *sdp* regulatory region (Fujita *et al.*, 2005). These cell-to-cell

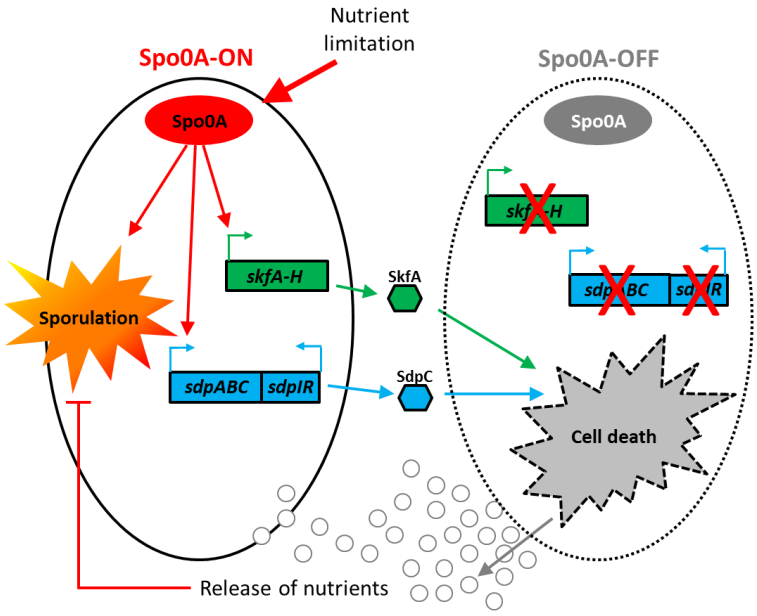

Fig. 1.10: Simplified schematic overview of the underlying mechanisms driving cannibalism. Cannibalism is based on a heterogeneous activation of Spo0A at the onset of stationary growth phase. Spo0A-ON cells activate transcription of the *skfABCEFGH* and *sdpABC-sdpRI* operons whereas in Spo0A-OFF siblings expression of these operons is repressed. Lysed cells supply the cannibal subpopulation with nutrients which delays sporulation significantly. This figure is adapted from (Engelberg-Kulka *et al.*, 2006).

variations of different levels of active Spo0A lead to a stochastic activation of the *sdpABC-sdpRI* and *skfABCEFGH* operons within one bacterial population giving rise to two subpopulations (Spo0A-ON and Spo0A-OFF) (Chung *et al.*, 1994, Chastanet *et al.*, 2010). Spo0A-ON cells do not only produce and secrete the respective cannibalism toxins but also simultaneously express immunity proteins to ensure that the producers are not killed by their own toxins (see also section 1.3). Accordingly, in Spo0A-OFF cells the cannibalism operons are still repressed by AbrB. As a consequence, neither toxins nor immunity proteins are made, rendering Spo0A-OFF cells sensitive to the toxins produced by their siblings (Gonzalez-Pastor *et al.*, 2003, Ellermeier *et al.*, 2006). As a result, they are prone to lyse and release nutrients to the starved environment. The cannibal cells are then able to feed on these nutrients and sporulation is arrested until the new nutrients are exhausted again. This cycle of starvation, initiation of cannibalism and resumption of growth continues until the majority of cells has transformed into spores.

The biological significance of cannibalism becomes evident when considering the fact that spore formation is highly energy-demanding and reversible only up to a certain point (Parker *et al.*, 1996). After this checkpoint, the cells are not able to resume vegetative growth although nutrients might be available again. Additionally, completion of sporulation takes several hours. This might result in having a disadvantage over other microorganisms in their natural environment or just over nonsporulating sister cells. Cannibalism helps to maintain a mixed population during stationary phase with few spores, some cells already committed to sporulation and many cells vegetatively growing.

1.7 Aims of this thesis

The LiaSR system of *B. subtilis* responds to a great variety of peptide antibiotics including the cyclic AMP bacitracin. It has been shown previously that the LiaSR system is highly induced by bacitracin. Whole population studies revealed a heterogeneous induction pattern of the LiaSR system depending on the extracellular bacitracin concentration. In CHAPTER II, the aim was to investigate this heterogeneity of the LiaSR response to different external concentrations of bacitracin on single cell level. We used quantitative fluorescence microscopy including time-lapse microscopy to elucidate the heterogeneous induction of the LiaSR system in a bacitracin-dependent manner.

Although the LiaSR system has been extensively studied over the last decade, its physiological role remained unclear. Despite its strong and fast induction by various cell wall antibiotics, the LiaSR system only seems to provide some secondary resistance layer when the primary resistance determinant is missing. While LiaF, LiaS and LiaR have been characterized well over the last years, the function of LiaI and LiaH remained elusive. The aim of CHAPTER III was to gain deeper insight into the physiological role of the LiaSR system by using time-lapse microscopy to study the subcellular localization and interaction of LiaI and LiaH in the presence and absence of bacitracin.

In addition to its strong and fast activation by external cell wall antibiotics, the LiaSR system was shown to be induced intrinsically without any external stimulus at the transition from exponential to stationary growth phase. This transition phase induction is partly due to Spo0A-mediated de-repression of the LiaSR system via inhibition of its negative regulator AbrB during logarithmic growth phase but is not sufficient for induction. In the course of studying this intrinsic activation, we observed that the BceRS and PsdRS 2CSs as well as the ECF σ factors σ^M, σ^X and σ^W are also induced in stationary growth phase by an unknown stimulus. In CHAPTER IV, the aim was to determine the stimuli leading to the intrinsic activation of these systems. We used a *lux*-reporter system to monitor target promoter activity of each system in a microplate reader and screened for a variety of peptide antibiotics and toxins produced by *B. subtilis* 168 in stationary growth phase.

CHAPTER II

Immediate and Heterogeneous Response of the LiaFSR Two-Component System of *Bacillus subtilis* to the Peptide Antibiotic Bacitracin

Sara Kesel, Andreas Mader, **Carolin Höfler**, Thorsten Mascher, Madeleine Leisner

PloS one **8**: e53457

OPEN ACCESS Freely available online

PLOS ONE

Immediate and Heterogeneous Response of the LiaFSR Two-Component System of *Bacillus subtilis* to the Peptide Antibiotic Bacitracin

Sara Kesel[1], Andreas Mader[1], Carolin Höfler[2], Thorsten Mascher[2], Madeleine Leisner[1]*

1 Center for NanoScience, Ludwig-Maximilians-University, Fakultät für Physik, Munich, Germany, **2** Department Biology I, Microbiology, Ludwig-Maximilians-University Munich, Planegg-Martinsried, Germany

Abstract

Background: Two-component signal transduction systems are one means of bacteria to respond to external stimuli. The LiaFSR two-component system of *Bacillus subtilis* consists of a regular two-component system LiaRS comprising the core Histidine Kinase (HK) LiaS and the Response Regulator (RR) LiaR and additionally the accessory protein LiaF, which acts as a negative regulator of LiaRS-dependent signal transduction. The complete LiaFSR system was shown to respond to various peptide antibiotics interfering with cell wall biosynthesis, including bacitracin.

Methodology and Principal Findings: Here we study the response of the LiaFSR system to various concentrations of the peptide antibiotic bacitracin. Using quantitative fluorescence microscopy, we performed a whole population study analyzed on the single cell level. We investigated switching from the non-induced 'OFF' state into the bacitracin-induced 'ON' state by monitoring gene expression of a fluorescent reporter from the RR-regulated *lial* promoter. We found that switching into the 'ON' state occurred within less than 20 min in a well-defined switching window, independent of the bacitracin concentration. The switching rate and the basal expression rate decreased at low bacitracin concentrations, establishing clear heterogeneity 60 min after bacitracin induction. Finally, we performed time-lapse microscopy of single cells confirming the quantitative response as obtained in the whole population analysis for high bacitracin concentrations.

Conclusion: The LiaFSR system exhibits an immediate, heterogeneous and graded response to the inducer bacitracin in the exponential growth phase.

Citation: Kesel S, Mader A, Höfler C, Mascher T, Leisner M (2013) Immediate and Heterogeneous Response of the LiaFSR Two-Component System of *Bacillus subtilis* to the Peptide Antibiotic Bacitracin. PLoS ONE 8(1): e53457. doi:10.1371/journal.pone.0053457

Editor: Tarek Msadek, Institut Pasteur, France

Received August 31, 2012; **Accepted** November 30, 2012; **Published** January 11, 2013

Copyright: © 2013 Kesel et al. This is an open-access article distributed under the terms of the Creative Commons Attribution License, which permits unrestricted use, distribution, and reproduction in any medium, provided the original author and source are credited.

Funding: Funding to ML, the authors thank excellence cluster Nano Initiative Munich and the Center for Nanoscience for funding. Funding to TM, funding is gratefully acknowledged by the Deutsche Forschungsgemeinschaft (MA2873/3-1). The funders had no role in study design, data collection and analysis, decision to publish, or preparation of the manuscript.

Competing Interests: The authors have declared that no competing interests exist.

* E-mail: madeleine.leisner@physik.uni-muenchen.de

Introduction

Two-component systems (TCS) are a fundamental principle of bacterial signal transduction that enables cells to respond to environmental stimuli [1–3]. These phosphotransfer systems involve two conserved components, a histidine protein kinase (HK) and a response regulator protein (RR). Extracellular stimuli are sensed by the HK, leading to its autophosphorylation [4]. The phosphoryl group is then transferred from the HK to the RR. The RR, now in its 'active' form, elicits the specific response. Bacteria such as *Escherichia coli* or *Bacillus subtilis* posses about 30 HKs and RRs [5,6], including well-known systems such as the EnvZ/OmpR TCS of the osmosensing pathway [7] or the HK CheA of the chemotaxis system phosphorylating two RRs, CheB and CheY [8]. In addition to functional characterization of TCS focusing on phosphorylation rates [9] accompanied by theoretical studies [10,11], specificity and crosstalk of TCS is of great interest [12] and several methods for two-component research have been developed to accommodate such studies [13]. While some TCS mediate differential expression of the output genes by a graded response [7], others result in an all-or-nothing response [14]. The latter is only triggered after a particular stimulus concentration has been overcome. The response itself can thereby be homogeneous (the whole population behaves in the same way) or heterogeneous with parts of the population behaving differently than the others. Regardless of the observed output, regulation of both types of systems can involve a number of auxiliary protein components. Systems involving accessory proteins [15–17], often referred to as three-component systems, also include peptide antibiotic-sensing systems of Gram-positive bacteria [18,19,20].

One such system is the LiaFSR cell envelope stress response module of *Bacillus subtilis* [21,22], which strongly responds to various peptide antibiotics such as bacitracin, nisin, vancomycin or daptomycin [23], but also to other less specific envelope perturbating conditions, such detergents or alkaline shock (summarized in [24] and [25]). The Lia system, is comprised of the LiaRS TCS, with the HK LiaS and the RR LiaR, and additionally the accessory protein LiaF (Figure 1). The latter is associated with all LiaRS-like TCS and acts as a negative regulator of LiaR-mediated gene regulation [21]. The mechanism by which

LiaF interferes with LiaRS-dependent signal transduction is not yet understood. The genes of the LiaFSR system, together with a forth protein of unknown function, LiaG, are encoded in the *liaGFSR* operon, which is expressed from the constitutive *liaG* promoter (P_{liaG}) in the absence of inducing conditions [21]. Activation of LiaR results in induction of the *liaI* promoter (P_{liaI}) resulting in a strong upregulation of the *liaIH* operon, but also the complete *lia* locus (Figure 1) [21,22]. The exact physiological role of LiaI and LiaH is not well understood, but the proteins seem to be involved in sensing and counteracting membrane damage [22]. In contrast to other cell wall antibiotic sensors of *B. subtilis*, such as the BceRS and PsdRS systems that directly sense peptide antibiotics and specifically mediate resistance against them [26], the Lia system seems to respond only indirectly to some quality of the damage caused by the diverse set of inducing conditions [27].

Here we focus on the activation of the P_{liaI} by LiaR in response to the external stimulus bacitracin, which is the strongest and most robust inducer of LiaRS activity [23,26]. As seen recently in other studies [28,29], signal transduction of TCS can result in heterogeneous expression of genes regulated by these TCS. Heterogeneous gene expression in genetically identical cells can result in phenotypic different outcomes, a phenomenon also known as phenotypic heterogeneity [30]. Gene expression in itself is a stochastic or 'noisy' process [31]. Two different kinds of noise can be distinguished: intrinsic noise, due to noise in transcription or translation of the particular gene studied; or extrinsic noise as caused by fluctuations in the amount of other cellular components affecting gene expression [31]. Independent of the source of the noise, the arising heterogeneity can be manifested in broad gene expression distributions or by bifurcation into distinct subpopulations [32], as has been observed in *B. subtilis* in case of the transition state and stationary phase differentiation [32,33].

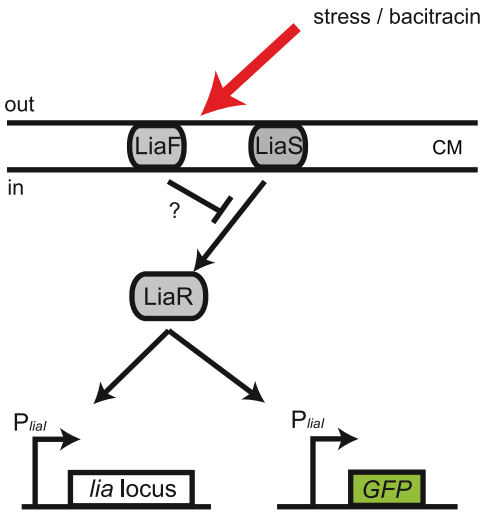

Figure 1. Core of the LiaFSR system. Arrows denote upregulation and T-shaped lines indicate inhibition. The LiaFSR system of *Bacillus subtilis* consists of the two-component signal transducing system LiaRS and the accessory membrane protein LiaF, a LiaRS-specific inhibitor. Stress represented e.g. by cell wall antibiotics such as bacitracin is sensed by LiaS/F and leads to expression of the *lialH - liaGFSR* ("*lia* locus" in the Figure) locus mediated by LiaR. To study the response of the Lia system to external stressors, we report activity of P_{lial} using the fluorescent marker GFP expressed under the control of the *lial* promoter, chromosomally inserted ectopically in addition to the native Lia system. CM indicates the cytoplasmic membrane.
doi:10.1371/journal.pone.0053457.g001

For the LiaFSR system, averaged data obtained by whole population studies revealed that the response of the P_{liaI} is dependent on the external antibiotic concentration [23]. However, a quantitative single cell analysis of the Lia response addressing heterogeneity in gene expression has not yet been performed. Using quantitative fluorescence microscopy [33,34], we focused on a whole population study analyzed at the single cell level. We monitored gene expression from P_{liaI} over time and found heterogeneity at low bacitracin concentrations. While expression levels from P_{liaI} increased with the externally provided bacitracin amount, we found the immediate response of the LiaFSR system independent of the antibiotic concentration. We defined a switching threshold from the non-induced 'OFF' state to the bacitracin-induced 'ON' state. The number of cells in the 'ON' state, as well as the basal expression rate of the P_{liaI} increased with bacitracin concentration. In addition, a well defined time window for switching into the 'ON' state was observed at all bacitracin concentrations.

Results

Gene expression increases at high bacitracin concentrations

In this study, we aimed at a deeper understanding of the response of the LiaFSR system to various concentrations of the peptide antibiotic bacitracin. We used the *B. subtilis* strain TMB 1172 [35], which carries a translational fusion of P_{liaI} with the green fluorescent protein GFPmut1. This GFP reporter has been integrated chromosomally in addition to the naturally occurring genes under the control of P_{liaI} and regulated by the RR LiaR (Figure 1). Therefore, we were able to study the response of the LiaFSR system by analyzing the expression of the GFP reporter, as it represents the expression of the LiaR regulated target genes. In particular, we studied the fluorescence development of the GFP reporter in dependence of bacitracin, a model component used to study cell envelope stress response modules of *Bacillus subtilis* [19,36]. We chose the stable GFP variant, GFPmut1, shown to have a half-life of more than 24 h [37,38], as we were only interested in the onset of gene expression. Thereby, we excluded possible variations in gene expression due to GFP decay.

Our cells were grown until mid-exponential phase before being induced with bacitracin to ensure that the recorded P_{liaI} response was only due to external induction via bacitracin rather than intrinsic induction via the transition state regulator AbrB or the master regulator of sporulation Spo0A as present in the stationary phase [39]. Prior to bacitracin induction, we quantified the fluorescence intensity (FI) of non-induced cells representing the autofluorescence level (FI_{auto}) and found it to be narrowly distributed with FI_{auto} 8 ± 1 FU (Figure 2A). After bacitracin induction, we monitored the fluorescence development for two hours with five to seven minute intervals. At high bacitracin concentrations all cells shifted from the autofluorescence level to intermediate and finally high GFP expression levels. The maximal fluorescence intensities were reached at 60 min after bacitracin induction as shown in Figure 2B–F. While at 30 μg/ml bacitracin maximal fluorescence intensities of 272 FU on average were reached, FI_{max} decreased with lower bacitracin concentrations (Table 1). FI_{max} thereby represents the average FI of all cells at time point 60 min (see Materials and Methods). As seen in earlier publications [23,36], we verified that even the highest bacitracin concentrations used had no negative effects on cell growth, thereby ruling out the risk of affecting gene expression (Figure S1). In addition, we performed control experiments using a promoter-less GFP mutant to ensure that the observed increase in fluorescence is

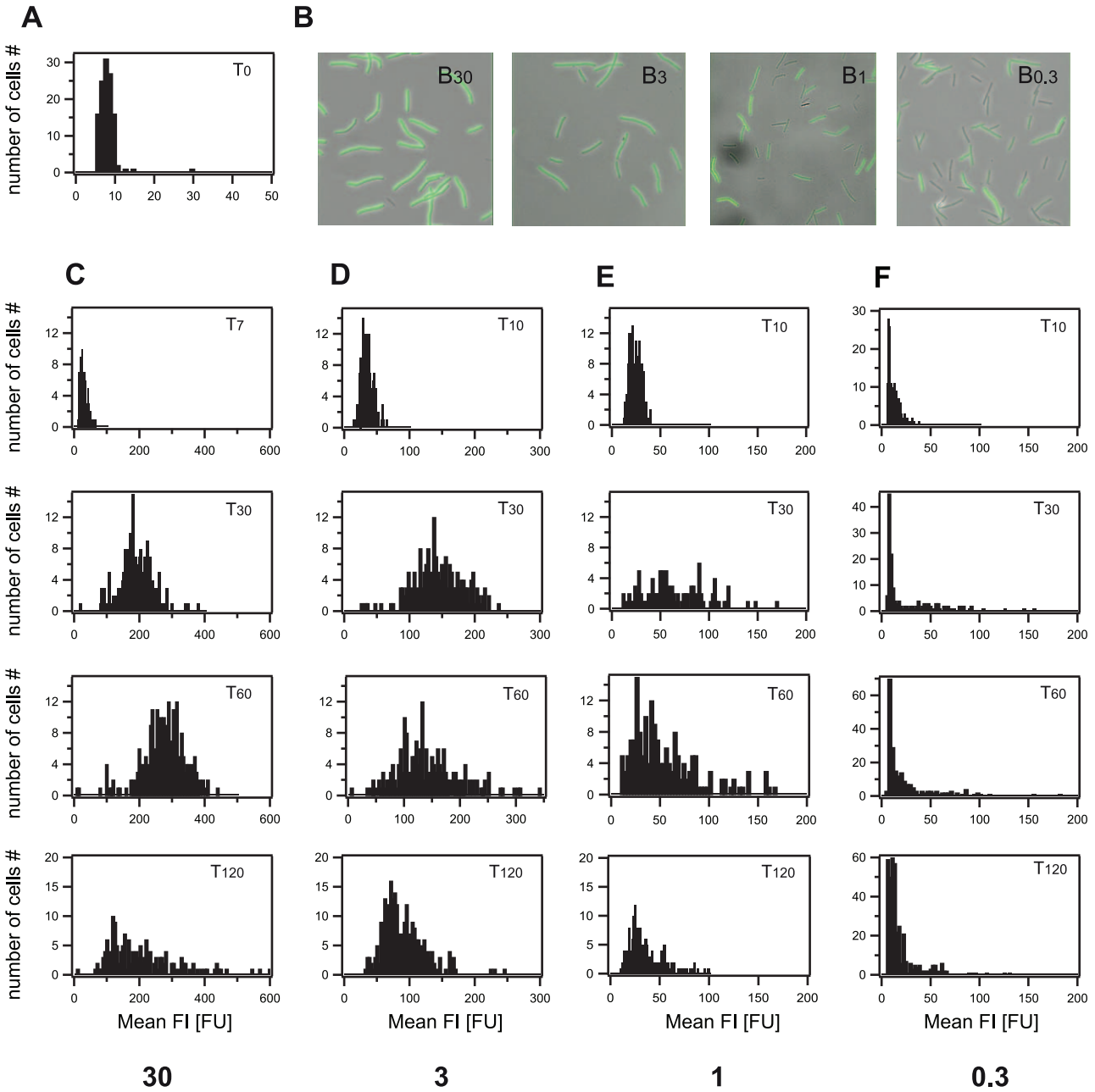

Figure 2. Expression profiles of the P_{lial} response in dependence of the bacitracin concentration. Addition of bacitracin induced GFP expression. At T_{60} all cells reached their maximum fluorescence intensities. While at high bacitracin concentrations all cells shifted to high fluorescence values, at low bacitracin concentrations (1 and 0.3 μg/ml) a fraction of cells did not express GFP. The observed decrease of fluorescence intensities after T_{60} is attributed to ongoing cell division. A) Autofluorescence (~8 FU) of *Bacillus subtilis* cells recorded shortly before bacitracin addition at T_0. B) Representative images of *B. subtilis* cells 60 min after bacitracin induction. Bacitracin concentration is given in the right upper corner of each image in μg/ml. C)–F) Histograms of GFP expression from the *lial* promoter for different time points, at C) 30 μg/ml bacitracin ($T_7 = 7$ min after bacitracin induction), D) 3 μg/ml bacitracin, E) 1 μg/ml bacitracin, and F) 0.3 μg/ml bacitracin.
doi:10.1371/journal.pone.0053457.g002

due to bacitracin induction. As expected no GFP expression could be detected in the promoter-less mutant (data not shown).

The general response of P_{liaI} was similar for all bacitracin concentrations (Figure 2C–F). First, the whole cell population responded within less than 10 min as at T_{10} a clear shift to higher fluorescence values was observable. Only at very low bacitracin concentrations (0.1 μg/ml) hardly any fluorescence could be detected within the 120 min observation period, as cells stayed at $FI_{auto} = 8 \pm 1$ FU (Figure S2). Second, FI_{max} was reached within 60 min. Third, after 60 min fluorescence levels decreased again probably due to ongoing cell division. Taken together our data demonstrate that the LiaFSR system exhibits a graded and fast response to the external stimulus bacitracin: The FI_{max} as obtained after 60 min of induction increased with the stimulus concentration. In addition, cells started expression of the fluorescent protein even at low inducer concentrations within less than 10 min, in contrast to other systems such as e.g. the arabinose utilization

Table 1. Quantitative Analysis of the LiaFSR response.

Bacitracin [μg/ml]	FI_{max} [FU]	f_{ONmax} [%]	P_{fONmax} [%/min]	$t(P_{fONmax})$ [min]	$FI_{basalmax}$ [FU]	Pa_{max} [FU/min]	$t(Pa_{max})$ [min]
30	272±2	99±0.2	10.6±1.1	11.3±1.3	NA	NA	NA
3	139±4	100±0	19.5±13.8	10.6±1.9	NA	NA	NA
1	44±4	78±2.4	9.7±2.9	14.2±1.1	21.6±0.7	2.3±0.4	8.0±0.35
0.3	26±2	26±2	3.9±2.6	14.3±1.5	11.9±0.4	0.3±0. 3	6.2±1.3
0.1	8±1	2.3±0.1	NA	NA	NA	NA	NA

FI_{max} = average maximal fluorescence intensity at T_{60}, f_{ONmax} = maximal fraction of cells in the 'ON' state, p_{fONmax} = maximal switching rate, $t_{(pfONmax)}$ = time point of maximal switching, $FI_{basalmax}$ = average maximal basal fluorescence intensity, Pa_{max} = maximal expression rate, $t_{(Pamax)}$ = time point of maximal expression rate.
doi:10.1371/journal.pone.0053457.t001

system where for low inducer concentrations cells responded only 20 min after induction [40].

Heterogeneity in gene expression is established at low bacitracin concentrations

As we had observed that FI_{max} decreased with lower bacitracin concentrations, the question arose whether this was due to general lower fluorescence intensities in all cells at T_{60} or due to a heterogeneous GFP expression in the population at low inducer concentrations, with only a fraction of cells expressing GFP at high levels. While for high bacitracin concentrations (30 and 3 μg/ml) all cells switched from FI_{auto} to FI_{max} by 60 min post-induction, this could not be observed at low bacitracin concentrations (1 and 0.3 μg/ml). Here, parts of the population were not induced by bacitracin, as indicated by fluorescence levels in the range of the autofluorescence. Therefore, a clear heterogeneity in gene expression levels was present at 60 min after bacitracin induction at low antibiotic concentrations (Figure 2B). Interestingly, no bimodality was observed at any time point for low bacitracin concentrations, as FI levels of cells expressing GFP ranged continuously from FI_{auto} to high FI values, making it difficult to separate the non-induced cells from cells with induced GFP expression corresponding to higher GFP levels. Therefore, we defined the switching threshold from the non-induced 'OFF' state to the induced 'ON' state in the following way: At high bacitracin induction all cells switched into the induced "ON" state. Although FI_{max} was not reached until T_{60}, all cells had clearly shifted away from the autofluoresce level FI_{auto} at T_7 (30 μg/ml bacitracin) and T_{10} (3 μg/ml bacitracin). We used these intermediate states as seen in experiments with high inducer concentrations (30 and 3 μg/ml bacitracin) to determine the switching threshold by applying a Gaussian fit to the histograms shown in Figure 3 (see Material and Methods, Table S1). This resulted in a switching threshold of 30 FU: cells showing expression levels above 30 FU (= three-fold above background) were considered as being in the 'ON' state. This threshold definition best reflected the observed fluorescence expression distributions (Figure 2C–F). Subsequently, we determined the fraction of cells in the 'ON' state as a function of time ($f_{ON}(T)$) (see Materials and Methods), which was well described by a sigmoid function (Figure 4 left, Table 1, Table S2). Around 20 min after bacitracin induction, the fraction of cells in the 'ON' state saturated at f_{ONmax}, ranging from 100% for high bacitracin concentrations to 2.3% for very low (0.1 μg/ml) antibiotic concentrations (Figure 4 left, Table 1, Figure S2). After these 20 min no further increase of the fraction of cells in the 'ON' state could be detected. The observed decrease of fluorescence intensities, and with it the fraction of cells in the 'ON' state, seen for low bacitracin concentrations (1 and 0.3 μg/ml), can be attributed to ongoing cell division. Our data show that the number of cells switching into the 'ON' state is dependent on the external antibiotic concentration and reaches a saturating level at 3 μg/ml bacitracin. Above this concentration all cells enter the 'ON' state.

Switching into the 'ON' state occurs within 20 min

We next investigated the time needed by the whole population to switch into the 'ON' state by analyzing the switching rate (Materials and Methods). We determined the switching rate (P_{fON}) as the first derivative of the fraction of cells in the 'ON' state with respect to time (Figure 4, right), which was well described by a Gaussian function (Material and Methods, Table S3). Maximal switching into the 'ON' state was observed at about 11 min for 3 and 30 μg/ml bacitracin and about 14 min for 1 and 0.3 μg/ml bacitracin. One possible explanation for this observation is heterogeneous timing [36]. Here, the time point of switching for individual cells is distributed over a longer time period. As the fraction of cells in the 'ON' state saturated 20 min after bacitracin induction, even for low bacitracin concentrations, and no further increase of the fraction of cells in the "ON" state could be observed thereafter, we find this explanation unlikely. Instead, we assume that cells still responding at low antibiotic concentrations need more time to do so (Figure 4 left, Table S4). The maximal switching rate (P_{fONmax}) was about 10 to 20%/min for high bacitracin concentrations (Table 1, Table S5), and was significantly reduced at 0.3 μg/ml bacitracin with about 4%/min. Therefore, the small number of cells entering the 'ON' state at this bacitracin concentration can be ascribed to the reduced switching rate.

Independent on the bacitracin concentration added, switching into the 'ON' state started approximately five minutes after bacitracin induction, ending 20 min later. This indicates the presence of a well-defined switching window of about 20 min in which cells can enter the 'ON' state. As soon as bacitracin, or any damage caused by it, is sensed by the LiaFSR system, cells start to switch into the 'ON' state. The shut-down of the LiaFSR response can be understand in the context of the complete bacitracin stress response network that the Lia system is embedded in: several TCS are present in *B. subtilis* [19] that sense the antibiotic bacitracin leading to the activation of bacitracin detoxification systems that remove the antibiotic from its site of action [19,32]. This in turn lowers the inducing stress that is sensed by the LiaFSR system, resulting in the observed 'switch-off' at about 20 min. Although, the fraction of cells in the 'ON' state does not increase any further 20 min after bacitracin induction, an increase in fluorescence intensities can be observed until T_{60}. We attribute this to the stability of the GFP-mRNA: as long as GFP-mRNA is present, translation can occur, resulting in the obtained increase in fluorescence intensity.

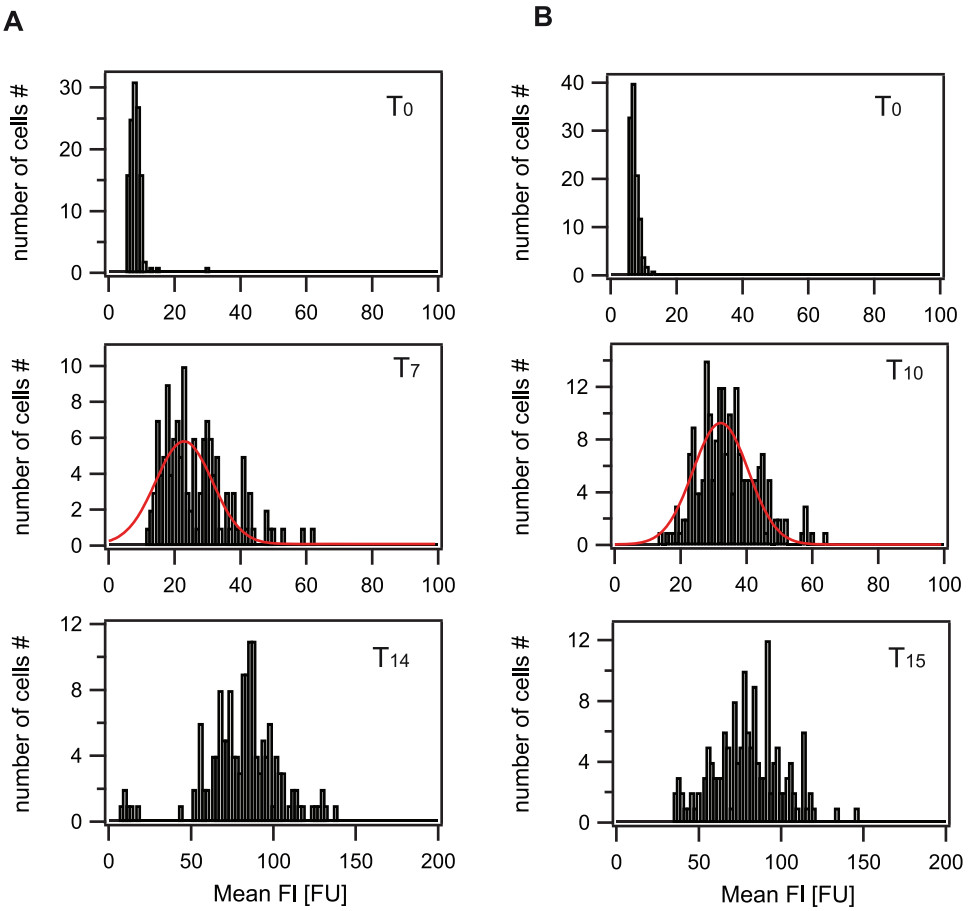

Figure 3. Definition of the switching threshold. Histograms of GFP fluorescence intensity at various time points. A) 30 µg/ml bacitracin, B) 3 µg/ml bacitracin. T_0: time point of bacitracin induction representing the autofluorescence with ~8 FU. T_7 and T_{10}: Time points 7 and 10 min after bacitracin induction representing the phase at which cells are switching into the 'ON' state. At T_{14} and T_{15} (14 and 15 min after bacitracin induction) all cells have switched and the fluorescence distribution is clearly shifted towards higher fluorescence values. T_7 and T_{10} therefore represent intermediate switching states and have therefore been used to determine the switching threshold as described in the Materials and Methods section. Red line: Gaussian fit. For details on the fit parameters see Table S1.
doi:10.1371/journal.pone.0053457.g003

Basal expression rate of P_{liaI} is dependent on bacitracin concentration

We observed that the maximal switching rate P_{fONmax} was reduced at 0.3 µg/ml bacitracin as compared to higher bacitracin concentrations and was reached at later time points. This raised the question whether the smaller switching rate at low bacitracin concentrations was due to a reduced P_{liaI} promoter activity. We addressed this question by analyzing the basal expression rate (Pa). As GFPmut1 and LiaI represent two different proteins, it is possible that GFPmut1 and LiaI have different proteolysis rates. Therefore, the concentration of GFPmut1 controlled by P_{liaI} is not necessarily a direct measure for the concentration of LiaI. However, the expression rates, i.e. the production rate of LiaI and GFPmut1, are expected to be similar, as the complete native P_{liaI} including all native signals for LiaI expression is present.

As a first step, we selected the cells that had not switched into the 'ON' state, as present in experiments with 1 and 0.3 µg/ml bacitracin. The average basal fluorescence value of cells that had not switched (FI_{basal}) shifted to higher values with time, saturating at the maximal basal fluorescence value $FI_{basalmax}$. This increase of fluorescence values of not-induced cells could be well described by a sigmoid fit function FI(T) (Table S6), similar to the fraction of cells in the 'ON' state. However, FI(T) was shifted towards earlier times as compared with $f_{ON}(T)$, indicating that the basal expression rate Pa had a maximum and that the maximum expression rate was shifted to earlier times as compared with the maximum switching rate P_{fON}. The maximal fluorescence values of not-induced cells as obtained at 20 min after bacitracin induction showed significantly higher values as compared to the autofluorescence (Figure 5 A,C), with about 22 and 12 FU for 1 and 0.3 µg/ml bacitracin, respectively (Table 1).

We determined the basal expression rate Pa as the first derivative with respect to time of the mean grey value of those cells that had not entered the 'ON' state (Figure 5 B and D), which was well described by a Gaussian function (Table S7). The maximum basal expression rate, Pa_{max} (Material and Methods), at 1 µg/ml was 2.3±0.4 FU/min exceeding the value of 0.3±0.3 FU/min at 0.3 µg/ml bacitracin by a factor of eight (Table S8). This indicated that the graded response of the LiaFSR system was merely due to a decreased basal expression rate at low bacitracin concentrations. As the maximal basal expression rate was reached at about 7 min at 1 and 0.3 µg/ml bacitracin as compared to the maximal switching rate at about 14 min (Table 1, Table S9), switching into the 'ON' state can be attributed to the increase of the basal expression rate at these bacitracin concentrations. As the basal expression rate is reduced again to zero

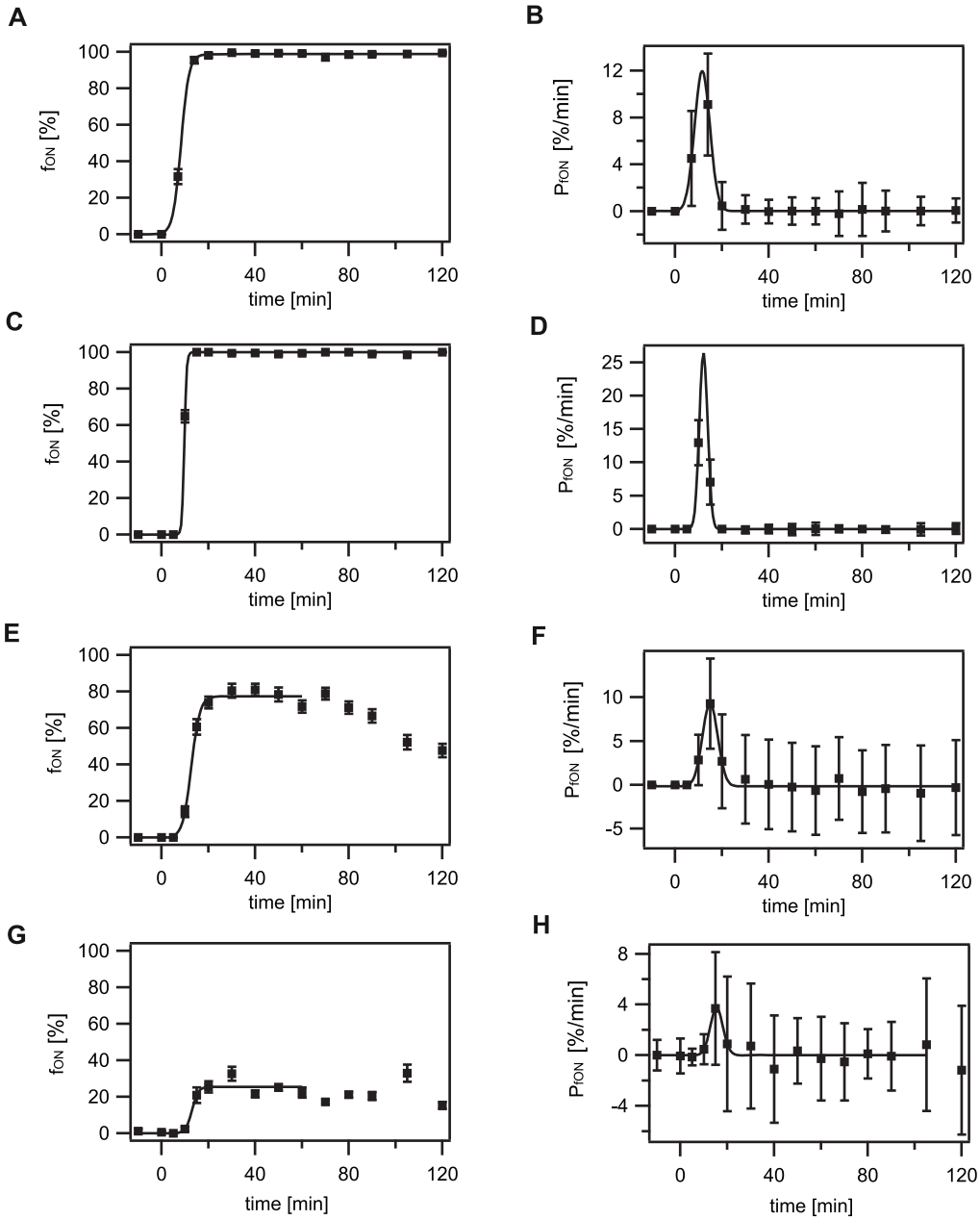

Figure 4. Fraction of cells in the 'ON' state as a function of time ($f_{ON}(T)$) and switching rate (P_{fON}). For definition of the switching threshold see description in the Materials and Method section. The fraction of cells in the 'ON' state (f_{ON}) increased with time, finally saturating at its maximal level. The maximal fraction of cells in the 'ON' state (f_{ONmax}) decreased with the bacitracin concentration. Similarly, the maximal switching rate (P_{fONmax}) decreased at low bacitracin concentrations (e.g. 0.3 μg/ml). A, C, E, G) Fraction of cells in the 'ON' state as a function of time (f_{ON}). Solid line: best fit to a sigmoid function as previously described in [33] (Table S2). B, D, F, H) Switching rate (P_{fON}). The switching rate was determined as the first derivative with respect to time of the fraction of cells in the 'ON' state. Solid line: best fit to a Gaussian function (Table S3). A and B: 30 μg/ml bacitracin; C and D: 3 μg/ml bacitracin; E and F: 1 μg/ml bacitracin, G and H: 0.3 μg/ml bacitracin.
doi:10.1371/journal.pone.0053457.g004

approximately 15–20 min after bacitracin induction, the duration of the switching window is well defined. The time delay between Pa_{max} and P_{fONmax} of about 6 to 8 min (Figure 5 E, F) is in the range of the maturation time of the used fluorescent protein GFPmut1 with 8 min (Figure S3, Table S10), demonstrating the immediate response of the LiaFSR system to the antibiotic bacitracin.

Switching initiation is similar for individual cells

So far, we have quantitatively analyzed the P_{liaI} response of the whole bacterial population grown in stirred liquid cultures as given by the averaged values of the single cells. In order to study the switching behavior of individual cells we developed a new protocol for fluorescent time-lapse microscopy of exponentially growing *B. subtilis* cells. Bacteria were fixed via attachment to microfluidic chambers coated with a specific silane (Materials and Methods) and flushed with fresh medium including the antibiotic bacitracin.

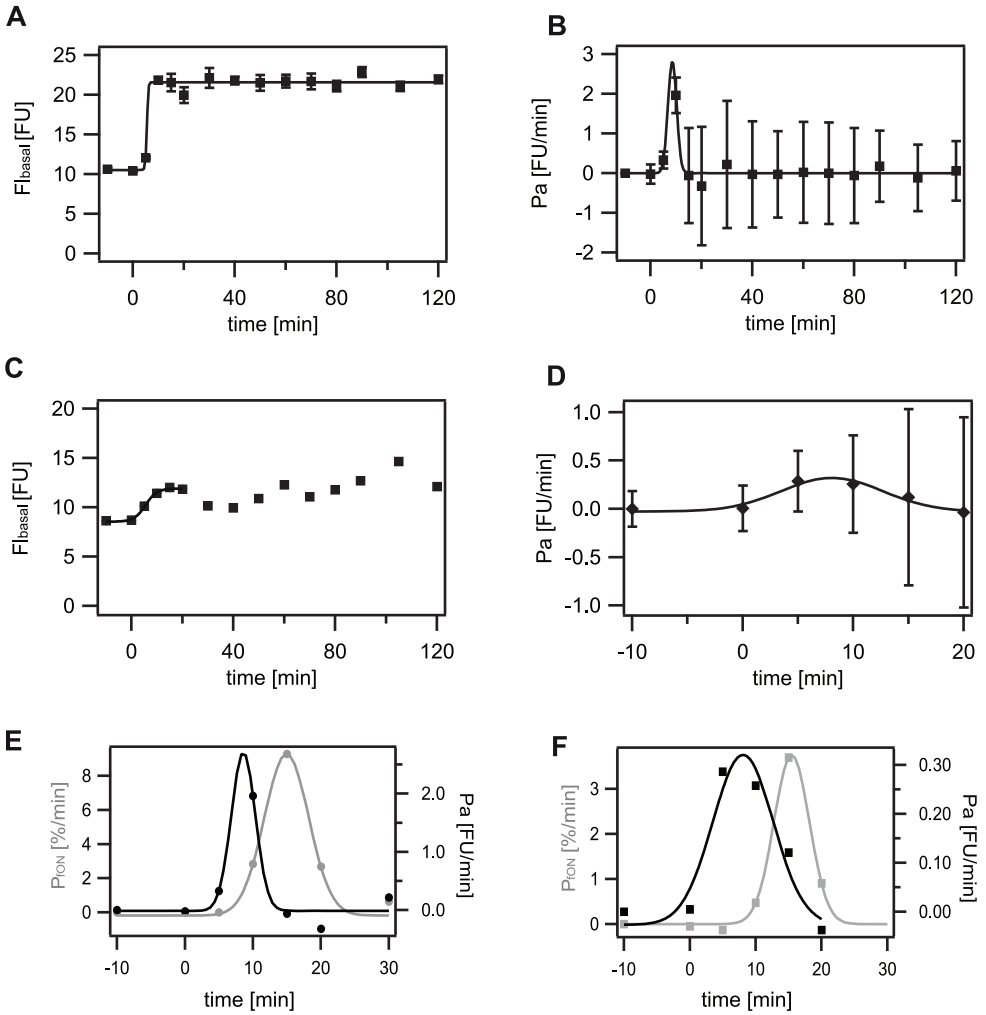

Figure 5. Basal expression rate (Pa) of P_{lial} at 1 and 0.3 μg/ml bacitracin. The average fluorescence intensities (Fl_{basal}) of cells in the 'OFF' state increased with time, saturating shortly thereafter. This enabled us to determine the basal expression rate (Pa) as described in the Material and Methods section. The maximal basal fluorescence intensity decreased with lower bacitracin concentrations. Similarly, the basal expression rate was significantly reduced in experiments with 0.3 μg/ml bacitracin as compared to 1 μg/ml bacitracin. A) and C) Fluorescence development of cells being in the 'OFF' state (Fl_{basal}). Solid line: best fit to a sigmoid function (Table S6). B) and D) Expression rate of P_{lial} as the first derivative of fluorescence development given in A) and C). Solid line: best fit to a Gaussian function (Table S7). A) and B): 1 μg/ml bacitracin, C) and D) 0.3 μg/ml bacitracin. E) and F) comparison of switching rate P_{fON} (grey) and basal expression rate Pa (black). E) 1 μg/ml bacitracin. F) 0.3 μg/ml bacitracin.
doi:10.1371/journal.pone.0053457.g005

As bleaching of the GFPmut1 molecules in single cells was significant, we corrected the obtained fluorescent values as described in the Materials and Methods section. Since the GFP expression levels for low bacitracin concentrations were in the range of the bleaching, we were only able to monitor the switching behavior of individual cells over time at 30 μg/ml bacitracin. Analyzing bleach-corrected fluorescence values (Material and Methods), we observed that cells started switching at about five minutes after bacitracin induction and all cells had switched into the 'ON' state within 15 min, as seen in experiments performed in liquid cultures. As expected, individual cells reached fluorescence values at 60 min post-induction between 200 and 600 FU (Figure 6). But in contrast to the experiments of whole populations described above, FI values increased until 80 min (200–800 FU) indicating that cell division was reduced for cells grown directly on the microscopic slide rather than in flask cultures. Nevertheless, the same overall switching behavior could be observed for individual cells growing in the microfluidic chamber as compared to cells grown in liquid culture, demonstrating the suitability of this approach. In a next step we compared the individual switching curves by applying a sigmoid function to the fluorescence development of single cells over time. This study revealed that cells initiated switching into the 'ON' state within the same time frame, but the individual switching curves showed a high variation with individual switching rates ranging from 6–15 FU/min (Figure 6). In accordance with our findings of whole population studies, our single cell data obtained by time-lapse microscopy demonstrate the fast response of the LiaFSR system to bacitracin.

Discussion

In this report, we quantitatively investigated the response of the LiaFSR system to an external signal, the peptide-antibiotic bacitracin, by performing a population study analyzed on the single cell level. Quantitative fluorescence microscopy (QFM) as described in this study, has been used previously to analyze switching of *Bacillus subtilis* into the competent state [33]. In this

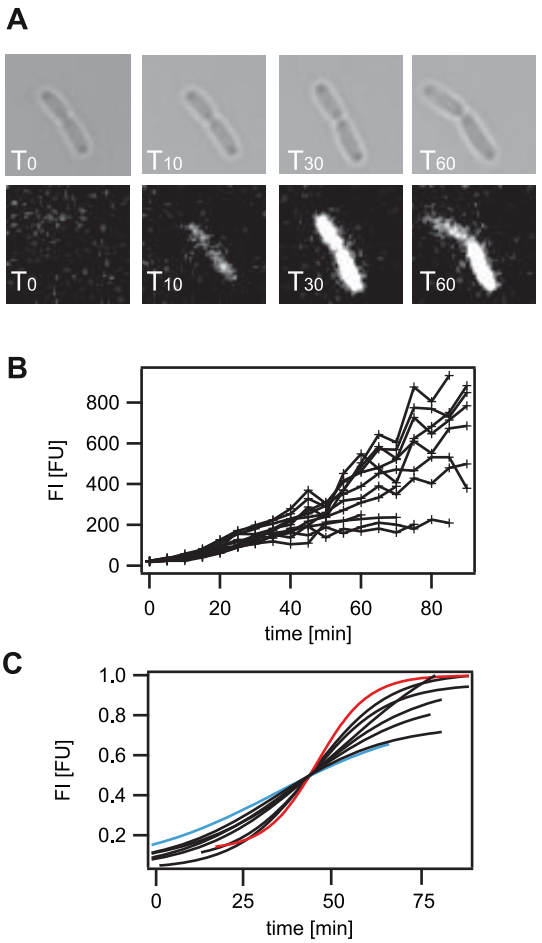

Figure 6. Switching characteristics of single cells at 30 μg/ml bacitracin. Fluorescence development of single cells over time at 30 μg/ml bacitracin was comparable to the data obtained by single cell analysis of the above described population study: All cells switched into the induced 'ON' state, exceeding the threshold fluorescence intensity within 15 min. In contrast to the whole population study the maximal fluorescence intensity was reached only after 80 min. A) Fluorescence development of one individual cell is shown. Top: bright field images at different time points. Bottom: fluorescence images at different time points. B) Fluorescence development of 13 individual cells is shown. C) Sigmoidal fits have been applied to eight fluorescence intensity traces in Figure 6B. The fluorescence intensity was normalized to the maximum fluorescence intensity and the time axis was shifted to T_{45}, where cells had half-maximum fluorescence intensity. Blue and red line: two individual fluorescence traces representing cells with the slowest and highest individual switching rates in this cell batch.
doi:10.1371/journal.pone.0053457.g006

particular case it was shown that the sensitivity of this approach is high enough to detect an increase of promoter activity by a factor of two. This result was confirmed independently, using fluorescence in situ hybridization (FISH), demonstrating the usability of quantitative fluorescence microscopy [41]. Another quantitative method to analyze single cells is flow cytometry. We performed flow cytometry experiments in order to study the LiaFSR response to various bacitracin concentrations (Figure S4), confirming our results obtained by QFM. Fluorescence values of single cells obtained by flow cytometry for low bacitracin concentrations were difficult to separate from the buffer background even after applying gating procedures. Therefore, we chose to focus on quantitative fluorescence microcopy to analyze our data in order to obtain the complete information of the LiaFSR response for high and low bacitracin concentrations.

We observed an immediate response of the system with cells switching in the bacitracin-induced 'ON' state within 20 min, irrespective of the externally provided bacitracin concentration. The switching rate shows its maximum approximately 7 min after the maximum of the basal expression rate. Importantly, this response time is in the range of the maturation time of the green fluorescent reporter with 8 min [42], indicating an almost instant burst of LiaR-dependent transcription initiation at P_{liaI}. This is in contrast to other studies, in which maximum RR-regulated mRNA concentrations [1] or the concentration of promoter-bound RR [10] could be detected only within 20–30 min after exposure to the externally provided signal. Functional characterization of all two-component signal transduction systems in *E. coli* revealed a wide span in auto-phosphorylation rates of the HK ranging from about 2 min to 10 min. Phospo-transfer to RRs by phosphorylated cognate HKs took place within less than ½ min [9]. As maximal switching into the 'ON' state of the LiaFSR system can be observed within 15 min after bacitracin addition, even at the lowest bacitracin concentration, this demonstrates that no further regulatory elements are involved in the bacitracin-dependent LiaFSR response. This is in line with our finding that the basal expression rate of the *liaI* promoter is dependent on the bacitracin concentration, indicating that the LiaR concentration is directly affecting gene expression from P_{liaI}. Recently, it was found that even at very high bacitracin concentrations (50 μg/ml) only about 20 molecules of LiaR are present within a single cell [43], while in the absence of bacitracin LiaR was not detectable. The amount of available LiaR controlling expression from P_{liaI} is therefore dependent on the bacitracin concentration. The low number of LiaR molecules can explain the observed variations in gene expression, in particular the heterogeneity present at low bacitracin concentrations, as cell-to-cell differences (noise [31]) in the exact number of LiaR directly affect gene expression from P_{liaI}.

Performing a population study analyzed at the single cell level, in combination with time-lapse microscopy, we quantitatively analyzed the response of the LiaFSR two-component system to bacitracin. As described above, the LiaFSR system responds within less than 15 min to the external stimulus. Cell-to-cell differences are present at all bacitracin concentrations and decrease at low bacitracin levels. The maximum switching rate as well as basal expression rate depends on the bacitracin concentration, reflecting the graded response of the LiaFSR system. For a stress sensor system, this kind of response is reasonable. Changing environmental conditions, including the presence of stressors, require fast stress sensing systems such as the LiaFSR system, that are shut-off as soon as the stressor is no longer present. Taken together, our data demonstrate that the LiaFSR system exhibits an immediate, heterogeneous and graded response to the peptide antibiotic bacitracin in the exponential growth phase.

Materials and Methods

Growth conditions

Bacillus subtilis strain TMB 1172 [35] carries a translational fusion of P_{liaI} with the green fluorescent reporter protein GFPmut1. TMB 1172 was grown in LB medium at 37°C, shaken at 300 rpm. Overnight cultures were diluted to OD_{600} of 0.1. Cells were grown to mid-logarithmic phase, then were again diluted to OD_{600} of 0.1 into fresh medium and grown for additional 30 min to ensure optimal growth conditions before induction with the peptide-antibiotic bacitracin (Sigma) at $T_0 = 30$ min and applying

the cells to the microscopic slides. This way any cross-over from intrinsic stationary phase induction [35] could be avoided. Experiments for each bacitracin concentration were performed in triplicates on three different days. For each time point a minimum of 100 cells was analyzed. The bacitracin concentrations used in this study are far below the minimal inhibitory concentration (MIC) [23,36] and have been shown to have no effect on growth (Figure S1).

Construction of promoter-less-gfp mutant strain

The promoter less vector pGFPamy [44] was transformed into *B. subtilis* as a negative control. The vector carries a chloramphenicol resistance cassette for selection in *B. subtilis*, and integrates into the *amyE* locus by double crossing-over, resulting in a stable integration of the promoter-less-gfp fusion. The plasmid was linearized with PstI and used to transform *B. subtilis* 168 with chloramphenicol selection (5 μg/ml). Successful integration into the *amyE* locus was confirmed by starch test.

Flow cytometry

For flow cytometry experiments, the cultures were grown as described above. Samples were taken every 10 min for 120 min and diluted 1:100 in PBS (phosphate buffered saline). The experiments were performed using a Partec CyFlow Space instrument and the software FlowMax. GFP was excited with a laser at 488 nm and its emission measured at 518 nm. The analysis of the cells was done at a flow-rate of 2 μl/s. In between measurements, the instrument was rinsed with PBS to eliminate cross-contamination. In addition to the different concentrations of bacitracin, not induced samples and PBS alone were analyzed for control purposes. To discriminate dead from healthy cells, appropriate gating procedures have been applied. 50000 cells lying in the appropriate gate have been analyzed for each time point.

Fluorescence Microscopy

Cells were sampled throughout growth as indicated in the main text. For image acquisition of the whole cell population, cells were permitted to attach to microscopic slides (eight-well IBIDI chamber, uncoated) and covered with 1% Agarose-patches.

For time-series of single cells, cells were allowed to attach to microfluidic chambers coated with 100% 1-[3-(Trimethoxysilyl)-propyl]urea (Sigma). Cells were induced already attached to the microfluidic channels and washed with fresh medium in the presence of bacitracin at a flow-rate of 0.3 ml/h.

Image acquisition was done using a Zeiss Axiovert 200 M microscope equipped with an Andor Digital Camera and a Zeiss EC Plan-Neofluar 100×/1.3 Oil immersion objective. Andor software was used for image acquisition. The stability of the absolute fluorescence values was verified using a microscope image intensity calibration kit (Invitrogen, FokalCheck^{TM} fluorescence microscope test slide #3). Microspheres showed a deviation of mean grey value of less than 1% under the experimental conditions used for detection of GFP fluorescence. Homogeneity of illumination was tested using fluorescent slides and the maximum deviation was less than 5%.

Image Analysis

Images were processed using ImageJ software. Image background was corrected using a rolling ball algorithm with a radius of 50. An intensity threshold tool was used to delimit the boundaries of the cells in the bright field image. The boundaries of the cells were obtained with the wand tool of the ImageJ software and transferred to the fluorescence image using the ROI manager of ImageJ. Only cells that were fully lying within the bright field image and were not in the process of cell division were considered. Furthermore, dead cells as observable by different contrast in the bright field image as compared to healthy cells were excluded from the single cell analysis. The remaining single cells were than analyzed with respect to their mean grey value. Data preparation was performed using the Software IGOR PRO 4.06 and Adobe Illustrator CS4.

Definitions and calculation methods

FI_{auto}: average autofluorescence/fluorescence intensity of cells not induced by bacitracin, given as fluorescence units [FU] as obtained by the mean grey value. The average autofluorescence level of cells prior bacitracin induction was $FI_{auto} = 8 \pm 1$ FU (Figure 2A).

FI_{max}: average maximal GFP expression/fluorescence intensity as observed at T_{60}. Upon induction with bacitracin cells expressed the GFP reporter. The resulting fluorescence intensities were obtained as the mean grey value of each single cell. The error of FI_{max} is given as the standard error.

Switching threshold: The switching threshold separates cells being in the 'OFF' state (no/basal expression) from cells being in the 'ON' state (induced GFP-expression). We used the intermediate states seen in experiments with high inducer concentrations (30 and 3 μg/ml bacitracin) to determine the switching threshold. A Gaussian fit was applied to the histograms shown in Figure 3 (Table S1). The values of the center of these distributions, in addition to the average fluorescence values of all cells at this time point, were averaged. The resulting value of 30 FU was then defined to be the switching threshold: any cell with fluorescent value above 30 FU (mean grey value) was considered as being in the 'ON' state.

f_{ON}: fraction of cells in the 'ON' state. We determined the fraction of cells in the 'ON' state as a function of time using the switching threshold. The fraction of cells in the 'ON' state was well defined by a sigmoid function with $f_{ON}(T) = f_{base} + f_{max}/1 + \exp(k(T_{half} - T))$. The fit parameter of this function can be found in Table S2. The maximal fraction of cells in the 'ON' state (f_{ONmax}) was determined using this fit function (Table S2). The error of the fraction of cells in the 'ON' state has been calculated according to: square root of $(p(1-p)/(n-1))$.

P_{fON}: average switching rate of cells switching into the 'ON' state. The switching rate was determined as the first derivative of the fraction of cells in the 'ON' state with respect to time. To reduce the error, the maximal switching rate (P_{fONmax}) was determined using two different calculation methods: a) P_{fonmax} = maximum of the 1st derivative of the exact data points of f_{ON}. b) by obtaining A of the Gaussian fit applied to the data Figure 4 right according to $P_{fON} = y_0 + A\exp(-((x-x_0)/\text{width})^2)$ (Table S5). The high error for data determined at 3 μg/ml bacitracin is attributed to the steep increase of the fraction of cells in the 'ON' state leading to a high fitting error. Additional data points in order to reduce the error could not be attained, as cells stored on ice for later image acquisition tended to lyse at bacitracin concentrations >1 μg/ml. Therefore image acquisition was performed immediately after sampling of the cells. The exact results of both calculation methods as well as the average values are given in Table S5. The error of the switching rate was calculated according to: Error P_{fON} at time point t_2 = square root of $((\text{error at } (t_2))^2 + (\text{error at } (t_1))^2)$, with t_1 and t_2 the time points of the derivated time interval. The individual errors here are the errors of f_{ON} as described above. Please note that error propagation has to be

taken into account when deriving data points, leading to the high errors in Figure 4, F and H.

$t(P_{fONmax})$: Time point of maximal switching rate. To reduce the error the time point of the maximal switching rate has been determined in three different ways: a) T_{half} of the sigmoidal fit applied to Figure 4 left according to $f_{ON}(T) = f_{base}+f_{max}/1+exp(k(T_{half}-T))$. b) Time point of P_{fONmax} = maximum of the 1st derivative of the exact data points of f_{ON}. c) by obtaining x_0 of the Gaussian fit applied to the data in Figure 4 right according to $P_{fON}(T) = y_0+A \exp(-((x-x_0)/width)^2)$ (Table S4).

FI_{basal}: average basal fluorescence intensity of cells in the 'OFF' state. The error is given as the standard error.

$FI_{basalmax}$: maximal average basal fluorescence intensity as obtained by applying a sigmoidal fit function $FI(T) = f_{base}+f_{max}/1+exp(k(T_{half}-T))$, with f_{base} baseline, f_{max} maximum basal fluorescence intensity, T_{half} half time and *k* rate (Table S6).

Pa: average basal expression rate of cells in the non-induced 'OFF' state. We determined the Pa as the first derivative with respect to time of the mean grey value of those cells that had not entered the 'ON' state. To reduce the error the maximal basal expression rate (Pa_{max}) has been determined in two different ways: a) Pa = maximum of the 1st derivative of the exact data points of FI_{basal}. b) by obtaining x_0 of the Gaussian fit applied to Figure 5 B, D according to $Pa(T) = y_0+Aexp(-((x-x_0)/width)^2)$ (Table S8). The error of the basal expression rate was calculated according to: Error Pa at time point t_2 = square root of $((error\ at\ (t_2))^2+(error\ at\ (t_1))^2)$, with t_1 and t_2 the time points of the derivated time interval. The individual errors here are the errors of FI_{basal} as described above. Please note that error propagation has to be taken into account when deriving data points, leading to the high errors in Figure 5 B and D.

$t(Pa_{max})$: The time point of the maximal basal expression rate has been determined in three different ways: a) T_{half} of the sigmoidal fit applied to Figure 5 A, C according to $FI(T) = f_{base}+f_{max}/1+exp(k(T_{half}-T))$ (Table S9). b) Pa_{max} = maximum of the 1st derivative of the exact data points of FI_{basal}. c) by obtaining x_0 of the Gaussian fit applied to Figure 5 right according to $Pa(T) = y_0+Aexp(-((x-x_0)/width)^2)$ (Table S9).

A summery of all data described here, as well as the average data obtained from the different calculation methods for $t(P_{fONmax})$, $t(Pa_{max})$, P_{fONmax} and Pa_{max} can be found in Table 1. The obtained data for each calculation method for $t(P_{fONmax})$, $t(Pa_{max})$, P_{fONmax} and Pa_{max} are given in Figure S5.

Bleach correction of single cell time-series

In time-series of individual cells, bleaching of GFP in these cells occurred. Hence, we applied a bleach correction to our time-series data. After each time-series a new spot was chosen at an appropriate distance to ensure that no bleaching had occurred yet on this spot. Twenty successive images were taken. One image was immediately taken after the previous one. For each cell of this spot the obtained 'bleach curve' was fitted exponentially. The resulting rates were averaged. The data obtained in the actual time-series were then divided by e^{-nk}, with n being the number of pictures already taken of this spot and k the average of the rates determined by the exponential fit of the 'bleach curves'.

GFPmut1 maturation

To determine the time delay between expression of the GFP reporter and the onset of fluorescence, strain TMB 1172 was grown in LB medium as described above. For induction of GFPmut1 expression bacitracin was added after 60 min at a final concentration of 30 μg/ml and erythromycin was added at 80 min, inhibiting protein biosynthesis. Increase of fluorescence after 80 min must therefore be due to folding of already synthesized GFP (Figure S3). Assuming a first-order kinetic we fitted the data with a single exponential function and obtained a characteristic maturation time of 7.9±0.69 min.

Supporting Information

Table S1 Fit parameter for the fluorescence distributions given in Figure 3.
(DOC)

Table S2 Fit parameters for the fraction of cells in the 'ON' state f_{ON}.
(DOC)

Table S3 Fit parameter for the switching rate P_{fON}.
(DOC)

Table S4 Time point of maximal switching rate $t(P_{fONmax})$.
(DOC)

Table S5 Maximal switching rate P_{fONmax}.
(DOC)

Table S6 Fit parameters for the basal fluorescence level FI_{basal}.
(DOC)

Table S7 Fit parameter for the basal expression rate Pa.
(DOC)

Table S8 Maximal basal expression rate Pa_{max}.
(DOC)

Table S9 Time point of maximal basal expression rate $t(Pa_{max})$.
(DOC)

Table S10 Maturation of GFPmut1.
(DOC)

Figure S1 Influence of bacitracin on cell growth. Cells were grown as described in the Material and Methods section in the presence of bacitracin at different final concentrations (Black: 0 μg/ml, grey: 0.1 μg/ml, blue: 0.3 μg/ml, yellow: 1 μg/ml, green: 3 μg/ml, red: 30 μg/ml). At these concentrations bacitracin has no influence on cell growth.
(EPS)

Figure S2 Expression profiles of the Lia response at 0.1 μg/ml bacitracin. At these very low inducing concentration of bacitracin nearly all cells stay in the non-induced 'OFF' state. A) Representative image of *B. subtilis* cells 60 min after bacitracin induction. B) Histograms of GFP expression from the *liaI* promoter for different time points (T_{10} = 10 min after bacitracin induction). Red arrows indicate the few cells in the 'ON' state at this bacitracin concentration.
(EPS)

Figure S3 Maturation of GFPmut1. Arrow indicates the addition of 400 μg/ml erythromycin at 80 min leading to immediate translation inhibition. Therefore any fluorescence development arising after erythromycin addition can be attributed to the maturation of the GFP fluorophore. Grey: cells grown in the absence of erythromycin. Black: Cells grown in the presence of erythromycin. Solid lines: best fit to an exponential function (Table S10).
(EPS)

Figure S4 Flow cytometry analysis of the P_{liaI} response of LiaFSR to bacitracin. Flow cytometry analysis verified the results obtained by quantitative fluorescence microcopy as shown in main Figure 2. Addition of bacitracin induced GFP expression. At T_{60} all cells reached their maximum fluorescence intensities. While at high bacitracin concentrations all cells shifted to high fluorescence values, at low bacitracin concentrations (1 and 0.3 μg/ml) a fraction of cells did not express GFP and stayed at the autofluorescence value. As low fluorescence intensities of induced cells were hard to distinguish from the background fluorescence of not induced cells using flow cytometry, we chose quantitative fluorescence microscopy for detailed analysis of the LiaFSR response. Data shown here represent the mean grey value of each single cell: mean FI [FU]. A) Background signal of the buffer PBS in the gated area. B) Autofluorescence of not induced *Bacillus subtilis* cells C)–F) Histograms of GFP expression from the *liaI* promoter for different time points, at C) 30 μg/ml bacitracin (T_{30} = 30 min after bacitracin induction), D) 3 μg/ml bacitracin, E) 1 μg/ml bacitracin, and F) 0.3 μg/ml bacitracin.
(EPS)

Figure S5 Maximal switching rate P_{fONmax} and maximal basal expression rate Pa_{max} for various bacitracin concentrations. As switching into the 'ON' state took place in a very short time period of less than 10–15 min, only few data points between the 'OFF' and the 'ON' state could be obtained. As cells treated with high bacitracin concentrations, although not showing any fitness defects, tended to lyse when stored on ice, a shorter experimental time resolution was not possible. Therefore, to reduce the error by simply fitting to the data, the maximal switching rate as well as the maximal basal expression rate was determined using several calculation methods as described in the Material and Methods section. This Figure gives an overview of the data obtained by the various methods used. A) Time point of maximum switching rate t(P_{fONmax}); Black, grey and light grey bars represent data obtained as described in Table S4 a–c. Blue: averaged data of the time point of maximal switching. B) Maximal switching rate P_{fONmax}: Black, and light grey bars represent data obtained as described in Table S5 a and b. Blue: averaged data of maximal switching rate P_{fONmax}. C) Time point of maximum basal expression rate t(Pa_{max}); Black, grey and light grey bars represent data obtained as described in Table S9 a–c. Blue: average data of t(Pa_{max}). D) Maximum basal expression rate Pa_{max}; Black and light grey bars represent data as described in Table S8 a and b. Blue: average date of maximal Pa_{max}.
(EPS)

Acknowledgments

We thank Prof. J. O. Rädler for the opportunity to use laboratory equipment, in particular the inverse microscope. We thank Sonja Westermayer, Andrea Ebert and Elke Hebisch for fruitful discussions.

Author Contributions

Conceived and designed the experiments: TM ML. Performed the experiments: CH AM SK. Analyzed the data: SK ML. Wrote the paper: TM ML.

References

1. Kato A, Mitrophanov Y, Groisman EY (2007) A connector of two-component regulatory systems promotes signal amplification and persistence of expression. Proc Natl Acad Sci U S A 104: 12063–12068.
2. Castelli M, Vescvi EG, Soncini FC (2000) The phosphatase activity is the target for Mg^{2+} regulation of the sensor protein PhoQ in *Salmonella*. J Biol Chem 275: 22948–22954.
3. Li M, Wang C, Feng Y, Pan X, Cheng G, et al. (2008) SalK/SalR, a two-component signal transduction system, is essential for full virulence of highly invasive *Streptococcus suis* serotype 2. PloS One 3(5): e2080. Accessed 09 June 2012.
4. Stock A, Robinson VL, Gourdreau PN (2000) Two-component signal transduction. Annu Rev Biochem 69: 183–215.
5. Nagasawa S, Tokishita S, Aiba H, Mizuno T (1997) A novel sensor-regulator protein that belongs to the homologous family of signal transduction proteins involved in adaptive responses in *Escherichia coli*. DNA Res 4:161–168.
6. Fabret C, Feher VA, Hoch JA (1999) Two-component signal transduction in *Bacillus subtilis*: How one organism sees its world. J Bacteriol 181:1975–1983.
7. Pratt LA, Silhavy TJ (1995) in Two-component signal transduction. In: Hoch, JA, Silhavy TJ, editors. Washington, DC: ASM press pp. 105–127.
8. Li J, Swanson RV, Simon MI, Weis RM (1995) The response regulators CheB and CheY exhibit competitive binding to the kinase CheA. Biochemistry 34: 14626–14636.
9. Yamamoto K, Hirao K, Oshima T, Aiba H, Utsumi R, et al. (2005) Functional characterization in vitro of all two-component signal transduction systems from *Escherichia coli*. J Biol Chem 280:1448–1456.
10. Ray JCJ, Igoshin OA (2010) Adaptable functionality of transcriptional feedback in bacterial two-component systems. Plos Comp Biol 6(2): e1000676. Accessed 06 August 2012.
11. Mitrophanov AY, Churchward G, Borodovsky M (2007) Control of *Streptococcus pyogenes* virulence: Modeling of the CovR/S signal transduction system. J Theo Biol 246:113–128.
12. Groban ES, Clarke EJ, Salis HM, Miller SM, Voigt CA (2009) Kinetic buffering of cross talk between bacterial two-component sensors. J Mol Biol 390:380–393.
13. Scharf BE (2010) Summary of useful methods for two-component system research. Curr Opin Microbiol 13:246–252.
14. Hoch JA (1995) Two-component signal transduction. Washington, DC: Am Soc Microbiol. pp. 129–144.
15. Szurmant H, Bu L, Brooks CLIII Hoch JA (2008) An essential sensor histidine kinase controlled by transmembrane helix interactions with its auxiliary proteins. Proc Natl Acad Sci U S A 105: 5891–5896.
16. Elsen S, Duche O, Colbeau A (2003) Interaction between the sensor HupUV and the histidine kinase HupT controls HupSL hydrogenase synthesis in *Rhodobacter capsulatus*. J Bacteriol 185: 7111–7119.
17. De Orue Lucana DO, Groves MR (2009) The three-component signaling system HbpS-SenS-SenR as an example of a redox-sensing pathway in bacteria. Amino Acids 37:479–486.
18. Li M, Lai Y, Villaruz AE, Cha DJ, Sturdevant DE, et al. (2007) Gram-positive three-component antimicrobial peptide-sensing system. Proc Natl Acad Sci U S A 104:9469–9474.
19. Rietkötter E, Hoyer D, Mascher T (2008) Bacitracin sensing in *Bacillus subtilis*. Mol Microbiol 68:768–785.
20. Gebhard S, Mascher T (2011) Antimicrobial peptide sensing and detoxification modules: unraveling the regulatory circuitry of *Staphylocccus aureus*. Mol Micro 81:581–587.
21. Jordan S, Junker A, Helmann JD, Mascher T (2006) Regulation of LiaRS-dependent gene expression in *Bacillus subtilis*: Identification of inhibitor proteins, regulator binding sites, and target genes of a conserved cell envelope stress-sensing two-component system. J Bacteriol 188:5153–5166.
22. Wolf D, Kalamorz F, Wecke T, Juszczak A, Mäder U, et al. (2010) In-depth profiling of the LiaR response of *Bacillus subtilis*. J Bacteriol 192:4680–4693.
23. Mascher T, Zimmer SL, Smith T-A, Helmann JD (2004) Antibiotic-inducible promoter regulated by the cell envelope stress-sensing two-component system LiaRS of *Bacillus subtilis*. AAC 48:2888–2896.
24. Jordan S, Hutchings MI, Mascher T (2008) Cell envelope stress response in Gram-positive bacteria. FEMS Microbiol Rev 32:107–146.
25. Schrecke K, Staron A, Mascher T (2012) Two-Component Signaling in the Gram-positive Envelope Stress Response: Intramembrane-sensing Histidine Kinases and Accessory Membrane Proteins. Two-component Systems in Bacteria. Book: EAN: 9781908230089.
26. Staron A, Finkeisen DE, Mascher T (2011) Peptide antibiotic sensing and detoxification modules of *Bacillus subtilis*. Antimicrob Agents Chemother 55:515–525.
27. Wolf D, Dominguez-Cuevas P, Daniel RA, Mascher T (2012). Cell envelope stress response in cell wall-deficient L-forms of *Bacillus subtilis*. Antimicrob Agents Chemother. DOI:10.1128.
28. Ghosh S, Sureka K, Ghosh B, Bose I, Basu J, et al. (2011) Phenotypic heterogeneity in mycobacterial stringent response. BMC Systems Biology 5:18. Available: http://www.biomedcentral.com/1752-0509/5/18. Accessed 2012 July 9.
29. Botella E, Hübner S, Hokamp K, Hansen A, Bisicchia P, et al. (2011) Cell envelope gene expression in phosphate-limited *Bacillus subtilis* cells. Microbiology 157:2470–2484.
30. Smits WK, Kuipers OP, Veening J-W (2006) Phenotypic variation in bacteria: the role of feedback regulation. Nature Reviews Microbiol 4:259–271.
31. Swain PS, Elowitz MB, Siggia ED (2002) Intrinsic and extrinsic contributions to stochasticity in gene expression. Proc Natl Acad Sci U S A 99:12795–12800.

32. Dubnau D, Losick R (2006) Bistability in bacteria. Mol Microbiol 61:564–572.
33. Leisner M, Stingl K, Rädler JO, Maier B (2007) Basal expression rate of *comK* sets a 'switching-window' into the K-state of *Bacillus subtilis*. Mol Microbiol 63:1806–1816.
34. Leisner M, Kuhr J-T, Rädler JO, Frey E, Maier B. (2009) Kinetics of genetic switching into the state of bacterial competence. Biophys J 96:1178–1188
35. Toymentseva A, Schrecke K, Sharipova MR, Mascher T (2012) The LIKE system, a novel protein expression toolbox for *Bacillus subtilis*, based on the *liaI* promoter. Microbial Cell Factories 2012, 11:143.
36. Mascher T, Margulis NG, Wang T, Rick WY, Helmann JD (2003) Cell wall stress responses in *Bacillus subtilis*: The regulatory network of the bacitracin stimulon. Mol Microbiol 50:1591–1604.
37. Hauser K, Haynes WJ, Kung C, Plattner H, Kissmehl R (2000) Expression of the green fluorescent protein in *Paramecium teraurelia*. Europ J Cell Biol 79:144–149.
38. Li X, Zhao X, Fang Y, Jiang X, Dueng T, et al. (1998) Generation of Destabilized Green Fluorescent Protein as a Transcription Reporter. J Biol Chem 273:34970–34975.
39. Jordan S, Rietkötter E, Strauch MA, Kalamorz F, Butcher BG, et al. (2007) LiaRS-dependent gene expression is embedded in the transition state regulation in *Bacillus subtilis*. Microbiology 153:2530–2540.
40. Megerle J, Fritz G, Gerland U, Jung K, Raedler JO (2008) Timing and dynamics of single cell gene expression in the arabinose utilization system. Biophys J 95:2103–2115.
41. Marmaar H, Raj A, Dubnau D (2007) Noise in Gene Expression Determines Cell Fate in *Bacillus subtilis*. Science 317: 525–529.
42. Izuka R, Yamagishi-Shirasaki M, Funatsu T (2011) Kinetic study of de novo chromophore maturation of fluorescent proteins. Anal Chem 414:173–178.
43. Schrecke K, Jordan S, Mascher T (2012) Stoichometry and Perturbation Studies of the LiaFSR System of *Bacillus subtilis*. Mol Microbiol accepted.
44. Bisicchia P, Botella E, Devine KM (2010) Suite of novel vectors for ectopic insertion of GFP, CFP and IYFP transcriptional fusions in single copy at the *amyE* and *bglS*loci in *Bacillus subtilis*. Plasmid: 10.1016/j.plasmid.2010.06

CHAPTER III

Subcellular localization, interactions and dynamics of the phage-shock protein-like Lia response in *Bacillus subtilis*

Julia Dominguez-Escobar, Diana Wolf, Georg Fritz, **Carolin Höfler**,
Roland Wedlich-Söldner, Thorsten Mascher

Molecular Microbiology **92**: 716-732

Molecular Microbiology (2014) 92(4), 716–732 ■
doi:10.1111/mmi.12586
First published online 15 April 2014

Subcellular localization, interactions and dynamics of the phage-shock protein-like Lia response in *Bacillus subtilis*

Julia Domínguez-Escobar,[1§] Diana Wolf,[2†§] Georg Fritz,[2,3] Carolin Höfler,[2] Roland Wedlich-Söldner[1‡] and Thorsten Mascher[2*]
[1]*Max Planck Institute of Biochemistry, AG Cellular Dynamics and Cell Patterning, Martinsried, Germany.*
[2]*Ludwig-Maximilians-Universität München, Department Biology I, AG Synthetic Microbiology, München, Germany.*
[3]*Ludwig-Maximilians-Universität München, Arnold Sommerfeld Center for Theoretical Physics, München, Germany.*

Summary

The *lialH* operon of *Bacillus subtilis* is the main target of the envelope stress-inducible two-component system LiaRS. Here, we studied the localization, interaction and cellular dynamics of Lia proteins to gain insights into the physiological role of the Lia response. We demonstrate that LialI serves as the membrane anchor for the phage-shock protein A homologue LiaH. Under non-inducing conditions, LialI locates in highly motile membrane-associated foci, while LiaH is dispersed throughout the cytoplasm. Under stress conditions, both proteins are strongly induced and colocalize in numerous distinct static spots at the cytoplasmic membrane. This behaviour is independent of MreB and does also not correlate with the stalling of the cell wall biosynthesis machinery upon antibiotic inhibition. It can be induced by antibiotics that interfere with the membrane-anchored steps of cell wall biosynthesis, while compounds that inhibit the cytoplasmic or extracytoplasmic steps do not trigger this response. Taken together, our data are consistent with a model in which the Lia system scans the cytoplasmic membrane for envelope perturbations. Upon their detection, LiaS activates the cognate response regulator LiaR, which in turn strongly induces the *lialH* operon. Simultaneously, LialI recruits LiaH to the membrane, presumably to protect the envelope and counteract the antibiotic-induced damage.

Accepted 18 March, 2014. *For correspondence. E-mail mascher@bio.lmu.de; Tel. (+49) 89 218074622; Fax (+49) 89 218074626. †Present address: Ruprecht-Karls-University, Center for Molecular Biology Heidelberg, AG Bacterial Signaling Networks, Heidelberg, Germany. ‡Present address: Westfälische Wilhelms-Universität Münster, Institute of Cell Dynamics and Imaging and Cells-in-Motion Cluster of Excellence (EXC 1003 – CiM), Münster, Germany. §These two authors contributed equally to this work.

© 2014 John Wiley & Sons Ltd

Introduction

The bacterial cell envelope, consisting of the cytoplasmic membrane, the cell wall, and – in Gram-negative bacteria – the outer membrane, is the first and major barrier of defence against threats from the environment. Hence, closely monitoring envelope integrity is crucial for survival of a bacterial cell in its natural habitat. Accordingly, complex regulatory networks have evolved in both Gram-negative and Gram-positive bacteria to respond to envelope stress by mounting protective countermeasures. The underlying signal transduction is predominantly mediated by two-component systems and alternative sigma factors of the extracytoplasmic function (ECF) protein family (Raivio, 2005; Jordan *et al.*, 2008; MacRitchie *et al.*, 2008). An additional protective layer is provided by the so-called phage-shock protein (PSP) response, which is centred around homologues of the ubiquitously distributed phage-shock protein A (PspA). Proteins belonging to the PspA/IM30 protein family are found in Gram-negative and Gram-positive bacteria, as well as in archaea and plant chloroplasts (reviewed in Model *et al.*, 1997; Darwin, 2005; Darwin, 2007; Bultema *et al.*, 2010; Joly *et al.*, 2010; Vothknecht *et al.*, 2012; Yamaguchi and Darwin, 2012).

The PSP response has been extensively studied in *Escherichia coli* (Model *et al.*, 1997; Darwin, 2005; Joly *et al.*, 2010). It is induced by filamentous phage infection, high osmolarity, heat shock, secretion stress or changes in lipid biosynthesis as well as in presence of protonophores, like CCCP (Brissette *et al.*, 1990; Bergler *et al.*, 1994; Model *et al.*, 1997; Jones *et al.*, 2003; DeLisa *et al.*, 2004). In *E. coli*, the PSP regulon consists of the *pspABCDE* operon and the separate genes *pspF* and *pspG* (Joly *et al.*, 2010). Transcription of the *psp* genes is initiated in a σ^{54}-dependent manner and controlled by the enhancer PspF. Under non-stress conditions, PspF is inhibited by cytosolic PspA (Elderkin *et al.*, 2002; 2005; Joly *et al.*, 2009). Upon induction, PspA is recruited to the plasma membrane via two transmembrane anchors, PspB and

PspC. This allows PspA to counteract membrane damage and at the same time releases the PspF enhancer from its inhibitory complex, thereby allowing expression of all *psp* genes (Huvet *et al*., 2011). A similar regulatory mechanism has been demonstrated for the PSP response in the closely related pathogenic bacterium *Yersinia enterocolitica* (Maxson and Darwin, 2006; Gueguen *et al*., 2009; 2011; Yamaguchi *et al*., 2010; 2013; Horstman and Darwin, 2012). In summary, data obtained so far indicates that the PSP response is regulated by an intricate set of transient protein interactions centred around PspA, which switches its interaction partners from PspF (non-inducing conditions) to PspB/C (stress conditions).

Despite our detailed molecular understanding of the PSP response, its physiological role is still not well defined. Mutants in *psp* genes often show only mild phenotypes but available data so far points to a function of PspABC in protecting and stabilizing the membrane against leakage and loss of membrane potential (Kobayashi *et al*., 2007; Vrancken *et al*., 2008; Horstman and Darwin, 2012). Moreover, the PSP response also seems to be important for virulence (Karlinsey *et al*., 2010; Yamaguchi and Darwin, 2012) and protein secretion (Jones *et al*., 2003; DeLisa *et al*., 2004; Seo *et al*., 2007; Wang *et al*., 2011; Mehner *et al*., 2012).

The genome of the Gram-positive model organism *Bacillus subtilis* encodes two PspA homologues, termed PspA and LiaH. Despite the clear sequence homology, the underlying regulation is significantly different from the *E. coli/Y. enterocolitica* blueprint (see below). Expression of *pspA* is controlled by the ECF sigma factor σ^W in response to envelope stress, SPP1 phage infection and alkaline shock (Wiegert *et al*., 2001; Hachmann *et al*., 2009; Wenzel *et al*., 2012), but its physiological role has not been determined. In contrast, the Lia response of *B. subtilis* has been intensively studied in the last decade (reviewed in Jordan *et al*., 2008; Schrecke *et al*., 2012).

LiaH is encoded in the *liaIH* operon, which is controlled by the LiaFSR three-component system (Wolf *et al*., 2010). The LiaFSR system is part of the regulatory network orchestrating cell envelope stress response in *B. subtilis* (Mascher *et al*., 2003). It consists of a classical bacterial two-component system, LiaSR, and the LiaSR-specific inhibitor protein, LiaF (Jordan *et al*., 2006; Wolf *et al*., 2010; Schrecke *et al*., 2013). In *B. subtilis*, this three-component system is encoded by the last genes of the *liaIH-liaGFSR* locus, which is expressed as two transcriptional units. While expression of the last four genes is ensured from a weak constitutive promoter, P_{liaG}, the *liaIH* operon is expressed from the strictly LiaR-dependent promoter P_{liaI}, which represents the only target of LiaFSR-dependent signalling (Mascher *et al*., 2004; Wolf *et al*., 2010). When challenged with cell wall antibiotics, such as bacitracin, nisin or vancomycin, this promoter is strongly induced in a concentration-dependent manner (Mascher *et al*., 2003; 2004; Jordan *et al*., 2006). Moreover, the *lia* operon is also more weakly induced by detergents, ethanol, alkaline shock, and secretion stress (Wiegert *et al*., 2001; Mascher *et al*., 2004; Hyyryläinen *et al*., 2005; Pietiäinen *et al*., 2005). Hence, the inducer spectrum of the Lia response is very reminiscent of the range of stimuli triggering the PSP response.

Additionally, P_{liaI} is embedded in the complex differentiation cascade ultimately leading to endospore formation. Here, the transition state repressor AbrB binds P_{liaI} during logarithmic growth, thereby maintaining its low basal activity. During transition state, AbrB repression is relieved by the action of Spo0A, the master regulator of sporulation, and LiaR is activated by an unknown intrinsic stimulus (Jordan *et al*., 2007). P_{liaI} seems to be the only relevant target promoter controlled by LiaR, which induces expression of the *liaIH* operon and thereby mounts a PSP-like response (Wolf *et al*., 2010). This operon encodes a small-membrane protein, LiaI, and the PspA homologue LiaH respectively. The latter forms large oligomeric ring structures (Wolf *et al*., 2010), reminiscent of those observed for other PspA-like proteins (Aseeva *et al*., 2004; Hankamer *et al*., 2004; Standar *et al*., 2008; Otters *et al*., 2013).

So far, the physiological role of LiaIH remains unclear. Despite its strong induction by antibiotics interfering with the lipid II cycle of cell wall biosynthesis, the Lia system does not mediate any resistance against them (Wolf *et al*., 2010). The only exception is the membrane-damaging antibiotic daptomycin, which triggers the Lia response that in turn provides some degree of protection against this compound (Hachmann *et al*., 2009; Wolf *et al*., 2010). On the other hand, mild sensitivity phenotypes have been observed in *liaIH* mutant against cell wall antibiotics interfering with cytoplasmic (fosfomycin) or extracellular steps (some β-lactams) of cell wall biosynthesis, as well as some generators of oxidative stress, none of which act as inducers of the Lia response (Wolf *et al*., 2010). Taken together, these and other preliminary data suggest a protective role of the Lia response by maintaining the integrity of the cytoplasmic membrane, rather than of the cell wall (D. Wolf and T. Mascher, unpublished).

Here, we aimed at increasing our knowledge of the physiological role of the Lia response by studying the interactions, cellular localization and protein dynamics of its main effectors, LiaI and LiaH.

Results

LiaI is a small-membrane protein with two transmembrane helices

Previously, we have demonstrated that the *liaIH* operon represents the only relevant target of LiaR-dependent

gene expression (Wolf *et al*., 2010). While *liaH* encodes a cytoplasmic protein that belongs to the widely conserved PspA/IM30 protein family, little was known about LiaI. Based on hydrophobicity plots and secondary structure predictions, LiaI seems to be a membrane protein of 126 amino acids with two putative transmembrane regions (TMRs) and a C-terminal cytoplasmic domain of about 60 amino acids (Fig. 1A). To verify these predictions of LiaI topology, we constructed translational fusions of two different *liaI* gene fragments, encoding the full-length protein (base pairs 1–338) and an N-terminal fragment (base pairs 1–126) that terminates between the two postulated TMRs, to the reporter genes *phoA* and *lacZ* (Fig 1A; fusion points are indicated by stars). The alkaline phosphatase PhoA is only active in extracytoplasmic space while activity of the β-galactosidase LacZ indicates a cytoplasmic localization (Manoil, 1991; Daley *et al*., 2005). On selective 5-bromo-4-chloro-3-indolylphosphate (BCIP 50 μg ml^{-1}) agar, we observed activity of phosphatase A (resulting in blue colonies) only for *E. coli* strains containing the short *liaI* fragment fused to *phoA*, but not the full-length fragment. The opposite behaviour was observed for the *lacZ*-fusions in *B. subtilis*: No colony coloration was found on X-Gal (100 μg ml^{-1}) agar plates with cells containing the short *liaI* fragment fused to *lacZ* but with cells containing the full-length *liaI-lacZ* fusion (Fig 1A and data not shown). These results indicate that LiaI is a membrane protein with both the N- and C-terminus in the cytoplasm and two TMRs, which are connected by a small extracellular loop.

LiaI functions as a membrane anchor for LiaH

The genes *liaI* and *liaH* form an operon that is conserved in Firmicutes bacteria harbouring LiaFSR homologues (Jordan *et al*., 2006) and is strongly induced under cell envelope stress conditions (Mascher *et al*., 2003; 2004), indicative of a functional link between the two encoded proteins. Moreover, the genes for homologous PspA proteins in proteobacteria are also genetically associated with genes encoding small-membrane proteins that function as membrane anchors for PspA proteins (Joly *et al*., 2009). Hence, we propose a similar cellular role for LiaI. Especially the cytoplasmic C-terminus with its 60 amino acids length represents a suitable docking interface for LiaH.

Initially, we investigated the interaction between LiaI and LiaH by bacterial two-hybrid assay (BACTH) (Karimova *et al*., 1998; 2000; see *Experimental procedures* for details). In addition to the full-length *liaH*, two versions of *liaI* were cloned in the BACTH vectors, encoding a full-length LiaI and a truncated version that terminates after the second TMR. We observed a strong interaction between LiaH and full-length LiaI (Fig. 1B) and also between both LiaI versions, indicative of the functional expression of all alleles. Since no interaction was observed between LiaH and the truncated version of LiaI containing both TMRs but lacking the cytoplasmic

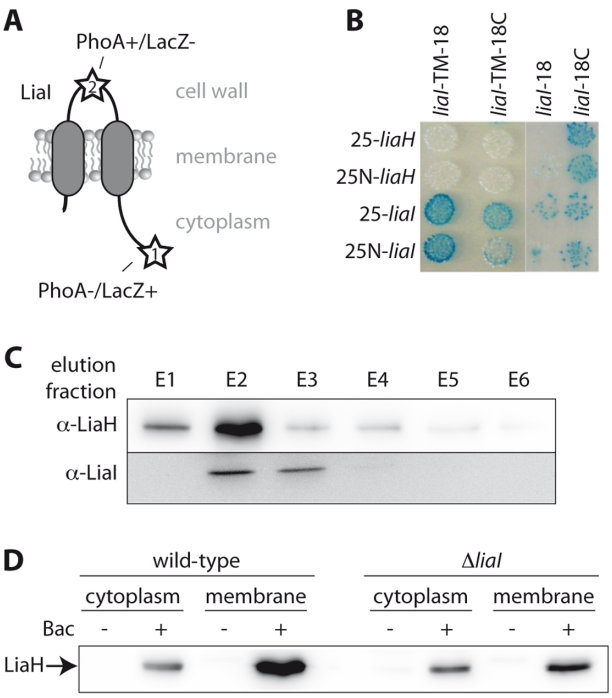

Fig. 1. LiaI is a membrane protein that interacts with LiaH.
A. Membrane topology of LiaI was studied by translationally fusing N-terminal *liaI* fragments to *lacZ* and *phoA*. The two fusion points are indicated by the stars, transmembrane helices are represented by grey bars). PhoA activity (PhoA+/LacZ–, star 2) indicates that the C-terminus of the corresponding fragment is localized in the extracellular space. LacZ activity (PhoA–/LacZ+, star 1), indicates that the C-terminus of LiaI is located in the cytoplasm. PhoA and LacZ activity was determined by colony colour on BCIP and X-Gal plates respectively (data not shown).
B. Interaction between LiaI and LiaH as inferred by bacterial two-hybrid assay (BACTH). Full-length genes of *liaI* and *liaH*, as well as a truncated allele encoding only the N-terminal half of LiaI until the end of the second transmembrane helix (*liaI*-TM) were translationally fused to the N- and C-terminus of the T18 or T25 fragment of the adenylate cyclase gene into the corresponding BACTH test vectors. The resulting co-transformants in *E. coli* BTH101 were assayed on LB/X-Gal plates. Blue colonies indicate protein interactions. See *Experimental procedures* for details.
C. Co-immunoprecipitation of LiaI with LiaH. A streptactin-tagged soluble C-terminal fragment LiaI was overexpressed in *B. subtilis* strain TMB688 and cross-linked under induced conditions with bacitracin (20 μg ml^{-1}). Twenty microlitres of each elution fraction E1-E6 was separated by SDS-PAGE and analysed by Western blot with α-StrepII (indicated as α-LiaI in the panel) and α-LiaH respectively (see *Experimental procedures*). Detection of LiaH and streptactin-tagged LiaI in identical elution fractions indicate a co-purification and interaction of both proteins.
D. Dependence of LiaH membrane association on LiaI. Strains W168 (wild-type) and TMB1394 (Δ*liaI*) were used to investigate LiaH localization under uninduced (–) and induced [+, bacitracin 20 μg ml^{-1} (Bac)] conditions. Protein samples (30 μg per lane) of cytoplasmic and membrane fraction of each strain were separated by SDS-PAGE and analysed for LiaH (marked by arrow) by Western blot using α-LiaH.

Table 1. Strains used in this study.

Strain	Relevant genotype[a]	Reference
Escherichia coli		
BTH101	F- *cya*-99 *araD*139 *galE*15 *galK*16 *rpsL*1 (str^R) *hsdR*2 *mcrA*1 *mcrB*1	Lab stock
CC118	F-Δ(*ara-leu*)7697 *araD*139Δ(*lac*)X74 *phoA*Δ20 *galE glaK thi rpsE rpoB argE recA*1	Lab stock
Bacillus subtilis		
W168	*trpC*2	Lab stock
3417	W168 Ω *mreC*::pSG5276 (P_{xyl} *gfp-mreC*) Ω cm^R	Leaver and Errington (2005)
RWSB432	W168 Ω *liaH*::pDW5101 (*liaH*-GFP) Ω *amyE*::RWB4 (mRFPruby-*mreB*) cm^R spec^R	This study
TMB321	W168 *amyE*::pSJ5402 (*liaH*-GFP) spec^R	This study
TMB322	W168 *amyE*::pSJ5401 (*liaI*-GFP) spec^R	This study
TMB688	W168 pDW3802 (cytoplasmic C-terminal part of *liaI*) mls^R	This study
TMB841	W168 pGP380 (empty vector control) mls^R	This study
TMB1172	W168 *amyE*::pAT6203 (P_{liaI}-GFP) cm^R	Toymentseva *et al.* (2012)
TMB1328	W168 Ω *liaH*::pDW5101 (*liaH*-GFP) Ω cm^R	This study
TMB1394	W168 Δ*liaI* markerless deletion	This study
TMB1407	W168 Δ*liaI* Ω *liaH*::pDW5101(*liaH*-GFP) Ω cm^R	This study
TMB1421	W168 Ω *liaI*::pDW5102 (*liaI*-GFP) Ω cm^R	This study
TMB1441	W168 amyE::pSJ5401(*liaI*-GFP) Ω *liaH*::pDW6401mRFPruby (RFP-*liaH*) Ω cm^R spec^R	This study
TMB1714	W168 Ω *liaH*::pDW6401mRFPruby (RFP-*liaH*) Ω cm^R	This study
TMB2204	W168 *amyE*::pCH5402 (P_{liaI}-*liaIH-gfp*)	This study
TMB2206	W168 Δ*liaIH amyE*::pCH5402 (P_{liaI}-*liaIH-gfp*)	This study

a. Resistance cassettes: cm, chloramphenicol; str, streptomycin; mls, macrolide-lincosamide-streptogramin B; spec, spectinomycin.

C-terminus, we conclude that the latter is necessary for the interaction with LiaH. The specificity of the BACTH results on LiaI-LiaH interaction was validated by a lack of interaction between LiaI and other membrane proteins, including LiaG or LiaF (data not shown).

To verify these observations, we next studied the interaction between LiaI and LiaH in more detail. By using the SPINE (Strep-Protein INteraction Experiment) approach (Herzberg *et al.*, 2007), we were able to demonstrate an interaction between LiaI and LiaH by *in vivo* cross-linking followed by co-purification and detection of both proteins via immunoblotting (Fig. 1C). Strain TMB688, which constitutively expresses a soluble Streptacin-tagged derivative of LiaI (Table 1), was grown in the presence of bacitracin (20 μg ml^{-1}) to induce the LiaRS system and hence LiaH production. At an OD_{600} of 1.0 formaldehyde was added to cross-link interacting proteins *in vivo* (Herzberg *et al.*, 2007). After incubation of the cytoplasmic cell extract with Strep-Tactin sepharose and subsequent thorough washing, we detected both proteins in the elution fractions by using LiaH- and Strep-tagII-specific antibodies respectively (Fig. 1C). In contrast, no signals for LiaH or the tag-specific antibodies were detected in the elution fractions of the control strain TMB841 (data not shown). We therefore conclude that LiaI and LiaH interact when the Lia-system is induced by cell envelope stress.

Given that both proteins interact *in vivo* and LiaI is a membrane protein, one would expect that LiaH should be detectable in membrane fractions under Lia-inducing conditions. To corroborate this hypothesis we incubated the wild-type strain in the presence and absence of bacitracin to compare the induced and uninduced state of expression of the *liaIH* operon respectively. Equal amounts of the cytoplasmic and membrane protein fraction harvested from both uninduced and induced cultures were separated by SDS-PAGE, followed by LiaH-specific Western analysis (see *Experimental procedures* for details). While no LiaH-specific signal could be observed in any fraction from uninduced cultures, a band of the appropriate size was detected in the cytoplasmic, and especially the membrane fraction under inducing conditions, thereby verifying not only the induction of LiaH production but also its specific association with the cytoplasmic membrane (Fig. 1D, lanes 1–4).

Based on the results described so far, it seems reasonable to assume that this membrane localization of the cytoplasmic protein LiaH depends on its membrane anchor LiaI. We therefore repeated the experiment described above with strain TMB1394, harbouring an in-frame markerless deletion of *liaI* (Table 1). Compared to the wild-type strain, the overall amount of LiaH was slightly reduced in the *liaI* mutant (lanes 2 + 4 compared to lanes 6 + 8 and data not shown), indicating translational coupling between the two overlapping genes. Moreover, the ratio of the LiaH-specific signal was clearly shifted from the membrane fraction towards the cytoplasmic fraction and simultaneously decreased in the membrane fraction of the Δ*liaI* strain (Fig. 1D, lanes 5–8), indicative of an important role of LiaI for the membrane tethering of LiaH. However, the results also indicate that upon induction LiaH was still able to associate with the cytoplasmic membrane, even in the absence of its identified membrane anchor LiaI. This observation might indicate that LiaH, just as its proteobacterial counterpart PspA, has more than

one interaction partner in the cytoplasmic membrane (Darwin, 2005). Alternatively, elevated levels of LiaH alone could be sufficient for its association with the membrane, as has been observed in a mutant of *Y. enterocolitica* that lacks the two known membrane anchors of PspA, PspB and PspC (Yamaguchi *et al.*, 2010). Both scenarios could be envisioned for LiaH and further experiments will be required to clarify this observation.

Taken together, our data demonstrate that LiaI is a membrane protein with two TMRs that functions as a membrane anchor for LiaH through its cytoplasmic C-terminal domain. Moreover, our data can be viewed as a first indication that *B. subtilis* LiaH is embedded in a larger protein interaction network that involves additional, so far unknown, proteins to ensure its proper positioning at the cytoplasmic membrane under conditions of cell envelope stress.

LiaI and LiaH colocalize in discrete foci under envelope stress conditions

The data described above indicate that – under envelope stress conditions – the cytoplasmic protein LiaH is recruited to the cytoplasmic membrane with the help of LiaI and presumably additional proteins. This would suggest that LiaI and LiaH should at least to some extent also colocalize within the cell. We therefore aimed at directly visualizing this localization by generating strains in which functional C-terminal LiaI-/LiaH-GFP fusions were integrated directly into the native *lia* locus and therefore also expressed under the native stress-inducible *liaI* promoter. The cellular localization of LiaH and LiaI in strains TMB1328 and TMB1421, respectively, was then analysed by total internal reflection fluorescence microscopy (TIRFM). With this technique, only an about 200 nm wide section of the cell closest to the glass slide, containing the cell wall, cytoplasmic membrane, but only a small part of the cytoplasm, will be excited by the laser. Compared to epifluorescence, TIRFM therefore greatly reduces background fluorescence and bleaching of fluorophores for membrane-associated proteins (Spira *et al.*, 2012).

In uninduced cells, only very faint signals could be detected for both proteins (Fig. 2A, left panels). While LiaH-GFP gave a diffuse signal, in line with a cytoplasmic localization, LiaI-GFP was always detected in a few distinct foci at the cytoplasmic membrane. While the number of LiaI-foci varied between cells, we never observed a dispersed signal at the membrane. Under inducing condition (addition of bacitracin, 20 μg ml^{-1} final concentration), the number of LiaI-foci greatly increased. Importantly, LiaH-GFP now showed a similar cellular distribution, indicative of a colocalization and possibly complex formation of LiaI and LiaH in the presence of envelope stress (Fig. 2A, right panels).

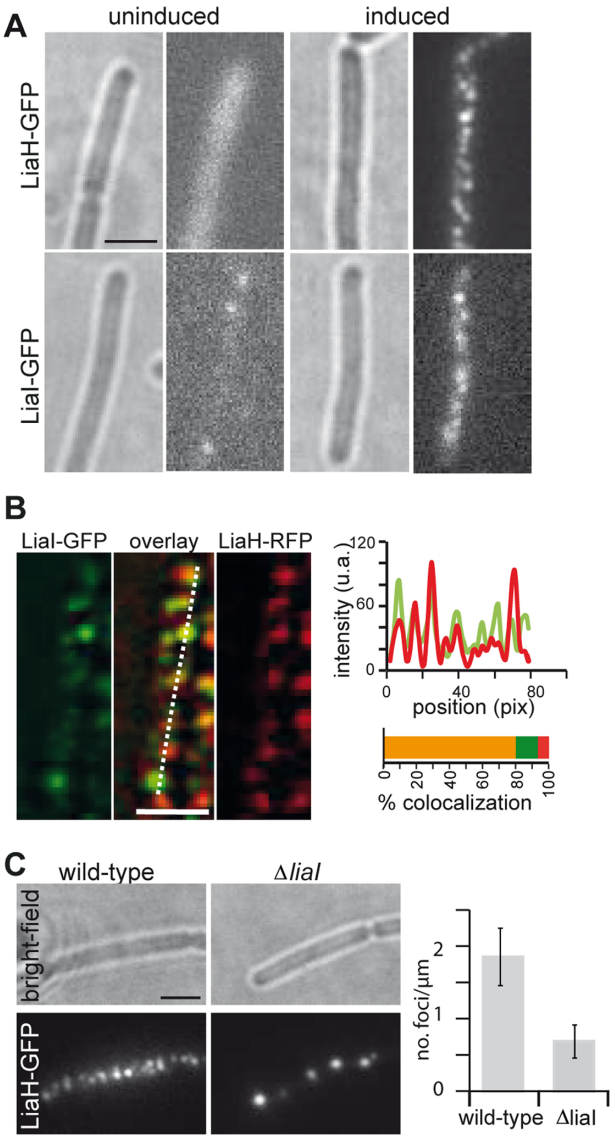

Fig. 2. LiaI is the membrane anchor of LiaH and both localize in discrete foci.
A. Localization of LiaI-GFP (TMB1421) and LiaH-GFP (TMB1328) under control of their native promoter in uninduced (left) and bacitracin-induced cells (right). Bright-field images (left) and TIRF images (right).
B. Colocalization of LiaI and LiaH (TMB1441). The linescan plotted on the right was taken along the dotted line. Colocalization (orange), LiaI-GFP foci (green) and LiaH-mRFPruby foci (red) (number of foci counted = 200).
C. Localization of LiaH-GFP in wild-type (TMB1328) and Δ*lialI* (TMB1407) cells. Bright-field images (top row) and corresponding TIRF images (bottom row). Quantification of LiaH-GFP foci per μm in wild-type and Δ*lialI* cells (means and standard deviations derived from 40 cells). The two conditions are statistically different in a *t*-test ($P < 0.001$). Cells were grown until OD_{600} 0.2–0.4 in LB (supplemented with 0.05% xylose in B) at 30°C and induced with bacitracin (20 μg ml^{-1}) for 30 min.
Scale bars for all microscopic images: 2 μm.

To determine whether the observed localization pattern (Fig. 2A) as well as the interaction (Fig. 1C and D) of LiaI and LiaH under stress conditions indeed reflects the formation of complexes, we generated strain TMB1441, which contains a LiaI-GFP fusion gene integrated in the *amyE* locus under the control of the xylose-inducible promoter P_{xyl}, together with a LiaH-mRFPruby fusion protein placed under the control of the native *liaI* promoter. While the amount of ectopically expressed LiaI-GFP was now xylose-dependent and uncoupled from envelope stress, its behaviour under stress and non-stress conditions was indistinguishable from LiaI-GFP in strain TMB1421, in which the expression of the corresponding gene was under control of the native P_{liaI} promoter (data not shown). As observed with LiaH-GFP in strain TMB1328, LiaH-mRFPruby exhibited a weak and diffuse signal in non-stressed cells, while LiaI-GFP formed distinct foci at the cytoplasmic membrane (data not shown). Upon bacitracin stress, LiaH was recruited to the membrane patches, with 80% of foci containing both LiaI-GFP and LiaH-mRFPruby (Fig. 2B). These numbers are in line with recent observations for the cell wall biosynthesis machinery of *B. subtilis* (Dominguez-Escobar *et al.*, 2011), thereby supporting the notion of a physical interaction between LiaI and LiaH at the membrane. This assumption was further supported by a reduction of the number of LiaH-GFP foci upon *liaI* deletion (Fig. 2C). In summary, our results support the notion that LiaI recruits LiaH to the membrane under envelope stress conditions.

LiaI foci are highly motile in non-stressed cells and become static under envelope stress conditions

Having observed formation of LiaI/LiaH patches at the cytoplasmic membrane we next studied the dynamics of these foci in real time. For this purpose, we analysed membrane recruitment of LiaH-GFP at different time points post induction through cell wall stress. Upon addition of bacitracin (20 μg ml^{-1}) the first visible foci already appeared within 3 min and foci number constantly increased over 15–20 min (Fig. 3A and B). The observed timing was in line with a recent report on kinetics of P_{liaI} induction, which demonstrated a rapid response of the LiaRS system to bacitracin shock (Kesel *et al.*, 2013). Interestingly, at early induction time points (3–7 min) LiaH foci were often motile (kymographs in Fig. 3A), while they became static after prolonged induction (Fig. 3A).

Since our results indicate that LiaI recruits LiaH under stress conditions, we reasoned that LiaI foci should also become static in the presence of envelope stress. Indeed, while LiaI foci in unstressed cells showed fast and randomly oriented movement (Fig. 3C and supplemental Movie S1), most LiaI foci became immobile in the presence of bacitracin (Fig. 3D and supplemental Movie S2).

Taken together, our data suggest that a small number of LiaI foci constantly scan the cytoplasmic membrane during normal growth. Under envelope stress conditions, LiaI and LiaH expression is strongly increased. LiaI, maybe together with additional unknown proteins, recruits LiaH to the membrane into large immobile protein complexes. Both stalling and complex formation might either occur at sites of membrane damage, or be the result of the strong upregulation of LiaIH expression itself in the presence of envelope stress conditions. The first idea would require that LiaI performs some sensory function in perceiving envelope damage, while the second would be independent of damage. To discriminate the two possibilities, we introduced a copy of the *liaIH* operon, including its native LiaR-dependent promoter P_{liaI} and encoding a C-terminal translational LiaH-GFP fusion protein, ectopically into the *amyE* locus, thereby placing it under the additional control of the xylose-dependent promoter P_{xyl} (Fig. 4A). This set-up allows for the separation of a mere dose-dependent *versus* a stress-dependent localization of LiaH-GFP.

In the absence of xylose and envelope stress, weak and polar LiaH-GFP foci can be seen (Fig. 4A). Induction with xylose leads to a significant increase in strength of these mostly polarly localized foci. Moreover, some cells also contain individual and very weak lateral foci. In contrast, induction with bacitracin again leads to occurrence of numerous discrete LiaH-GFP foci (Fig. 4A), a distribution identical to the one observed before (Figs 2 and 3). To rule out any interference from the presence of the second native copy of the *liaIH* operon, we also performed similar experiments in an isogenic *liaIH* deletion strain. While the intensity of the foci was slightly weaker throughout, we basically achieved the same results (Fig. 4A). This result provides a first clear hint that foci formation is indeed coupled to envelope stress and not merely a result of an increase in protein amounts as a result of induction.

To substantiate our findings, we next investigated the dynamics of an ectopically expressed copy of LiaI-GFP, the expression of which was uncoupled form envelope stress, by time-lapse TIRF microscopy (Fig. 4B). Induction with xylose results in a strong increase in the number LiaI foci, which were highly motile. Hence, the behaviour of LiaI foci was comparable to the situation described for the uninduced wild-type (Fig. 3C), despite the significant increase in protein amounts and hence foci numbers. If bacitracin was simultaneously added, the number of LiaI-GFP foci did not increase further, but now all foci remained static. This again supports the hypothesis that foci stalling is primarily a consequence of envelope stress rather than a result of the increased protein amounts in the cell.

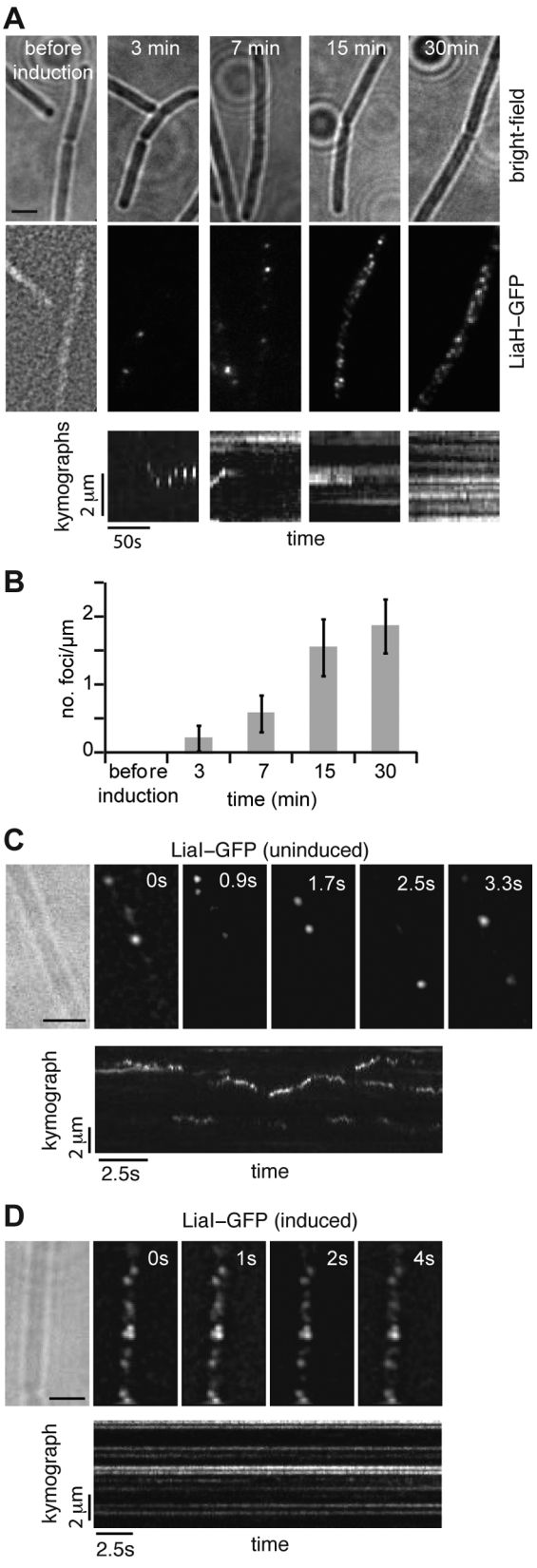

Fig. 3. LiaI and LiaH display dynamic localization.
A. TIRFM time-lapse image series of LiaH-GFP (TMB1328) in *B. subtilis* cells induced with 20 µg ml^{-1} bacitracin. Bright-field (top), TIRFM (middle) and representative kymographs of protein dynamics (bottom).
B. Quantification of LiaH-GFP static foci µm^{-1} for every time point (mean and standard deviation derived from more than 40 cells per time point).
C. TIRFM time-lapse of LiaI-GFP (TMB1421) under uninducing conditions and typical kymograph along a line parallel to the cell axis.
D. TIRFM time-lapse of LiaI-GFP in cells induced with bacitracin and typical kymograph. Cells were grown until exponential phase (OD_{600} 0.4–0.6) in LB at 30°C and induced with bacitracin (20 µg ml^{-1}) when indicated.
Scale bars for all microscopic images: 2 µm.

Recruitment of LiaH to static membrane foci is specifically induced by antibiotics that interfere with the lipid II cycle of cell wall biosynthesis

We have previously shown that the Lia system can be specifically triggered by cell wall antibiotics that interfere with the lipid II cycle of cell wall biosynthesis, such as bacitracin, nisin, or vancomycin, resulting in an over 200-fold increased *liaIH* expression for the first three compounds, and an about 50-fold induction in case of vancomycin (Mascher *et al.*, 2004; Staroń *et al.*, 2011 and references therein). But despite its strong induction, the Lia system does not mediate resistance against these inducers (Wolf *et al.*, 2010). Of the three cell wall antibiotics for which *B. subtilis* shows a Lia-dependent change in susceptibility – fosfomycin, some β-lactams, and daptomycin – only the latter acts as an inducer. We therefore wanted to determine how cellular localization and dynamics of LiaI and LiaH were influenced by treatment with different antibiotics that affect cell wall biosynthesis and envelope integrity (Fig. 5A).

Both the strong induction and the recruitment of LiaH-GFP to membrane foci were readily observed for the known inducers of the Lia response, bacitracin, daptomycin, vancomycin and nisin. But despite the fact that a *liaIH* mutant shows increased fosfomycin sensitivity (Wolf *et al.*, 2010), LiaH remained dispersed in the cytoplasm after a challenge with fosfomycin or ampicillin (Fig. 5A). Hence, cell wall antibiotics that affect cytoplasmic or extracellular steps of cell wall biosynthesis neither act as inducers of the Lia response, nor do they affect localization of LiaH (Fig. 5A) and LiaI (data not shown). Taken together, these observations demonstrate that the localization of LiaH into static membrane foci correlates with the inducer profile of the Lia response and hence the strong upregulation of LiaI and LiaH production, but not with the antibiotic sensitivity phenotypes associated with LiaIH.

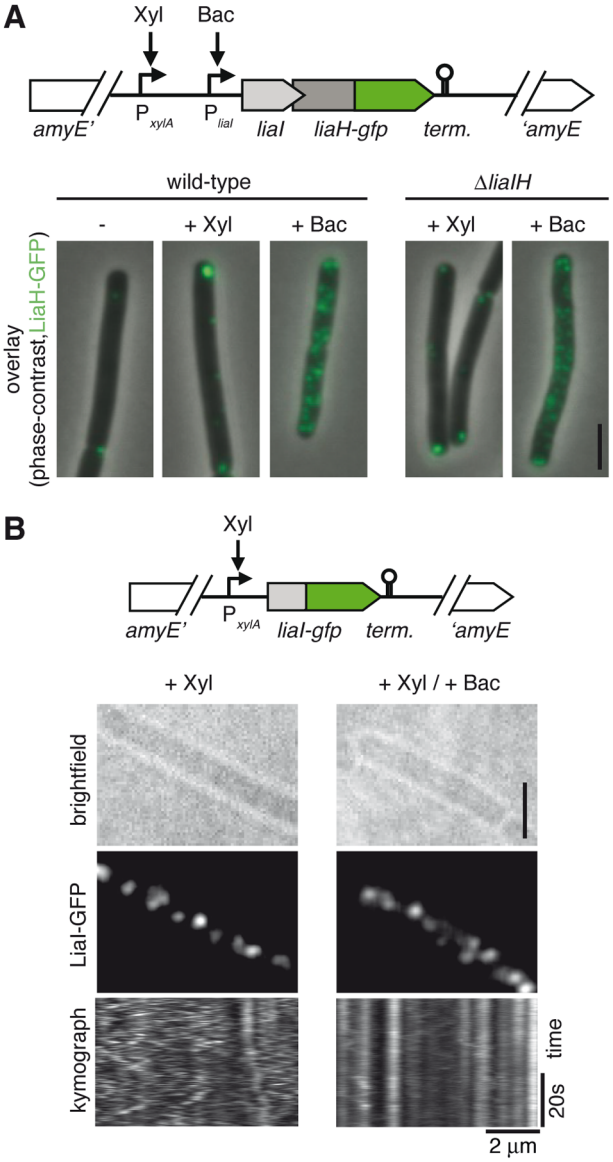

Fig. 4. Stalling of LiaI/LiaH foci depends on envelope damage, not protein overproduction.
A. Ectopic expression of the *liaIH* operon under dual control of the xylose-dependent promoter P_{xylA} and the native, bacitracin-dependent promoter P_{lial} in strains TMB2204 and TMB2206 (isogenic markerless *liaIH* deletion mutant derived from TMB2204) allows discrimination between foci-stalling that is based on protein overproduction (+Xyl, addition of xylose, 0.2% final concentration) and stalling in response to envelope stress (+Bac, addition of bacitracin, 20 µg ml^{-1} final concentration). A schematic diagram of the genotype is provided above, overlay microscopic images from strains TMB2204 (wild-type) and TMB2206 (Δ*liaIH*) are shown below.
B. Ectopic expression of a *liaI-gfp* fusion under control of P_{xylA} in the presence of only xylose (+Xyl, addition of xylose, 0.05% final concentration) and in combination with envelope stress [+Xyl/+Bac, addition of xylose (0.05%) and bacitracin (20 µg ml^{-1})]. A schematic diagram of the genotype is provided above, the TIRFM data (bright-field and fluorescence image, as well as the corresponding kymographs) is shown below.

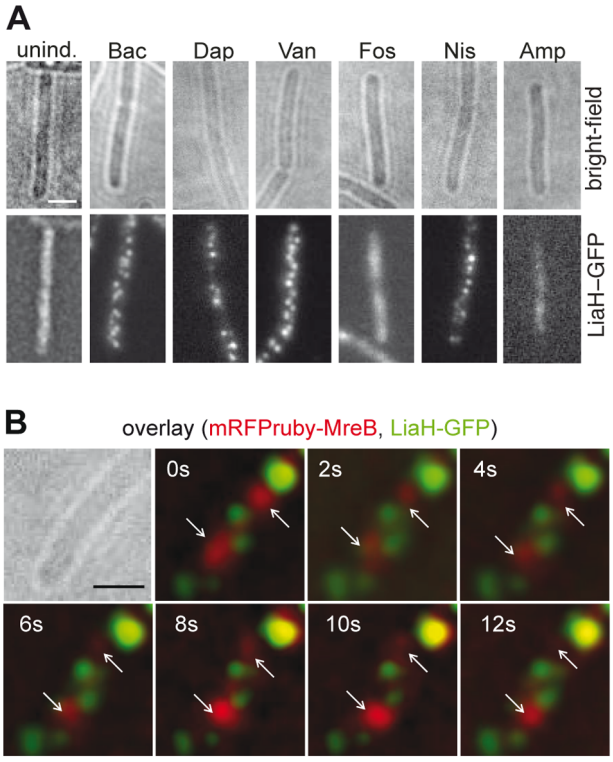

Fig. 5. Membrane localization of LiaH foci is induced by antibiotics interfering with the lipid II cycle of cell wall biosynthesis and is independent of the cell wall biosynthesis machinery.
A. LiaH-GFP *B. subtilis* cells (TM1328) untreated and treated with bacitracin (20 µg ml^{-1}), daptomycin (1 µg ml^{-1}), vancomycin (10 µg ml^{-1}), fosfomycin (50–700 µg ml^{-1}), nisin (20 µg ml^{-1}) and ampicillin (50–100 µg ml^{-1}). Cells were grown until OD_{600} 0.2–0.4 in LB at 30°C and induced with the indicated antibiotic for 30 min. Scale bar: 2 µm.
B. Movement of mRFPruby-MreB patches (arrows) in *B. subtilis* cells treated with bacitracin. TIRFM time-lapse images of cells expressing LiaH-GFP (green) and mRFPruby-MreB (red). Cells were grown until exponential phase (OD_{600} 0.4–0.6) in LB supplemented with 0.5% xylose at 30°C and induced with bacitracin (20 µg ml^{-1}). Scale bars: 2 µm.

Movement and localization of LiaI foci are independent of the cell wall biosynthesis machinery

In rod-shaped bacteria, the cell wall biosynthesis machinery is co-ordinated by the actin-like MreB, which spatially organizes the enzymatic activities required for proper bacterial growth (Chastanet and Carballido-Lopez, 2012; White and Gober, 2012). Recently, it was reported that contrary to previous models cell wall biosynthesis is not driven by treadmilling of MreB filaments, but instead that intracellular MreB patches are actively moved by peptidoglycan biosynthesis (Dominguez-Escobar *et al.*, 2011; Garner *et al.*, 2011). Accordingly, addition of cell wall antibiotics resulted in slowing or arrest of MreB motility (Dominguez-Escobar *et al.*, 2011). It had previously been suggested that in *E. coli* MreB is crucial for PspA-mediated stress response, but not stress-induction of the

pspA operon (Engl *et al*., 2009). Because of the known link between cell wall biosynthesis and MreB, and in light of the induction of the Lia response by cell wall antibiotics, especially since the motility of LiaI and LiaH foci was also negatively affected by the action of cell wall antibiotics, we wondered if the cellular localization of LiaIH and the dynamics of the MreB-associated cell wall biosynthesis machinery might overlap in the presence of severe envelope stress. To address this question, we studied the colocalization of mRFPruby-MreB and LiaH-GFP (Fig. 5B and supplementary Movie S3). While both LiaI and MreB form motile patches at the membrane, their modes of movement are very different. While MreB patches are moved perpendicular to the long cell axis in a highly directed manner (Dominguez-Escobar *et al*., 2011; Garner *et al*., 2011), LiaI diffuses randomly within the membrane on a much faster timescale. Despite the fact that the mobility of both MreB and LiaI patches can be stopped in the presence of cell wall antibiotics, this response occurs at very different antibiotic concentration. In fact, Lia foci seem to be significantly more susceptible to antibiotic-induced stalling (Fig. 5B): In the presence of bacitracin (20 μg ml^{-1}) movement of LiaH patches was already stalled, while MreB remained motile, clearly demonstrating that MreB, and hence the cell wall biosynthesis machinery was not associated with LiaIH, even under conditions of severe envelope stress (Fig. 5B and supplementary Movie S3).

These data, together with the antibiotic profile triggering the Lia response described above (Fig. 5A), indicate that the positions of LiaIH foci are independent of the cell wall biosynthesis machinery. Instead, it is reasonable to assume that LiaIH motility is most likely affected by changes in membrane properties as a result of antibiotic action. But the exact molecular nature of this stimulus remains to be identified.

The intrinsic stationary-phase induction of the Lia response is heterogeneously distributed but also results in the colocalization of LiaI and LiaH in foci

In addition to the very strong (about 200-fold) and immediate induction of the Lia response by the extrinsic addition of some cell wall antibiotics, the expression of *liaIH* operon also increases a moderate 10-fold at the onset of stationary phase, as quantified by β-galactosidase assays as an average over the whole population (Jordan *et al*., 2007). This intrinsic transition state induction of the Lia response is still poorly understood. We could previously demonstrate that under these conditions the activity of both the LiaRS system and Spo0A, the master regulator of differentiation and sporulation in *B. subtilis* are required (Jordan *et al*., 2007). But the nature of the intrinsic trigger still remains elusive, as does the reason for the much weaker promoter activities under these conditions.

In the course of the present studies, we noticed that LiaH-GFP and LiaI-GFP also localized in discrete foci in the stationary growth phase, similarly to the bacitracin-induced cells during mid-exponential phase (Fig. 6A). Remarkably, both induction and foci formation could only be observed in a small subset of cells, especially in late stationary-phase cultures (about 6% at an OD_{600} of 2.7; Fig. 6B). To verify this observation, we analysed the behaviour of a transcriptional P_{liaI}-*gfp* fusion, and again we could detect a strong GFP signal in only about 5–10% of the cells (Fig. 6C). This behaviour could reproducibly be observed even after re-inoculation from a single colony, e.g. an isogenic population, demonstrating that this behaviour represents a phenotypic heterogeneity rather than a genetically manifested trait.

Hence, our data show that the weak population-averaged Lia response upon intrinsic stimulation (Jordan *et al*., 2007) is the result of only a subpopulation of cells that is fully induced, compared to the full induction of all cells within the population observed upon bacitracin induction with 20 μg ml^{-1} (Kesel *et al*., 2013). Moreover, one input to P_{liaI}, Spo0A, is known to exhibit phenotypic heterogeneity in stationary phase (Veening *et al*., 2005), and hence, we speculate that the bifurcation of the Lia response at the onset of stationary phase might be a direct consequence of this.

Quantitative analysis of LiaI protein dynamics indicates subdiffusive motion under envelope stress conditions

So far, the cellular motility of only very few proteins has been studied in *B. subtilis*. Among those, it was shown that the actin-like cytoskeletal element MreB and several components of the cell wall elongation machinery move in a highly directed manner circumferentially around the cell (Dominguez-Escobar *et al*., 2011; Garner *et al*., 2011). In contrast, trajectories obtained from single particle tracking of LiaI under uninducing and inducing conditions (Fig. 7A and B) suggest that LiaI diffuses randomly within the cytoplasmic membrane, further supporting that the Lia response is not directly associated with cell wall biosynthesis.

To characterize the diffusive motion of LiaI, we analysed the single particle trajectories at a quantitative level. In particular, we studied how the mean squared displacement (MSD), which provides a measure for the spatial extent of random motion, scales as a function of the time lag τ between two successive observations. In the case of LiaI foci, it became apparent that the MSD curves increased much faster in cells that were uninduced compared to cells that were induced with bacitracin (Fig. 7C). From these data we estimated the apparent diffusion

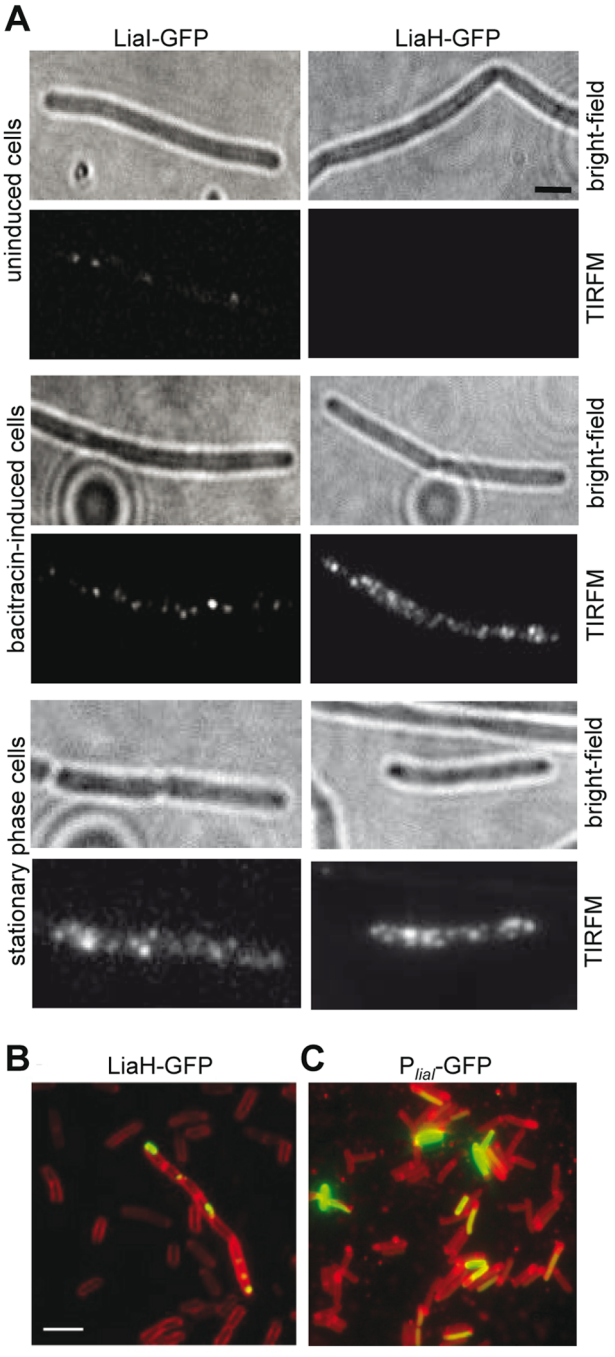

Fig. 6. Heterogeneous induction of the Lia response during transition state.
A. TIRFM analysis of uninduced and bacitracin-induced (20 μg ml^{-1} final concentration) cells during exponential growth (OD_{600} 0.4–0.6, grown in LB at 30°C) and stationary-phase cells without external induction. A similar expression and subcellular pattern of LialH-GFP is observed between the latter two conditions.
B and C. (B) TIRFM image of LialH-GFP (strain TMB1328). FM4–64 membrane staining (red) and LialH-GFP (green). (C) P_{lial}-*gfp* (strain TMB1172).
Scale bar: 2 μm (A) and 4 μm (B).

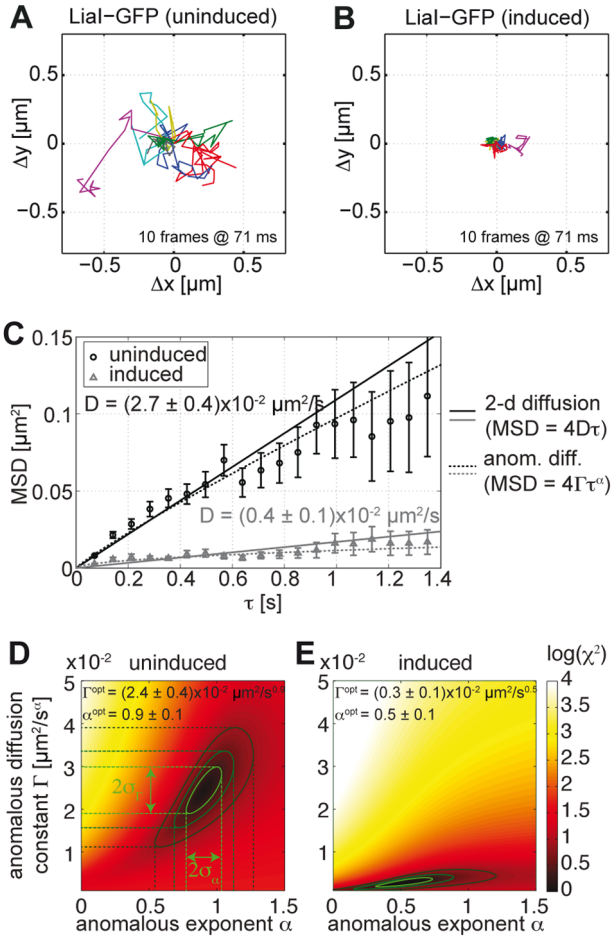

Fig. 7. Quantitative analysis of LialH protein dynamics.
A and B. Representative trajectories obtained by single particle tracking for LialH-GFP under uninducing (A) and inducing (B) conditions. Each plot shows 10 trajectories (colours) followed over 10 frames recorded at a frame rate of 71 ms.
C. Mean squared displacement (MSD) analysis of LialH protein dynamics in uninduced and bacitracin-induced cells as a function of the lag time τ between two observations. Symbols represent mean experimental MSDs and error bars the corresponding standard errors to the mean, based on $n = 57$ (LialH-GFP –bac) and $n = 85$ (LialH-GFP +bac) single particle trajectories, as described in *Experimental procedures*. Solid and dotted lines are fits of a simple two-dimensional diffusion model (MSD = $4D\tau$) and an anomalous diffusion model (MSD = $4\Gamma\tau^{\alpha}$) respectively. The apparent diffusion constants D obtained from the simple model are indicated next to the fits. The anomalous diffusion model describes the data significantly better than the simple one, as indicated by an F-test with P-values of 0.008 (LialH unind.) and 3×10^{-9} (LialH ind.).
D and E. Best-fit parameters of the anomalous diffusion model and their corresponding confidence intervals [66.8% (light green), 95% (dark green) and 99% (black)]. The colour codes for log(χ^2), where a low χ^2 indicates high quality of the fit for a given combination of model parameters.

constant D by linear fits, as one expects a linear dependence of the MSD on the time lag for two-dimensional Brownian motion (MSD = $4D\tau$). Accordingly, the apparent diffusion constant of LialH was reduced from $D = (2.7 \pm 0.4)$

$\times 10^{-2}$ μm^2 s^{-1} in the uninduced samples to $D = (0.4 \pm 0.1) \times 10^{-2}$ μm^2 s^{-1} in induced samples.

However, in both cases it is clearly visible that the MSD is not fully linear, but has a rather concave shape. In fact, it is known that most experimental diffusion measurements within cell membranes do not display simple linear relationships, but that an anomalous diffusion model ($MSD = 4\Gamma\tau^{\alpha}$) is often more suitable to explain the data (Saxton and Jacobson, 1997). In general terms, anomalous diffusion can be the result of both obstacles to diffusion and traps with a distribution of binding energies or escape times. Fits to the MSD curves in Fig. 7C showed that the anomalous diffusion model in fact explains our data significantly better than simple diffusion (*P*-values < 0.008, see caption to Fig. 7). While the anomalous diffusion constants Γ obtained for LiaI were similar to the apparent diffusion constants *D* under both conditions, the scaling exponent α was reduced from $\alpha = 0.9 \pm 0.1$ under uninducing to $\alpha = 0.5 \pm 0.1$ under inducing conditions (Fig. 7C–E).

While for eukaryotic membrane proteins anomalous diffusion seems to be the rule rather than the exception (Saxton and Jacobson, 1997), it has also been reported that in bacteria the three-dimensional cell geometry can lead to a sublinear increase of the MSD curves even when the particles undergo simple Brownian diffusion (Deich *et al*., 2004; Niu and Yu, 2008). Accordingly, it seems likely that the deviation of the anomalous scaling exponent obtained for LiaI under non-inducing conditions ($\alpha \approx 0.9 \pm 0.1$) from the Brownian diffusion case ($\alpha = 1$) can be attributed to such geometrical factors. However, the strong reduction of α for LiaI foci under cell envelope stress conditions ($\alpha = 0.5 \pm 0.1$) clearly indicates subdiffusive motion, because the cell geometry does not change upon antibiotic treatment.

These findings show that treatment with bacitracin does not only reduce the mobility of LiaI by a factor of eight, but also suggest that either damaged areas within the cell envelope or oligomerization with LiaH serve as obstacles and/or diffusional traps for LiaI foci under cell envelope stress conditions. The apparent diffusion coefficient for LiaI obtained under non-inducing conditions [$D = (2.7 \pm 0.4) \times 10^{-2}$ μm^2 s^{-1}] is near the lower end of the range of diffusion constants measured for other bacterial membrane proteins (Deich *et al*., 2004; Mullineaux *et al*., 2006; Lenn *et al*., 2008). This might suggest that LiaI forms larger complexes or locates within less mobile fractions of the bacterial membrane, but the limited amount of reference data does not permit a final conclusion.

Discussion

In this study, we demonstrated that LiaI is a small-membrane protein with two transmembrane helices that acts as a membrane anchor for the phage-shock protein homologue LiaH through its C-terminal cytoplasmic domain (Fig. 1). Our analyses further showed that under non-inducing conditions, LiaI is organized in a few membrane-anchored foci that appear to rapidly scan the cytoplasmic membrane in a diffusive pattern (Figs 2 and 3). Upon envelope stress, the *liaIH*-operon is strongly induced (Mascher *et al*., 2004; Jordan *et al*., 2006). Accordingly, the number of LiaI foci rapidly increases (Fig. 3). Moreover, these foci seem to recruit LiaH to the membrane and become mostly static under envelope stress conditions (Figs 2–4). These observations indicate that LiaI foci could be sensors of some aspect of membrane-linked envelope stress, reminiscent of PspC (Darwin, 2005; 2007). Complex formation could then be the result of strongly increased LiaH amounts under inducing conditions, e.g. in the presence of envelope stress, potentially at the sites of envelope damage (Fig. 4).

Functionality of GFP-fusion proteins of LiaI and LiaH

Translational GFP-fusions are a powerful way to study the subcellular localization of proteins *in vivo*, and such approaches have revealed numerous important insights into their biological function in the past (Margolin, 2000; Phillips, 2001). While the self-contained domain structure of GFP often does not interfere with the functionality of its fusion partner, introduction of GFP-fusion proteins can nevertheless generate artefacts, leading to misinterpretations. Basically, such artefacts can be the result of any of the following three issues: (i) alterations of the protein amount due to copy-number effects, e.g. if expressed from a replicative plasmid, (ii) generation of artificial situations due to uncoupling the production of a fusion-protein from its native regulation, e.g. if expressed ectopically from an inducible or constitutive promoter without the corresponding partner genes and/or outside its normal regulatory context, and (iii) disruption of the proteins' functionality by the fused GFP, in case that the fusion end is functionally important.

By introducing the *gfp*-fusion genes at their native locus, we avoided copy-number effects and ensured that expression of the fusion proteins, together with their coexpressed partner proteins, remained under their native regulation. While functionality of LiaI is indicated by its ability to interact with LiaH, we currently have no reliable read-out for LiaH-GFP functionality. While we cannot rule out the possibility of interfering with LiaH functionality due to the GFP-fusion, a vast body of evidence argues against such issues. PspA/IM30-like proteins are highly conserved, such that even distantly related family members can complement for each other, as recently demonstrated by the functional complementation of an *E. coli pspA*

mutant with VIPP1 from *Arabidopsis* (Zhang *et al*., 2012). Over the years, a number of functional GFP-fusions of PspA or VIPP1 proteins have been generated and rigorously evaluated in different organisms, such as *E. coli, Y. enterocolitica, Chlamydomonas reinhardtii*, and *Arabidopsis thaliana* (Zhang *et al*., 2012). Moreover, we observe a relocalization of LiaH from a diffuse cytoplasmic distribution to membrane-associated patches both upon bacitracin stress and at the onset of stationary phase without any external inducer, but not with other cell wall antibiotics. It is hard to imagine that such a specific response based on demonstrated protein–protein interactions could be the result of a translational GFP-fusion, especially in light of similar redistributions of functional PspA-GFP fusion proteins in the other organisms. Nevertheless, in the absence of a clear LiaH-dependent phenotype that could be used to demonstrate the full functionality of translational GFP-fusions to LiaH, this potential caveat needs to be taken into account when interpreting the data presented in this work.

Foci formation and motility is a universal feature of PspA/IM30 proteins

Our observations are reminiscent of a recent report on the cellular dynamics of the proteins that mount the PSP response in *Y. enterocolitica*, the phage-shock protein PspA, the enhancer protein PspF, and the membrane proteins PspB and PspC (Yamaguchi *et al*., 2013). Under non-inducing conditions, all four proteins appear as highly motile foci either in the cytoplasm (PspA, PspF) or at the cytoplasmic membrane (PspB and PspC), with PspA and PspF directly interacting with each other. Under stress-inducing conditions, PspA switches its partner and re-associates with PspC that together with PspB can then be found in large static complexes at the cytoplasmic membrane (Yamaguchi *et al*., 2013). Moreover, membrane association of PspA requires induction of the PSP response (Yamaguchi *et al*., 2010), just as described here for the Lia response. A complex formation of PspA in lateral and highly motile patches has previously also been observed for *E. coli* (Engl *et al*., 2009; Lenn *et al*., 2011).

Overall, the behaviour of PSP proteins from *Y. enterocolitica* is very similar to the dynamics of Lia proteins in *B. subtilis*. One difference is that LiaH is present in very low amounts dispersed in the cytoplasm under non-inducing conditions, where it exerts no known function and does not seem to have a protein-interaction partner. Taken together, the available data on the cellular dynamics of PSP-proteins emphasizes the striking similarities between the Lia responses of *B. subtilis*, a low G+C Gram-positive bacterium, and the PSP response in Gram-negative γ-proteobacteria, despite the mechanistically different molecular regulation mechanisms (Fig. 8). This

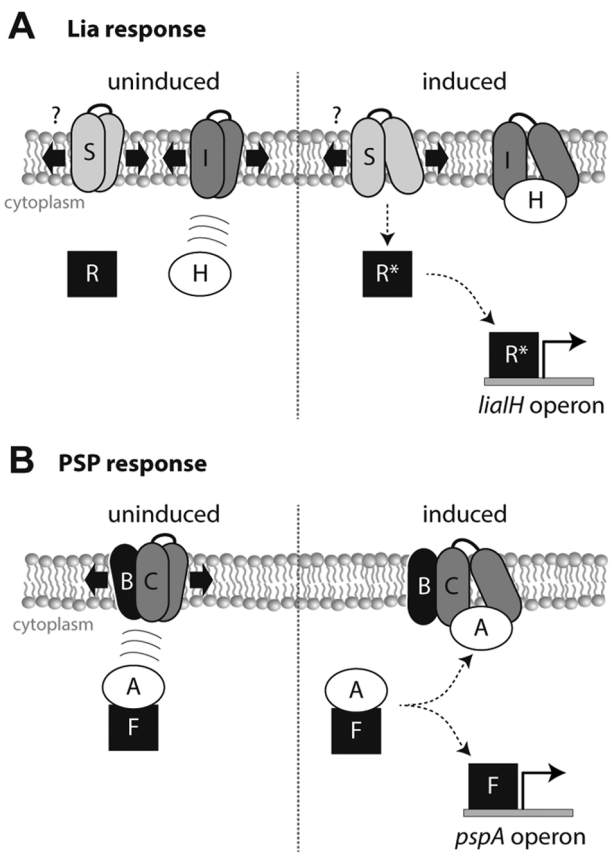

Fig. 8. Graphical model illustrating the dynamics of LiaI and the relocalization of LiaH during the Lia stress response of *B. subtilis* (A) in comparison to the partner switching model of PspA dynamics during the PSP stress response of *Y. enterocolitica* shown in (B). The cytoplasmic membrane and the individual proteins are shown. Arrows indicate the mobility of proteins in the presence and absence of stress. Figure 8B is adapted from Yamaguchi *et al*. (2013). See *Discussion* for details.

similarity seems to even reach beyond bacterial PspA-/IM30 family members. Two recent reports on the eukaryotic PspA-homologue VIPP1 from the alga *C. reinhardtii* and the plant *A. thaliana* demonstrated the formation of VIPP1-spots and even filaments within chloroplasts (Nordhues *et al*., 2012; Zhang *et al*., 2012). In the latter case, VIPP1 foci also showed dynamic movement, but in contrast to PspA and LiaH only under stress conditions (Zhang *et al*., 2012). Collectively, a unifying picture emerges that PspA/IM30 proteins exhibit their function in larger mobile or static complexes through protein–protein interactions at membrane interfaces. The close similarity of PspA-like proteins is also supported by the recent demonstration that *Arabidopsis* VIPP1 can functionally complement an *E. coli pspA* mutant (Zhang *et al*., 2012).

Coupling of stress response and gene regulation

A bacterial stress response usually is the combination of two cellular processes: (i) recruiting stress response pro-

teins to their site of action, and – often coupled to this – (ii) upregulation of the corresponding genes through a signal transducing mechanism. Along those lines, the model in Fig. 8 highlights an important difference between the proteobacterial PSP response and the Lia response in *B. subtilis*. In proteobacteria, the ultimate stress response and underlying gene regulation are tightly interlinked since they are mediated through the same mediator protein, PspC. In response to envelope stress PspC recruits PspA to the membrane and thereby elicits its protective role against cell envelope stress. At the same time, the latter releases its inhibitory grip on PspF, which is then able to induce expression of the *pspA* operon from a σ^{54}-dependent promoter (Darwin, 2005; Joly *et al*., 2010). Hence PspC, as the sensory input of the PSP response is also the mediator of the output – recruitment of PspA to the membrane. Accordingly, the PspC dynamics follows that of PspA: the foci become static under inducing conditions (Yamaguchi *et al*., 2013).

In contrast, the regulation is very different in *B. subtilis* and presumably other Firmicutes bacteria that harbour LiaIH homologues under control of the LiaFSR three-component system (Jordan *et al*., 2008; Schrecke *et al*., 2012). It seems that the membrane protein LiaI scans the envelope for damage and turns static once the cells encounter envelope stress and LiaH is recruited to the membrane. Since the LiaFSR-dependent stress regulation is fully functional in a *liaIH* deletion strain (Jordan *et al*., 2006), it seems that in *B. subtilis* – in contrast to the proteobacterial PSP response – there is just a regulatory but not a physical interaction between LiaFSR and LiaIH. Consequently, the ultimate stress response (recruitment of LiaH to the membrane) is uncoupled from stress-induced gene regulation, as also indicated by the data shown in Fig. 4. But it will require additional work on the cellular dynamics of LiaFSR before such hypotheses can be explored further.

Experimental procedures

Bacterial strains and growth conditions

All bacterial strains and plasmids are listed in Table 1 and Table S1 respectively. In general, *B. subtilis* and *E. coli* were grown in LB medium or on plates at 37°C with aeration. *B. subtilis* strains used in this study are derivatives of the laboratory wild-type strain W168.

DNA manipulations and cloning

Molecular cloning techniques were performed as described (Sambrook and Russell, 2001). For topology investigation vectors pHA-4 and pAC7 were used. Fragments of *liaI* were amplified (primers see Table S2) and cloned into pHA-4 to generate plasmids pDW401 and pDW402. LacZ fusions (pDW1001 and pDW1002, see Table S1) were constructed by cloning *liaI* fragments, fused with the promoter P_{veg} (primer TM856, see Table S2), into the promoter-less vector pAC7. The replicative vector pGP380 was used for protein overexpression to study protein interactions via SPINE. The cytoplasmic C-terminus of *liaI* was amplified (Table S2), restricted and cloned into pGP380 (Herzberg *et al*., 2007). *B. subtilis* W168 was transformed with the resulting plasmid pDW3802, generating the strain TMB688 (Table 1). As a control, *B. subtilis* W168 transformed with the empty vector pDG380 was used (TMB841). For BACTH analysis, genes were amplified from chromosomal DNA of *B. subtilis* (Table S2) and cloned into pUT18, pUT18C, pKT25 and pKT25N (Karimova *et al*., 1998) (Table S1).

GFP- and mRFPruby-fusion constructs were designed for fluorescence microscopy (Table S1). Fragments of *liaH* and *liaI* were amplified and cloned into pSG1151 (Lewis and Marston, 1999; Feucht and Lewis, 2001) to construct C-terminal GFP fusions via endogenous recombination into the native *lia*-locus (pDW5101 and pDW5102). Full-length versions of *liaI* and *liaH* were amplified and cloned into pSG1154 (Lewis and Marston, 1999; Feucht and Lewis, 2001) to generate C-terminal GFP fusions under the control of P_{xyl}, which were integrated into the *amyE* locus of *B. subtilis* W168 (pSJ5401and pSJ5402). The vector pRWB2 (Dominguez-Escobar *et al*., 2011) was used to fuse N-terminal mRFPruby to *liaH* under the control of P_{xyl} and later to integrate the plasmid (pDW6401) into the endogenous *lia*-locus by transformation of *B. subtilis* W168, generating strain TMB1714.

Construction of markerless liaI deletion

Markerless deletion of *liaI* was constructed using the vector pMAD (Arnaud *et al*., 2004). Genomic regions approximately 1 kb up- and downstream of the gene were amplified using primers listed in Table S2, and restricted. The two fragments were cloned into pMAD, generating pDW106. Mutants generation was performed as previously described (Arnaud *et al*., 2004). In brief: *B. subtilis* W168 was transformed with pDW106 and incubated at 30°C with MLS selection on LB agar plates supplemented with X-Gal (100 μg ml^{-1}). Blue colonies were selected and incubated for 6–8 h at 42°C in LB medium with MLS selection, resulting in the integration of pDW106 into the chromosome. Again, blue colonies were picked from LB (X-Gal) plates and incubated at 30°C for 6 h in LB medium without selection. Subsequently, the liquid culture was shifted to 42°C for 3 h, and the cells were then plated on LB (X-Gal) plates, this time without selective pressure. White colonies that had lost the plasmid were picked and checked for MLS sensitivity. The resulting strain TMB1394 was subsequently analysed by PCR and sequenced for the integrity of the desired genetic modifications.

PhoA/LacZ activity assay

The topology of LiaI was tested by using the PhoA/LacZ activity assay. *E. coli* strain CC118 was transformed with plasmids containing *phoA*-fusions (pDW401and pDW402 Table S1) and streaked on agar plates with 5-brom-4-chlor-3-indolylphosphate (BCIP 50 μg ml^{-1}), ampicillin (100 μg ml^{-1}) and arabinose (0.2% w/v). Plasmids containing *lacZ*-fusions

(pDW1001 and pDW1002; Table S1) were transformed into *B. subtilis* W168 and streaked on agar plates with kanamycin (10 μg ml^{-1}) and X-Gal (100 μg ml^{-1}). Plates were incubated at 37°C overnight, followed by blue-white screening (Manoil, 1991).

In vivo *cross-linking (SPINE)*

SPINE (Strep-protein interaction experiment) was performed as described (Herzberg *et al*., 2007) by using formaldehyde, a cross-linking agent (final concentration 0.6%). In brief, cells were grown in LB at 37°C to an OD_{600} of 1.0. Formaldehyde was added and after 20 min cells were harvested and washed in cell disruption buffer (50 mM Tris-HCl, 100 mM NaCl, pH 7.5). Again, cell pellets were resuspended in cell disruption buffer, then PMSF (1 mM) was added and cells were disrupted by sonication. After centrifugation, strep-tag purification was performed by using Strep-tactin columns (1 ml Strep-Tactin® sepharose, IBA, Goettingen, Germany). Proteins were separated on 12.5% SDS-PAGE and cross-linked proteins were detected by Western blot.

Cell fractionation

Bacillus subtilis cells were grown in LB at 37°C to an OD_{600} of 1.0 and then fractionated into cytoplasmic and membrane components as described (Schöbel *et al*., 2004): the cell pellet was resuspended in cell disruption buffer and disrupted by sonication. After centrifugation, the supernatant was ultracentrifuged at 4°C, 30 000 *g* for 1 h and the supernatant was again collected (= cytoplasmic fraction). The membrane pellet was washed and ultracentrifuged again (4°C, 30 000 *g*, 30 min). Finally, the membrane pellet was resuspended in cell disruption buffer. Protein concentrations of all collected fractions were determined by using BCA reagent (PIERCE) and 30 μg total protein was loaded per lane.

Immunoblotting

Immunoblotting by using α-Strep-Tactin horseradish peroxidase conjugate was performed according to the manufacturer's protocol (IBA, Goettingen). Western analysis with α-LiaH (1:5000) and α-rabbit horseradish peroxidase conjugate secondary antibody (1:7500) was done as described (Jordan *et al*., 2007).

Bacterial two-hybrid analysis

BACTH analysis was carried out as described (Karimova *et al*., 1998). *E. coli* BTH101 was co-transformed with plasmids containing genes of interest and either T18 or T25 fragments. After transformation, cells were spotted on agar plates with kanamycin (25 μg ml^{-1}), ampicillin (50 μg ml^{-1}), X-Gal (40 μg ml^{-1}) and IPTG (0.5 mM) and incubated at 30°C for 40 h. Blue colonies indicate potential protein–protein interactions. Empty vectors or vectors carrying fusions of the leucine zipper of GCN4 to the T18/T25 fragments were used as negative and positive controls respectively.

Sample preparation for microscopy

Overnight pre-cultures of *B. subtilis* were grown in LB medium supplemented with xylose (0.05%) and appropriate antibiotic selection from freshly isolated colonies on plate. Day cultures were performed by diluting pre-culture to an OD_{600} of 0.01–0.05 in LB and grown at 30°C. Expression of fluorescent xylose-inducible fusions was induced by addition of xylose to 0.05%. Samples for microscopic observation were taken at exponential phase (OD_{600} of 0.3–0.6) or stationary phase (OD_{600} of 1.7–2.0) and immobilized on 1.2% agarose-coated microscope slides as described (Glaser *et al*., 1997). To stain the bacterial membranes, the vital membrane dye FM4–64 was added to obtain the final concentration of 2 μg ml^{-1} in uninduced cells. To induce with bacitracin, cells were diluted to an OD_{600} in uninduced cells of 0.2, then 1 ml of culture was harvested and resuspended in LB medium with 20 μg ml^{-1} bacitracin, cells were incubated again to an OD_{600} of 0.4 and samples were taken for microscopic observations.

Microscopy

All images were acquired on a custom TIRFM set-up from Till Photonics based on a fully automated iMIC-stand with climate control chamber and an Olympus 1.45 NA 100× objective. DPSS lasers with output powers of 75 mW at 488 nm (Coherent Sapphire) and 75 mW at 561 nm (Cobolt Jive) were used as light sources. Lasers were selected through an AOTF and directed through a broadband fibre to the iMIC. A galvanometer-driven 2-axis scanner head was used to adjust TIRFM incidence angles. Images were collected with an AndoriXON DU-897 EM CCD camera at maximum gain setting (300) attached to a 2× magnification lens. Acquisition was controlled by the Live Acquisition (Till Photonics) software package. For two-colour TIRFM experiments a double colour filter set was used. Incidence angles and z-position were adjusted individually for both channels to obtain comparable evanescent wave penetration depth and focus position. Time-lapse movies were taken on at least three different days for each strain. To follow LiaH dynamics exposure times of 100 ms and frame rates of 200 ms, for LiaI 50 ms and frame rates of 71 ms and for MreB exposure times of 100 ms and frame rates of 2 s were used. All images were processed in Metamorph v7.1.2 (Molecular Devices) using local background subtraction (flatten background function) and Gaussian filtering (kernel 1-3-1; 3-7-3; 1-3-1). Kymographs, linescans, colour overlay and image montages were performed with the respective functions in Metamorph. Images were rotated and zoomed for visualization purposes only. Number of foci per length quantification was made in ImageJ 1.43 (Wayne Rasband, National Institute of Health, USA).

Single particle tracking and MSD analysis

For the automated detection and quantitative analysis of particle trajectories a two-dimensional (2D) particle tracker Mosaic (Sbalzarini and Koumoutsakos, 2005) was used. For LiaI-GFP movies of 71 ms between frames (200 frames with exposure times of 50 ms) were analysed. For particle detection a radius of 3, a cut-off of 0, a percentile of 0.1–0.2% and for particle linking a link range of 2 and a displacement of 2

pixels were used. Trajectories of less than 10 frames were filtered. The tracking software returns the *x* and *y* positions of the traces in the respective frame of the movie, from which the mean squared displacement (MSD) was calculated. To that end, the squared displacement for each trajectory $\Delta r^2(t,\tau) = [x(t+\tau) - x(t)]^2 + [y(t+\tau) - y(t)]^2$ was averaged over all available *t*, resulting in the MSD of each trajectory $<\Delta r^2>(\tau)$. Finally, the MSD was averaged over about 100 trajectories for each protein species and condition. The resulting MSD curves were fitted with the normal and anomalous diffusion models described in the main text by using a trust-region reflective Newton method (MATLAB, The MathWorks). Standard deviations on estimated parameters were determined from 66.8% confidence intervals as described (Press *et al.*, 1992). Since the fitted models are nested, an *F*-test was performed to test whether the anomalous diffusion describes the data significantly better than the normal diffusion model.

Comparative genomic analysis

Domain-based analysis of protein sequences was performed using the SMART database (Schultz *et al.*, 1998) and the microbes-online website. Secondary predictions of the protein LiaI was carried out using database JPred3 (Cole *et al.*, 2008) (http://www.compbio.dundee.ac.uk/www-jpred/).

Acknowledgements

The authors would like to thank Elisa Granato, Sebastian Dintner, Johannes Schneider, Karen Schrecke, and Annika Sprenger for the construction of plasmids and strains. Moreover, we are indebted to Robyn Emmins (Newcastle) for the introduction to the bacterial two-hybrid system used in this study. Work in the author's labs was funded by grants from the Deutsche Forschungsgemeinschaft (DFG Grant MA2837/1-3 and MA2837/3-1 to TM, a start-up grant through the DFG priority programme SPP1617 to GF and the Cells-in-Motion Cluster of Excellence (EXC 1003 – CiM) at the University of Münster (RW-S)) and the Human Frontier Science Program (HFSP-RGY0067/2009-C to RW-S).

References

Arnaud, M., Chastanet, A., and Debarbouille, M. (2004) New vector for efficient allelic replacement in naturally nontransformable, low-GC-content, gram-positive bacteria. *Appl Environ Microbiol* **70:** 6887–6891.

Aseeva, E., Ossenbuhl, F., Eichacker, L.A., Wanner, G., Soll, J., and Vothknecht, U.C. (2004) Complex formation of Vipp1 depends on its a-helical PspA-like domain. *J Biol Chem* **279:** 35535–35541.

Bergler, H., Abraham, D., Aschauer, H., and Turnowsky, F. (1994) Inhibition of lipid biosynthesis induces the expression of the *pspA* gene. *Microbiology* **140:** 1937–1944.

Brissette, J.L., Russel, M., Weiner, L., and Model, P. (1990) Phage shock protein, a stress protein of *Escherichia coli*. *Proc Natl Acad Sci USA* **87:** 862–866.

Bultema, J.B., Fuhrmann, E., Boekema, E.J., and Schneider, D. (2010) Vipp1 and PspA: related but not twins. *Commun Integr Biol* **3:** 162–165.

Chastanet, A., and Carballido-Lopez, R. (2012) The actin-like MreB proteins in *Bacillus subtilis*: a new turn. *Front Biosci* **4:** 1582–1606.

Cole, C., Barber, J.D., and Barton, G.J. (2008) The Jpred 3 secondary structure prediction server. *Nucleic Acids Res* **36:** W197–W201.

Daley, D.O., Rapp, M., Granseth, E., Melen, K., Drew, D., and von Heijne, G. (2005) Global topology analysis of the *Escherichia coli* inner membrane proteome. *Science* **308:** 1321–1323.

Darwin, A.J. (2005) The phage-shock-protein response. *Mol Microbiol* **57:** 621–628.

Darwin, A.J. (2007) Regulation of the phage-shock-protein stress response in *Yersinia enterocolitica*. *Adv Exp Med Biol* **603:** 167–177.

Deich, J., Judd, E.M., McAdams, H.H., and Moerner, W.E. (2004) Visualization of the movement of single histidine kinase molecules in live *Caulobacter cells*. *Proc Natl Acad Sci USA* **101:** 15921–15926.

DeLisa, M.P., Lee, P., Palmer, T., and Georgiou, G. (2004) Phage shock protein PspA of *Escherichia coli* relieves saturation of protein export via the Tat pathway. *J Bacteriol* **186:** 366–373.

Dominguez-Escobar, J., Chastanet, A., Crevenna, A.H., Fromion, V., Wedlich-Söldner, R., and Carballido-Lopez, R. (2011) Processive movement of MreB-associated cell wall biosynthetic complexes in bacteria. *Science* **333:** 225–228.

Elderkin, S., Jones, S., Schumacher, J., Studholme, D., and Buck, M. (2002) Mechanism of action of the *Escherichia coli* phage shock protein PspA in repression of the AAA family transcription factor PspF. *J Mol Biol* **320:** 23–37.

Elderkin, S., Bordes, P., Jones, S., Rappas, M., and Buck, M. (2005) Molecular determinants for PspA-mediated repression of the AAA transcriptional activator PspF. *J Bacteriol* **187:** 3238–3248.

Engl, C., Jovanovic, G., Lloyd, L.J., Murray, H., Spitaler, M., Ying, L., *et al.* (2009) *In vivo* localizations of membrane stress controllers PspA and PspG in *Escherichia coli*. *Mol Microbiol* **73:** 382–396.

Feucht, A., and Lewis, P.J. (2001) Improved plasmid vectors for the production of multiple fluorescent protein fusions in *Bacillus subtilis*. *Gene* **264:** 289–297.

Garner, E.C., Bernard, R., Wang, W., Zhuang, X., Rudner, D.Z., and Mitchison, T. (2011) Coupled, circumferential motions of the cell wall synthesis machinery and MreB filaments in *B. subtilis*. *Science* **333:** 222–225.

Glaser, P., Sharpe, M.E., Raether, B., Perego, M., Ohlsen, K., and Errington, J. (1997) Dynamic, mitotic-like behavior of a bacterial protein required for accurate chromosome partitioning. *Genes Dev* **11:** 1160–1168.

Gueguen, E., Savitzky, D.C., and Darwin, A.J. (2009) Analysis of the *Yersinia enterocolitica* PspBC proteins defines functional domains, essential amino acids and new roles within the phage-shock-protein response. *Mol Microbiol* **74:** 619–633.

Gueguen, E., Flores-Kim, J., and Darwin, A.J. (2011) The *Yersinia enterocolitica* phage shock proteins B and C can form homodimers and heterodimers *in vivo* with the possibility of close association between multiple domains. *J Bacteriol* **193:** 5747–5758.

Hachmann, A.-B., Angert, E.R., and Helmann, J.D. (2009) Genetic analysis of factors affecting susceptibility of *Bacillus subtilis* to daptomycin. *Antimicrob Agents Chemother* **53:** 1598–1609.

Hankamer, B.D., Elderkin, S.L., Buck, M., and Nield, J. (2004) Organization of the AAA(+) adaptor protein PspA is an oligomeric ring. *J Biol Chem* **279:** 8862–8866.

Herzberg, C., Weidinger, L.A., Dörrbecker, B., Hübner, S., Stülke, J., and Commichau, F.M. (2007) SPINE: a method for the rapid detection and analysis of protein-protein interactions *in vivo*. *Proteomics* **7:** 4032–4035.

Horstman, N.K., and Darwin, A.J. (2012) Phage shock proteins B and C prevent lethal cytoplasmic membrane permeability in *Yersinia enterocolitica*. *Mol Microbiol* **85:** 445–460.

Huvet, M., Toni, T., Sheng, X., Thorne, T., Jovanovic, G., Engl, C., *et al*. (2011) The evolution of the phage shock protein response system: interplay between protein function, genomic organization, and system function. *Mol Biol Evol* **28:** 1141–1155.

Hyyryläinen, H.L., Sarvas, M., and Kontinen, V.P. (2005) Transcriptome analysis of the secretion stress response of *Bacillus subtilis*. *Appl Microbiol Biotechnol* **67:** 389–396.

Joly, N., Burrows, P.C., Engl, C., Jovanovic, G., and Buck, M. (2009) A lower-order oligomer form of phage shock protein A (PspA) stably associates with the hexameric AAA(+) transcription activator protein PspF for negative regulation. *J Mol Biol* **394:** 764–775.

Joly, N., Engl, C., Jovanovic, G., Huvet, M., Toni, T., Sheng, X., *et al*. (2010) Managing membrane stress: the phage shock protein (Psp) response, from molecular mechanisms to physiology. *FEMS Microbiol Rev* **34:** 797–827.

Jones, S.E., Lloyd, L.J., Tan, K.K., and Buck, M. (2003) Secretion defects that activate the phage shock response of *Escherichia coli*. *J Bacteriol* **185:** 6707–6711.

Jordan, S., Junker, A., Helmann, J.D., and Mascher, T. (2006) Regulation of LiaRS-dependent gene expression in *Bacillus subtilis*: identification of inhibitor proteins, regulator binding sites and target genes of a conserved cell envelope stress-sensing two-component system. *J Bacteriol* **188:** 5153–5166.

Jordan, S., Rietkötter, E., Strauch, M.A., Kalamorz, F., Butcher, B.G., Helmann, J.D., and Mascher, T. (2007) LiaRS-dependent gene expression is embedded in transition state regulation in *Bacillus subtilis*. *Microbiology* **153:** 2530–2540.

Jordan, S., Hutchings, M.I., and Mascher, T. (2008) Cell envelope stress response in Gram-positive bacteria. *FEMS Microbiol Rev* **32:** 107–146.

Karimova, G., Pidoux, J., Ullmann, A., and Ladant, D. (1998) A bacterial two-hybrid system based on a reconstituted signal transduction pathway. *Proc Natl Acad Sci USA* **95:** 5752–5756.

Karimova, G., Ullmann, A., and Ladant, D. (2000) A bacterial two-hybrid system that exploits a cAMP signaling cascade in *Escherichia coli*. *Methods Enzymol* **328:** 59–73.

Karlinsey, J.E., Maguire, M.E., Becker, L.A., Crouch, M.L.V., and Fang, F.C. (2010) The phage shock protein PspA facilitates divalent metal transport and is required for virulence of *Salmonella enterica* sv. Typhimurium. *Mol Microbiol* **78:** 669–685.

Kesel, S., Mader, A., Höfler, C., Mascher, T., and Leisner, M. (2013) Immediate and heterogeneous response of the LiaFSR two-component system of *Bacillus subtilis* to the peptide antibiotic bacitracin. *PLoS ONE* **8:** e53457.

Kobayashi, R., Suzuki, T., and Yoshida, M. (2007) *Escherichia coli* phage-shock protein A (PspA) binds to membrane phospholipids and repairs proton leakage of the damaged membranes. *Mol Microbiol* **66:** 100–109.

Leaver, M., and Errington, J. (2005) Roles for MreC and MreD proteins in helical growth of the cylindrical cell wall in *Bacillus subtilis*. *Mol Microbiol* **57:** 1196–1209.

Lenn, T., Leake, M.C., and Mullineaux, C.W. (2008) Clustering and dynamics of cytochrome bd-I complexes in the *Escherichia coli* plasma membrane *in vivo*. *Mol Microbiol* **70:** 1397–1407.

Lenn, T., Gkekas, C.N., Bernard, L., Engl, C., Jovanovic, G., Buck, M., and Ying, L. (2011) Measuring the stoichiometry of functional PspA complexes in living bacterial cells by single molecule photobleaching. *Chem Commun* **47:** 400–402.

Lewis, P.J., and Marston, A.L. (1999) GFP vectors for controlled expression and dual labelling of protein fusions in *Bacillus subtilis*. *Gene* **227:** 101–110.

MacRitchie, D.M., Buelow, D.R., Price, N.L., and Raivio, T.L. (2008) Two-component signaling and gram negative envelope stress response systems. *Adv Exp Med Biol* **631:** 80–110.

Manoil, C. (1991) Analysis of membrane protein topology using alkaline phosphatase and β-galactosidase gene fusions. *Methods Cell Biol* **34:** 61–75.

Margolin, W. (2000) Green fluorescent protein as a reporter for macromolecular localization in bacterial cells. *Methods* **20:** 62–72.

Mascher, T., Margulis, N.G., Wang, T., Ye, R.W., and Helmann, J.D. (2003) Cell wall stress responses in *Bacillus subtilis*: the regulatory network of the bacitracin stimulon. *Mol Microbiol* **50:** 1591–1604.

Mascher, T., Zimmer, S.L., Smith, T.A., and Helmann, J.D. (2004) Antibiotic-inducible promoter regulated by the cell envelope stress-sensing two-component system LiaRS of *Bacillus subtilis*. *Antimicrob Agents Chemother* **48:** 2888–2896.

Maxson, M.E., and Darwin, A.J. (2006) Multiple promoters control expression of the *Yersinia enterocolitica* phage-shock-protein A (*pspA*) operon. *Microbiology* **152:** 1001–1010.

Mehner, D., Osadnik, H., Lunsdorf, H., and Brüser, T. (2012) The Tat system for membrane translocation of folded proteins recruits the membrane-stabilizing Psp machinery in *Escherichia coli*. *J Biol Chem* **287:** 27834–27842.

Model, P., Jovanovic, G., and Dworkin, J. (1997) The *Escherichia coli* phage-shock-protein (*psp*) operon. *Mol Microbiol* **24:** 255–261.

Mullineaux, C.W., Nenninger, A., Ray, N., and Robinson, C. (2006) Diffusion of green fluorescent protein in three cell environments in *Escherichia coli*. *J Bacteriol* **188:** 3442–3448.

Niu, L., and Yu, J. (2008) Investigating intracellular dynamics of FtsZ cytoskeleton with photoactivation single-molecule tracking. *Biophys J* **95:** 2009–2016.

Nordhues, A., Schottler, M.A., Unger, A.K., Geimer, S., Schönfelder, S., Schmollinger, S., *et al*. (2012) Evidence for a role of VIPP1 in the structural organization of the photosynthetic apparatus in *Chlamydomonas*. *Plant Cell* **24:** 637–659.

Otters, S., Braun, P., Hubner, J., Wanner, G., Vothknecht, U.C., and Chigri, F. (2013) The first alpha-helical domain of the vesicle-inducing protein in plastids 1 promotes oligomerization and lipid binding. *Planta* **237:** 529–540.

Phillips, G.J. (2001) Green fluorescent protein – a bright idea for the study of bacterial protein localization. *FEMS Microbiol Lett* **204:** 9–18.

Pietiäinen, M., Gardemeister, M., Mecklin, M., Leskela, S., Sarvas, M., and Kontinen, V.P. (2005) Cationic antimicrobial peptides elicit a complex stress response in *Bacillus subtilis* that involves ECF-type sigma factors and two-component signal transduction systems. *Microbiology* **151:** 1577–1592.

Press, W.H., Teukolsky, S.A., Vetterling, W.T., and Flannerty, B.P. (1992) *Numerical Recipes in C: The Art of Scientific Computing*. New York: Cambridge University Press.

Raivio, T.L. (2005) Envelope stress responses and Gram-negative bacterial pathogenesis. *Mol Microbiol* **56:** 1119–1128.

Sambrook, J., and Russell, D.W. (2001) *Molecular Cloning – A Laboratory Manual*. Cold Spring Harbor, NY: Cold Spring Harbor Laboratory Press.

Saxton, M.J., and Jacobson, K. (1997) Single-particle tracking: applications to membrane dynamics. *Annu Rev Biophys Biomol Struct* **26:** 373–399.

Sbalzarini, I.F., and Koumoutsakos, P. (2005) Feature point tracking and trajectory analysis for video imaging in cell biology. *J Struct Biol* **151:** 182–195.

Schöbel, S., Zellmeier, S., Schumann, W., and Wiegert, T. (2004) The *Bacillus subtilis* σ^W anti-sigma factor RsiW is degraded by intramembrane proteolysis through YluC. *Mol Microbiol* **52:** 1091–1105.

Schrecke, K., Staroń, A., and Mascher, T. (2012) Two-component signaling in the Gram-positive envelope stress response: intramembrane-sensing histidine kinases and accessory membrane proteins. In *Two Component Systems in Bacteria*. Gross, R., and Beier, D. (eds). Hethersett, Norwich, UK: Horizon Scientific Press, pp. 199–229.

Schrecke, K., Jordan, S., and Mascher, T. (2013) Stoichiometry and perturbation studies of the LiaFSR system of *Bacillus subtilis*. *Mol Microbiol* **87:** 769–788.

Schultz, J., Milpetz, F., Bork, P., and Ponting, C.P. (1998) SMART, a simple modular architecture research tool: identification of signaling domains. *Proc Natl Acad Sci USA* **95:** 5857–5864.

Seo, J., Savitzky, D.C., Ford, E., and Darwin, A.J. (2007) Global analysis of tolerance to secretin-induced stress in *Yersinia enterocolitica* suggests that the phage-shock-protein system may be a remarkably self-contained stress response. *Mol Microbiol* **65:** 714–727.

Spira, F., Dominguez-Escobar, J., Müller, N., and Wedlich-Söldner, R. (2012) Visualization of cortex organization and dynamics in microorganisms, using total internal reflection fluorescence microscopy. *J Vis Exp* **63:** e3982.

Standar, K., Mehner, D., Osadnik, H., Berthelmann, F., Hause, G., Lunsdorf, H., and Brüser, T. (2008) PspA can form large scaffolds in *Escherichia coli*. *FEBS Lett* **582:** 3585–3589.

Staroń, A., Finkeisen, D.E., and Mascher, T. (2011) Peptide antibiotic sensing and detoxification modules of *Bacillus subtilis*. *Antimicrob Agents Chemother* **55:** 515–525.

Toymentseva, A.A., Schrecke, K., Sharipova, M.R., and Mascher, T. (2012) The LIKE system, a novel protein expression toolbox for *Bacillus subtilis* based on the *liaI* promoter. *Microb Cell Fact* **11:** 143.

Veening, J.-W., Hamoen, L.W., and Kuipers, O.P. (2005) Phosphatases modulate the bistable sporulation gene expression pattern in *Bacillus subtilis*. *Mol Microbiol* **56:** 1481–1494.

Vothknecht, U.C., Otters, S., Hennig, R., and Schneider, D. (2012) Vipp1: a very important protein in plastids? *J Exp Bot* **63:** 1699–1712.

Vrancken, K., Van Mellaert, L., and Anne, J. (2008) Characterization of the *Streptomyces lividans* PspA response. *J Bacteriol* **190:** 3475–3481.

Wang, Y.Y., Fu, Z.B., Ng, K.L., Lam, C.C., Chan, A.K., Sze, K.F., and Wong, W.K. (2011) Enhancement of excretory production of an exoglucanase from *Escherichia coli* with phage shock protein A (PspA) overexpression. *J Microbiol Biotechnol* **21:** 637–645.

Wenzel, M., Kohl, B., Munch, D., Raatschen, N., Albada, H.B., Hamoen, L., *et al*. (2012) Proteomic response of *Bacillus subtilis* to lantibiotics reflects differences in interaction with the cytoplasmic membrane. *Antimicrob Agents Chemother* **56:** 5749–5757.

White, C.L., and Gober, J.W. (2012) MreB: pilot or passenger of cell wall synthesis? *Trends Microbiol* **20:** 74–79.

Wiegert, T., Homuth, G., Versteeg, S., and Schumann, W. (2001) Alkaline shock induces the *Bacillus subtilis* σ^W regulon. *Mol Microbiol* **41:** 59–71.

Wolf, D., Kalamorz, F., Wecke, T., Juszczak, A., Mäder, U., Homuth, G., *et al*. (2010) In-depth profiling of the LiaR response of *Bacillus subtilis*. *J Bacteriol* **192:** 4680–4693.

Yamaguchi, S., and Darwin, A.J. (2012) Recent findings about the *Yersinia enterocolitica* phage shock protein response. *J Microbiol* **50:** 1–7.

Yamaguchi, S., Gueguen, E., Horstman, N.K., and Darwin, A.J. (2010) Membrane association of PspA depends on activation of the phage-shock-protein response in *Yersinia enterocolitica*. *Mol Microbiol* **78:** 429–443.

Yamaguchi, S., Reid, D.A., Rothenberg, E., and Darwin, A.J. (2013) Changes in Psp protein binding partners, localization and behaviour upon activation of the *Yersinia enterocolitica* phage shock protein response. *Mol Microbiol* **87:** 656–671.

Zhang, L., Kato, Y., Otters, S., Vothknecht, U.C., and Sakamoto, W. (2012) Essential role of VIPP1 in chloroplast envelope maintenance in *Arabidopsis*. *Plant Cell* **24:** 3695–3707.

Supporting information

Additional supporting information may be found in the online version of this article at the publisher's web-site.

CHAPTER IV

Cannibalism Stress Response in *Bacillus subtilis*

Carolin Höfler, Judith Heckmann, Anne Fritsch, Philipp Popp, Susanne Gebhard, Georg Fritz, Thorsten Mascher

Microbiology, published ahead of print, doi: 10.1099/mic.0.000176

Cannibalism Stress Response in *Bacillus subtilis*

Carolin Höfler[a], Judith Heckmann[a], Anne Fritsch[a], Philipp Popp[a], Susanne Gebhard[a,1], Georg Fritz[a,2], and Thorsten Mascher[a,3,*]

[a]Department Biology I, Ludwig-Maximilians-Universität München, Großhaderner Str. 2-4, 82152 Planegg-Martinsried, Germany

[1]Present address: Department of Biology and Biochemistry, University of Bath, Claverton Down, Bath BA2 7AY, United Kingdom

[2]Present address: LOEWE-Center for Synthetic Microbiology, Philipps-Universität Marburg, Hans-Meerwein-Str. 6, 35043 Marburg, Germany

[3]Present address: Technische Universität Dresden, Institute of Microbiology, Zellescher Weg 20b, 01217 Dresden, Germany

Keywords: Cell envelope stress response, antimicrobial peptides, stationary phase survival, Bce system, ECF σ factors.

Subject category: Regulation

Running Title: Cannibalism stress response in *B. subtilis*

Word count: 5221

[*]Corresponding author: Prof. Dr. Thorsten Mascher, Tel.: +49 351 463-40420, Fax: +49 351 463-37715, Email: thorsten.mascher@tu-dresden.de

4.1 Abstract

When faced with carbon source limitation, the Gram-positive soil organism *Bacillus subtilis* initiates a survival strategy called sporulation, which leads to the formation of highly resistant endospores that allow *B. subtilis* to survive even long periods of starvation. In order to avoid commitment to this energy-demanding and irreversible process, *B. subtilis* employs another strategy called cannibalism to delay sporulation as long as possible. Cannibalism involves the production and secretion of two cannibalism toxins, the sporulation delaying protein, SDP, and the sporulation killing factor, SKF, which are able to lyse sensitive siblings. The lysed cells are thought to provide nutrients for the cannibals to slow down or even prevent them from entering sporulation. In this study, we uncovered the role of the cell envelope stress response (CESR), especially the Bce-like antimicrobial peptide detoxification modules, in cannibalism stress response during stationary phase. SDP and SKF specifically induce Bce-like systems and some ECF σ factors in stationary phase cultures, but only the latter provide some degree of protection. A full Bce response is only triggered by mature toxins, but not by toxin precursors. Our study provides insights into the close relationship between stationary phase survival and the CESR of *B. subtilis*.

4.2 Introduction

In their natural environment, microorganisms constantly compete for nutrients. In order to defend their habitat against invading species, many bacteria produce and secrete antimicrobial peptides (AMPs) that interfere with the integrity or biosynthesis of the cell envelope. AMP action leads to an arrest in cell growth and often to cell lysis (Silver, 2003, Walsh, 2003, Silver, 2006). To defend against such antimicrobial attacks, many bacteria induce a complex cell envelope stress response (CESR). In *Bacillus subtilis*, the underlying regulatory network is orchestrated by four two-component systems (TCS) and seven extracytoplasmic function (ECF) σ factors (Helmann, 2002, Jordan *et al.*, 2007, Schrecke *et al.*, 2012).

While it is generally accepted that the CESR network has evolved to maintain envelope integrity in the face of AMPs produced by competing species, little is known about the extent to which it is also involved in responding to endogenously produced AMPs. For instance, although it is known that the AMPs are co-expressed with dedicated immunity proteins that prevent cells from autolysis (Gonzalez-Pastor *et al.*, 2003, Ellermeier *et al.*, 2006, Dubois *et al.*, 2009), it is conceivable that the level of self-protection via these mechanisms can be insufficient, raising the need for additional protection by the CESR network. In fact, we recently reported that in early stationary phase a subpopulation of *B. subtilis* cells strongly induces one of the CESR modules, the LiaRS system, even in the absence of competitors and without any external addition of AMPs (Jordan *et al.*, 2007, Dominguez-Escobar *et al.*, 2014). Here, we set out to test whether other systems of the CESR network of *B. subtilis* also displayed such an intrinsic induction behavior during stationary phase and, if so, whether this was causally related to the endogenous production of AMPs.

To study these questions, we focused on the expression of the core of the CESR network, comprising the AMP-resistance modules, BceRS and PsdRS, as well as the ECF σ factors σ^M, σ^X and σ^W. While the BceRS and PsdRS systems regulate ABC transporters (BceAB and PsdAB, respectively) that specifically confer resistance against a number of AMPs (Staroń *et al.*, 2011), the regulons of the ECF σ factors are known to play a more promiscuous role in cell envelope stress response to antimicrobial compounds (Missiakas & Raina, 1998, Helmann, 2002, Mascher *et al.*, 2007, Kingston *et al.*, 2013). σ^M, σ^X and σ^W each regulate a set of about 30-60 target genes with partially overlapping specificity (Mascher *et al.*, 2007, Kingston *et al.*, 2013), and all are activated in a growth phase- and growth medium-dependent manner (Huang *et al.*, 1998): While σ^M and σ^X are induced mainly in late logarithmic growth phase, σ^W only becomes active in early stationary phase (Huang *et al.*, 1998, Nicolas *et al.*, 2012).

So far, no growth phase dependency has been observed for the BceRS and PsdRS modules. Both systems respond to and mediate resistance against a variety of peptide antibiotics: The BceRS system responds to the cyclic peptide antibiotic bacitracin and to a lesser extent also to the lantibiotics actagardine and mersacidin (Mascher *et al.*, 2003, Rietkötter *et al.*, 2008), while the PsdRS system responds primarily to lantibiotics, such as nisin or gallidermin (Staroń *et al.*, 2011). Since the *B. subtilis* strain W168 is known to produce and secrete a variety of similar AMPs, it was conceivable that they might also act as inducers of the BceRS and PsdRS modules.

In this study, we show that the BceRS and PsdRS system are, in fact, intrinsically activated during stationary phase growth of *B. subtilis*, and single out the inducers amongst a number of endogenously produced AMP candidates. The biological role of these AMPs has previously been implicated in a process termed “cannibalism”, in which the stationary phase population bifurcates into a fraction of AMP-producing cells that feed on another fraction of non-producing cells (Chung *et al.*, 1994, Gonzalez-Pastor *et al.*, 2003). Our data reveals that the CESR network not only serves as a defense against extrinsic attacks from competing species, but also plays a novel role in the intrinsic cannibalism stress response. Interestingly, we show that induction of the BceRS and PsdRS modules by cannibalism toxins critically hinges on the presence of the cognate immunity proteins, providing further insight into the mode of stimulus perception by these systems.

4.3 Methods

4.3.1 Media and growth conditions

B. subtilis and *E. coli* were routinely grown in Luria Bertani (LB) medium or MCSE (Radeck *et al.*, 2013) including 0.2% fructose (w/v) as C-source at 37°C with agitation. The final composition of MCSE is as follows: 1× MOPS (from 10× MOPS buffer: 83.72 g l^{-1} MOPS, 33 g l^{-1} $(NH_4)_2SO_4$, 3.85 mM KH_2PO_4, 6.15 mM K_2HPO_4; adjusted to pH 7 with KOH), 50 mg l^{-1} Tryptophan, 22 mg l^{-1} ammonium ferric citrate, 1× III’-salts (232 mg l^{-1} $MnSO_4x4H_2O$, 12.3 g l^{-1} $MgSO_4x7H_2O$), 0.8% (w/v) K-glutamate, 0.6% (w/v) Na-succinate, 0.2% (w/v) fructose. MCSE results in well-defined growth behavior and supports sporulation of *B. subtilis* under the growth conditions applied. Selective

media for *B. subtilis* contained chloramphenicol (5 µg ml^{-1}), kanamycin (10 µg ml^{-1}), spectinomycin (100 µg ml^{-1}), or erythromycin (1 µg ml^{-1}) plus lincomycin (25 µg ml^{-1}) for macrolide-lincosamide-streptogramin B (MLS) resistance. Selective media for *E. coli* contained ampicillin (100 µg ml^{-1}) or chloramphenicol (35 µg ml^{-1}). Solid media additionally contained 1.5% (w/v) agar.

4.3.2 Bacterial strains and plasmids

Transcriptional promoter fusions to bacterial luciferase (*luxABCDE*) were constructed in pAH328 (Schmalisch *et al.*, 2010) or the pAH328 derivative pBS3Clux (Radeck *et al.*, 2013) using *Not*I/*Sal*I or *EcoR*I/*Spe*I restriction enzymes, respectively. All strains used in this study are listed in Table 1 (at the end of section 4.3). All *B. subtilis* strains in this study are derivatives of the laboratory wild type strain W168. All plasmids and oligonucleotides are listed in Table 2 and 3, respectively (at the end of section 4.3).

4.3.3 DNA manipulations

All plasmids were constructed by standard cloning techniques and ligation mixtures were transformed into *E. coli* competent cells (DH5α, XL1-blue). The plasmids were verified by sequencing and transformed into *B. subtilis* as described previously (Harwood & Cutting, 1990). Plasmid integration into the *B. subtilis* chromosome was checked by colony-PCR. Preparation of chromosomal DNA from *B. subtilis* for transformation was prepared according to standard procedure (Cutting & Van der Horn, 1990).

4.3.4 Allelic replacement mutagenesis of *sdpAB*, *sdpC*, *sdpI*, *skfA-H*, *skfA*, *skfBC*, *skfEF*, *skfGH*, *skfH*, *sunA* and *yydF-J* using LFH-PCR

Long Flanking Homology PCR (LFH-PCR) technique was performed as described previously (Mascher *et al.*, 2003). The constructed strains are listed in Table 1 and the corresponding primers are listed in Table 3 (at the end of section 4.3).

4.3.5 Luminescence Assay

Promoter activities were detected by following luminescence in a Synergy™2 multi-mode microplate reader from BioTek® (Winooski, VT, USA) using Gen5™ software. Strain cultivation was performed as follows: Freshly prepared and pre-warmed (37°C) MCSE medium was inoculated 1:500 from overnight cultures and incubated at 37°C with agitation until OD_{600} 0.2. The culture was subsequently diluted to an OD_{600} of 0.05 with MCSE and 100 µl were transferred to one well of a 96-well plate (black walls, clear bottom; Greiner Bio-One, Frickenhausen, Germany). OD_{600} and luminescence were recorded every ten minutes for 18 hours. Incubation was performed at 37°C with agitation (medium intensity). Raw luminescence data were normalized to cell density by dividing luminescence per OD_{600} at each data point (relative luminescence units (RLU) / OD_{600}). For each individual sample, OD_{600} and luminescence were background-corrected by subtracting the respective mean values measured for MCSE medium only and TMB1578 (pAH328 empty) over every time point. Subsequently, RLU/OD_{600} values were calculated for each measurement and

mean values and SEM (standard error of the mean) were determined from at least three independent biological replicates.

Table 1: Strains used in this study.

E. coli	**Genotype**	**Reference**
DH5α	*recA1 endA1 gyrA96 thi hsdR17*rK- mK+*relA1 supE44* *ϕ*80Δ*lacZ*Δ*M15* Δ(*lacZYA-argF*)*U169*	(Sambrook & Russell, 2001)
XL1-blue	*endA1 gyrA96*(*nal*^{R}) *thi*-1 *recA1 relA1 lac gln*V44 F′[Tn10 *proAB*$^{+}$ *lacI*^{q} Δ(*lacZ*)*M15*] *hsdR17*(rK^{-} mK^{+}) *tet*^{R}	lab stock
B. subtilis	**Genotype**	**Reference**
W168	*trpC2*	lab stock
TMB1518	W168 Δ*bceRSAB psdRSAB yxdJKLM yxeA* (clean)	(Gebhard *et al.*, 2014)
TMB1528	W168 *sdpI*::mls	this study
TMB1578	W168 *sacA*::*luxABCDE* (without promoter)	this study
TMB1619	W168 *sacA*::pCHlux103 (P_{bceA}-*lux*)	this study
TMB1620	W168 *sacA*::pCHlux104 (P_{bcrC}-*lux*)	this study
TMB1768	W168 *sdpC*::kan	this study
TMB1770	W168 *sacA*::pCHlux103 (P_{bceA}-*lux*) *sdpC*::kan	this study
TMB1773	W168 *sacA*::pCHlux103 (P_{bceA}-*lux*) *skfA-H*::spec	this study
TMB1775	W168 *sacA*::pCHlux103 (P_{bceA}-*lux*) *yydF-J*::spec	this study
TMB1843	W168 *sacA*::pCHlux103 (P_{bceA}-*lux*) *sunA*::kan	this study
TMB1985	W168 *sacA*::pJHlux102 (P_{sdpA}-*lux*)	this study
TMB2009	W168 *sacA*::pJHlux104 (P_{psdA}-*lux*)	this study
TMB2015	W168 *sacA*::pCHlux103 (P_{bceA}-*lux*) *sdpC*::kan *skfA-H*::spec	this study
TMB2016	W168 *sacA*::pJHlux105 (P_{skfA}-*lux*)	this study
TMB2047	W168 *sacA*::pJHlux104 (P_{psdA}-*lux*) *sdpC*::kan	this study
TMB2048	W168 *sacA*::pJHlux104 (P_{psdA}-*lux*) *skfA-H*::spec	this study
TMB2118	W168 *sacA*::pCHlux103 (P_{bceA}-*lux*) *sdpI*::mls	this study
TMB2164	W168 *sacA*::pCHlux103 (P_{bceA}-*lux*) *skfA-H*::spec *sdpAB*::mls	this study
TMB2166	W168 Δ*bceRSAB psdRSAB yxdJKLM yxeA* (clean) *sdpI*::mls	this study
TMB2207	W168 *sacA*::pCHlux104 (P_{bcrC}-*lux*) *sdpC*::kan	this study
TMB2208	W168 *sacA*::pCHlux104 (P_{bcrC}-*lux*) *skfA-H*::spec	this study
TMB2209	W168 *sacA*::pCHlux104 (P_{bcrC}-*lux*) *sunA*::kan	this study
TMB2210	W168 *sacA*::pCHlux104 (P_{bcrC}-*lux*) *yydF-J*::spec	this study
TMB2211	W168 *sacA*::pJHlux102 (P_{sdpA}-*lux*) *sdpI*::mls	this study
TMB2212	W168 *sacA*::pJHlux105 (P_{skfA}-*lux*) *sdpI*::mls	this study
TMB2221	W168 *sacA*::pCHlux104 (P_{bcrC}-*lux*) *sdpC*::kan *skfA-H*::spec	this study
TMB2222	W168 *sacA*::pJHlux104 (P_{psdA}-*lux*) *sdpC*::kan *skfA-H*::spec	this study
TMB2223	W168 *sacA*::pJHlux104 (P_{psdA}-*lux*) *yydF-J*::spec	this study
TMB2224	W168 *sacA*::pJHlux104 (P_{psdA}-*lux*) *sunA*::kan	this study
TMB2240	W168 *spo0A*::spec	this study
TMB2257	W168 *sacA*::pCH3Clux02 (P_{sigX}-*lux*)	this study
TMB2259	W168 *sacA*::pCH3Clux04 (P_{ydaH}-*lux*)	this study
TMB2260	W168 *skfA*::mls	this study

Table 1: continued.

TMB2262	W168 *skfEF*::mls	this study
TMB2265	W168 *sacA*::pCHlux103 (P_{bceA}-*lux*) *skfA*::mls	this study
TMB2266	W168 *sacA*::pCHlux103 (P_{bceA}-*lux*) *skfBC*::spec	this study
TMB2267	W168 *sacA*::pCHlux103 (P_{bceA}-*lux*) *skfEF*::mls	this study
TMB2268	W168 *sacA*::pCHlux103 (P_{bceA}-*lux*) *skfH*::kan	this study
TMB2299	W168 *sacA*::pASp3Clux01 (P_{pspA}-*lux*)	this study
TMB2339	W168 *sacA*::pCHlux103 (P_{bceA}-*lux*) *skfGH*::kan	this study
TMB2806	W168 *sacA*::pCHlux103 (P_{bceA}-*lux*) *sdpC*::kan *skfGH*::mls	this study
TMB2909	W168 Δ*bceRSAB psdRSAB yxdJKLM yxeA* (clean) *skfEF*::mls	this study

Table 2: Vectors and plasmids used in this study.

Plasmid/vector	Genotype[a]	Primers used for cloning	Reference/source
pAH328	*sacA*'…'*sacA*, *luxABCDE*, *bla*, *cat*		(Schmalisch *et al.*, 2010)
pBS3Clux	pAH328 derivative; *sacA*'…'*sacA*, *luxABCDE*, *bla*, *cat*		(Radeck *et al.*, 2013)
pCHlux103	pAH328 derivative, *sacA*::P_{bceA}-*lux*, *cat*	TM2513/2514	this study
pCHlux104	pAH328 derivative, *sacA*::P_{bcrC}-*lux*, *cat*	TM2515/2516	this study
pJHlux102	pAH328 derivative, *sacA*::P_{sdpA}-*lux*, *cat*	TM2785/2786	this study
pJHlux104	pAH328 derivative, *sacA*::P_{psdA}-*lux*, *cat*	TM2781/2782	this study
pJHlux105	pAH328 derivative, *sacA*::P_{skfA}-*lux*, *cat*	TM2783/2784	this study
pCH3Clux02	pAH328 derivative, *sacA*::P_{sigX}-*lux*, *cat*	TM3262/3263	this study
pCH3Clux04	pAH328 derivative, *sacA*::P_{ydaH}-*lux*, *cat*	TM3266/3267	this study
pASp3Clux01	pAH328 derivative, *sacA*::P_{pspA}-*lux*, *cat*	TM3268/3269	this study

[a]Resistance cassettes: *bla* = ampicillin, *cat* = chloramphenicol

Table 3: Oligonucleotides used in this study.

Primer name	Sequence 5' – 3'[a]
Construction of transcriptional promoter-lux fusions	
TM2513 P_{bceA} *Not*I fwd	a***gcggccgc***ACGCGGTGAAATACAGCGAAG
TM2514 P_{bceA} *Sal*I rev	taa***gtcgac***TATATTGGATAATCTCATTATAAAAAG
TM2515 P_{bcrC} *Not*I fwd	a***gcggccgc***GGCCTTCAAAAAGCACATACG
TM2516 P_{bcrC} *Sal*I rev	taa***gtcgac***TTACATTTTTATATTTAGTAGACTAATC
TM2785 P_{sdpA} *EcoR*I fwd	ttatag***gaattc***cgcggccgcttctagagGATGACGCTTACGGAATTATCTG
TM2786 P_{sdpA} *Spe*I rev	ctataa***actagt***TTTTTTGATGTAGATTACCTCCTC
TM2781 P_{psdA} *EcoR*I fwd	ttatag***gaattc***cgcggccgcttctagagTGATGCTGCAAACGGCCC
TM2782 P_{psdA} *Spe*I rev	ctataa***actagt***TTTCTTTATTATAAAAAGGAAGTCAGC
TM2783 P_{skfA} *EcoR*I fwd	ttatag***gaattc***cgcggccgcttctagagATGACAGATTCGTATTGCCGG
TM2784 P_{skfA} *Spe*I rev	ctataa***actagt***TCAATTTTTGCATAGAGTCTATTGAC

Table 3: continued.

TM3262 P_{sigX} *EcoR*I fwd	ttatag***gaattc***cgcggccgcttctagagACTCCGGGTCTGGCATACC
TM3263 P_{sigX} *Spe*I rev	ctataa***actagt***TCACTTTTTTGTCGTATGAATAGCTTG
TM3266 P_{ydaH} *EcoR*I fwd	ttatag***gaattc***cgcggccgcttctagagTTTGAGAGAGAAGCTTACCGC
TM3267 P_{ydaH} *Spe*I rev	ctataa***actagt***AATTTCATCCTAGAGATAAGACTGG
TM3268 P_{pspA} *EcoR*I fwd	ttatag***gaattc***cgcggccgcttctagagTCCGGTGACATCAATTGACTC
TM3269 P_{pspA} *Spe*I rev	ctataa***actagt***AAAGCTAATTCGGTAACCCTTG
Allelic replacement mutagenesis (LFH-PCR)	
TM2748 *sdpC* up fwd	GAAGGTTATATTGACACCTATAATCC
TM2749 *sdpC* up rev	*CCTATCACCTCAAATGGTTCGCTG*GTTACCATGGAAACAATCAATAGCC
TM2750 *sdpC* do fwd	*CGAGCGCCTACGAGGAATTTGTATCG*GCTGCTGCAAAAACCCTAAAATTG
TM2751 *sdpC* do rev	CAAATATCTAAATGTCTAAATGTTTTTTTGTAAAG
TM2744 *skf* up fwd	TGGTGCGTTAGGGGTTATGATTGC
TM2745 *skf* up rev	*CCTATCACCTCAAATGGTTCGCTG*CTCACAGATTCCCATTCTTTTTGG
TM2746 *skf* do fwd	*CGAGCGCCTACGAGGAATTTGTATCG*GGAGATGTTGGTTGGGATAAGATG
TM2747 *skf* do rev	GATTTGCTGCCGTTTTGGTAAGAC
TM2723 *sunA* up fwd	GTATCACGATGGATATTTATAGATGC
TM2724 *sunA* up rev	*CCTATCACCTCAAATGGTTCGCTG*GTTTTCGAGTTCCTCTAGTTTAACTTC
TM2725 *sunA* do fwd	*CGAGCGCCTACGAGGAATTTGTATCG*GAGCTGTTGCTTGTCAAAACTATC
TM2726 *sunA* do rev	GGGAGAATAATTGTTAAGAAAAGAATG
TM3138 *sdpAB* up fwd	CAGACAATTGAATGCTTCCC
TM3139 *sdpAB* up rev	*CCTATCACCTCAAATGGTTCGCTG*GCTAAAGTAATAAGAAGAAAATAATAG
TM3140 *sdpAB* do fwd	*CGAGCGCCTACGAGGAATTTGTATCG*GGTGAATCAGTCAAGTTTCTTAC
TM3141 *sdpAB* do rev	GTGGAAATTCTATGCAGCTAG
TM0307 *spo0A* up fwd	TATCAGAGATTCTGCTGCTGGC
TM0308 *spo0A* up rev	*CCTATCACCTCAAATGGTTCGCTG*AGCGACAGGCATTCCTGTCC
TM0309 *spo0A* do fwd	*CGAGCGCCTACGAGGAATTTGTATCG*GTTGCGGATAAGCTGAGG
TM0310 *spo0A* do rev	GGAAGAACCTGAGACACCG
TM3315 *skfA* do fwd	*CGAGCGCCTACGAGGAATTTGTATCG*CGTGTTTGTGCACTTCCGCATC
TM3316 *skfA* do rev	GCTTCCCTAAGCTGTATTTGAACC
TM3317 *skfBC* up fwd	GTACAGTACGATTGCCTTGATCG
TM3318 *skfBC* up rev	*CCTATCACCTCAAATGGTTCGCTG*GAACCGCTAACTCTGGCAAATC
TM3319 *skfBC* do fwd	*CGAGCGCCTACGAGGAATTTGTATCG*GAAACATATGCATCATGATCAGCC
TM3320 *skfBC* do rev	CTGCCATTTGACTTGGTAATCG
TM3321 *skfEF* up fwd	CAGTACTTATTGGTACATAGCGG
TM3322 *skfEF* up rev	*CCTATCACCTCAAATGGTTCGCTG*CATCACCATTTCGATAGCATTTGC
TM3323 *skfEF* do fwd	*CGAGCGCCTACGAGGAATTTGTATCG*CATAGGGAGCCTAAGTTGGTG
TM3324 *skfEF* do rev	CATCGTTTTAGTAATGATCTGACC
TM3325 *skfH* up fwd	GAATTGTCAGACATTCTCAATCAG
TM3326 *skfH* up rev	*CCTATCACCTCAAATGGTTCGCTG*CTTGGCCATTCAGTCAACATTTG
TM3393 *skfGH* up fwd	GTGCCAGAACAGTGAAGAAAATG
TM3394 *skfGH* up rev	*CCTATCACCTCAAATGTTCGCTG*GAACAGATAACGACAATTTATCACC
TM0137 kan fwd	CAGCGAACCATTTGAGGTGATAGG

Table 3: continued.

TM0138 kan rev	CGATACAAATTCCTCGTAGGCGCTCGG
TM0139 mls fwd	CAGCGAACCATTTGAGGTGATAGGGATCCTTTAACTCTGGCAACCCTC
TM0140 mls rev	CGATACAAATTCCTCGTAGGCGCTCGGGCCGACTGCGCAAAAGACATAATCG
TM0141 spec fwd	CAGCGAACCATTTGAGGTGATAGGGACTGGCTCGCTAATAACGTAACGTGACTGGCAAGAG
TM0142 spec rev	CGATACAAATTCCTCGTAGGCGCTCGGCGTAGCGAGGGCAAGGGTTTATTGTTTTCTAAAATCTG
Check primers	
TM2505 *sacA* front check fwd	CTGATTGGCATGGCGATTGC
TM2506 *sacA* front check rev	ACAGCTCCAGATCCTCTACG
TM2507 *sacA* back check fwd	GTCGCTACCATTACCAGTTG
TM2508 *sacA* back check rev	TCCAAACATTCCGGTGTTATC
TM2262 pAH328 check fwd	GAGCGTAGCGAAAAATCC
TM2263 pAH328 check rev	GAAATGATGCTCCAGTAACC

[a]Restriction sites are highlighted in bold italics; BioBrick overhang sequences are underlined; overhang sequences for resistance cassettes are marked in italics.

4.4 Results and Discussion

4.4.1 Intrinsic induction of CESR target promoters during stationary phase growth

Initially, we aimed at investigating if other modules within the CESR network displayed induction profiles similar to the LiaRS system, which – when grown into stationary phase – displayed a clear induction pattern in the absence of any external stimulus (Dominguez-Escobar *et al.*, 2014). To this end, we fused the target promoters of the BceRS system (P_{bceA}), of the PsdRS system (P_{psdA}) and selected target promoters of σ^M, σ^X, and σ^W (P_{ydaH}, P_{sigX}, and P_{pspA}, respectively) and one promoter which is regulated by all three σ factors, P_{bcrC}, to a promoter-less *luxABCDE* reporter (Schmalisch *et al.*, 2010, Radeck *et al.*, 2013). The resulting promoter-*lux* fusions were integrated into the chromosome of *B. subtilis* W168 wild type cells. Automated incubation of the resulting reporter strains in a microplate reader revealed that all but the σ^W target promoter P_{pspA} displayed a marked increase in luminescence activity between two and four hours after the onset of stationary phase (Fig. 4.1; t=7-8 h). The amplitude of this intrinsic stationary phase induction was highest for the BceRS and PsdRS target promoters (both approx. 500-fold induction; Fig. 4.1b), but also the ECF target promoters displayed a 10-20-fold increase in promoter activity (Fig. 4.1d). From these observations, we conclude that large parts of the CESR network in *B. subtilis* perceive one or multiple stimuli that are endogenously produced between two to four hours after entry into stationary phase.

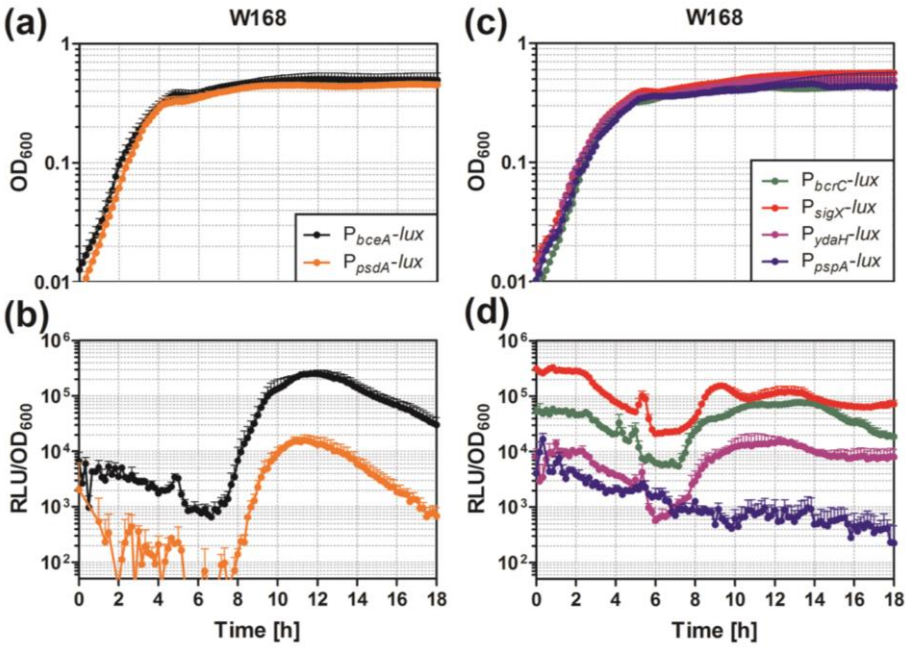

Fig. 4.1: Intrinsic late stationary phase induction of P_{bceA}-*lux*, P_{psdA}-*lux* (a, b) and ECF σ factor target promoters in W168 (c, d). Promoter activity was detected by following luminescence of 100 µl cultures growing in a microplate reader (Biotek®, Synergy™2; 96-well plate, 37°C, shaking) over time. The upper graphs (a, c) show the growth curves (OD_{600}) of the respective strains in MCSE medium. The lower graphs (b, d) show the promoter activities as relative luminescence units (RLU) per OD_{600}. Late stationary phase induction is shown for both the P_{bceA} (black) and P_{psdA} (orange) after 7-8 h of growth (b). Induction of P_{bcrC} controlled by σ^M, σ^X and σ^W after 7-8 h of growth is shown in green (d). Intermediate induction of σ^X- and σ^M-dependent promoters (P_{sigX} and P_{ydaH}) is shown in red and purple, respectively, after 7-8 h of growth. The σ^W-dependent P_{pspA} (blue) stays uninduced under our cultivation conditions. Please note that the small peak at t=5 h in this and all the following figures does not represent a regulated transition phase promoter induction, since it was observed for any promoter studied in MCSE so far, including a set of known constitutive promoters (Radeck *et al.*, 2013). All graphs show mean values and SEM (standard error of the mean) of at least three independent replicates.

4.4.2 AMPs and cannibalism toxins induce CESR systems

Both the BceRS and PsdRS system have been shown to respond to different peptide antibiotics that interfere with the cell wall biosynthetic pathway during exponential growth (Breukink & de Kruijff, 2006, Staroń *et al.*, 2011). In order to elucidate the mechanism behind the observed intrinsic stationary phase activation, we asked whether it could be caused by endogenously produced AMPs of *B. subtilis* W168. The first AMP we considered was Sublancin 168 (SunA), which is a SPβ prophage-derived bacteriocin described as an S-linked glycopeptide active against Gram-positive bacteria (Oman *et al.*, 2011). Its production is known to be repressed during exponential growth phase by the transcriptional regulators AbrB and Rok (Albano *et al.*, 2005, Strauch *et al.*, 2007). Another peptide that might trigger stationary phase induction of the CESR is the YydF peptide, which has been shown to be an endogenous inducer of the LiaRS system (Butcher *et al.*, 2007). Its production is also negatively controlled by AbrB during logarithmic growth (Butcher *et al.*, 2007). Subtilosin A (SboA) is another bacteriocin produced by *B. subtilis* W168. Although it is known to be transcriptionally regulated by AbrB and by the two-component regulatory proteins ResDE (Nakano *et al.*, 2000, Strauch *et al.*, 2007), it has been reported to be produced only under anaerobic growth conditions (Nakano *et al.*, 2000). Indeed, we found the *sboA* promoter to be inactive over the whole

time course under our cultivation conditions (data not shown). The last two potential AMPs were the two cannibalism toxins sporulation delaying protein, SdpC and sporulation killing factor, SkfA (referred to as SDP and SKF hereafter).

To study the effect of the AMPs on the induction of the CESR network, we analyzed P_{bceA}, P_{psdA} and P_{bcrC} promoter activation in mutants deleted for each gene encoding the respective antimicrobial peptides (Fig. 4.2).

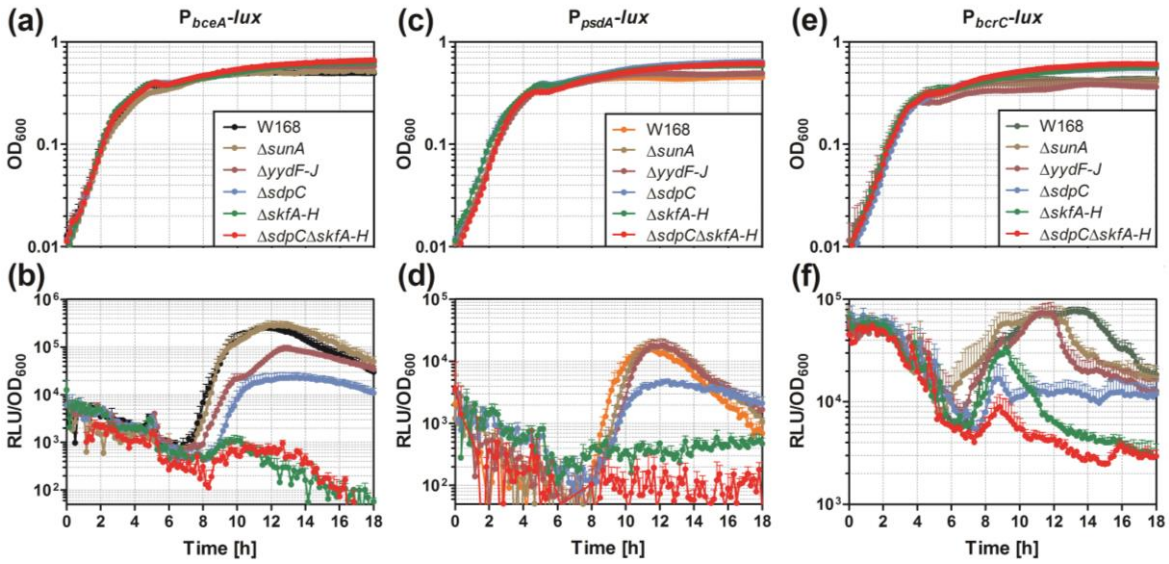

Fig. 4.2: Late stationary phase induction of P_{bceA}-*lux* (a, b), P_{psdA}-*lux* (c, d) and P_{bcrC}-*lux* (e, f) in deletion backgrounds. Promoter activity was detected by following luminescence in a microplate reader (for details see legend Fig. 4.1). Lower panels (b), (d) and (f) show the effect of different strains deleted for various antimicrobial peptide loci on each promoter: Δ*sunA* (Sublancin) in light brown, Δ*yydF-J* (YydF peptide) in dark purple, Δ*sdpC* (SDP) in blue, Δ*skfA-H* (SKF) in green, Δ*sdpC*Δ*skfA-H* in red. Δ*sunA* had no effect on either promoter. Δ*yydF-J* showed only minor effects on P_{bceA}, P_{psdA} and P_{bcrC} activity in stationary phase. Deletion of *sdpC* revealed 10-fold decrease on P_{bceA} activity and approx. 7-fold on P_{psdA} and P_{bcrC} activity. The *skfA-H* deletion resulted in approx. 100-fold reduced P_{bceA} and P_{psdA} activity but only 4-fold reduced P_{bcrC} induction.

Deletion of *sunA* (Sublancin 168) had no effect on any promoter activity and deletion of *yydF-J* only showed a minor effect on P_{bceA} promoter activity. In contrast, *sdpC* and *skfA-H* mutants revealed the most prominent reduction in luciferase activity for all three promoters tested. Deletion of *sdpC* resulted in an approx. 10-fold reduced P_{bceA} activity (Fig. 4.2b, blue curve), and deletion of *skfA-H* decreased the activity about 100-fold (Fig. 4.2b, green curve). The effect of an *sdpC* deletion on P_{psdA} induction was moderate (about 3-fold decrease), but P_{psdA} activity was almost completely lost in a *skfA-H* mutant (Fig. 4.2d). In contrast, P_{bcrC} activity was more strongly decreased in the *sdpC* mutant (about 4-fold, Fig. 4.2f) than in the *skfA-H* deletion strain (max. 2-fold). Moreover, in an *sdpC skfA-H* double mutant, stationary phase activity of P_{bceA} and P_{psdA} was fully abolished, while P_{bcrC} still displayed mild induction. Hence, we could identify the two cannibalism toxins SDP and SKF as strong inducers of all three CESR target promoters in stationary phase.

While induction of ECF σ factors was expected, given the described role in mounting a secondary layer of defense against SDP (Butcher & Helmann, 2006), this is the first time that an intrinsic growth phase-dependent induction has been observed for Bce-like systems. Since the

effect was most prominent for the *bceA* promoter, subsequent investigations of the cannibalism stress response were restricted to the BceRS system alone, but key findings were also verified for the PsdRS system, demonstrating similar behavior (data not shown).

4.4.3 Toxin production correlates with P_{bceA} induction

We next tested how stationary phase induction of P_{bceA} was correlated with the activation of *sdpC* and *skfA* expression. SDP is under dual control of first its own promoter P_{sdpC} and second under the promoter driving the whole *sdpABC* operon P_{sdpA} (Fig. 4.3).

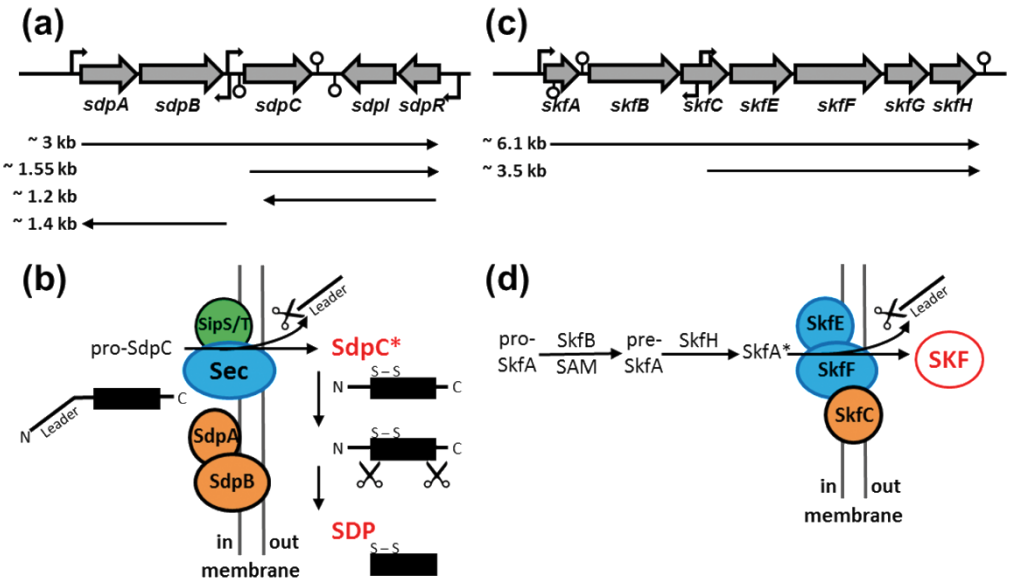

Fig. 4.3: Schematic overview of SDP and SKF maturation and genomic context. Panels (a) and (c) show main transcripts of the *sdpABC-sdpRI* and *skfA-H* operons, each based on recent microarray studies (Nicolas *et al.*, 2012). Panels (b) and (d) show the hypothesized schematic maturation pathway of SDP and SKF precursors until release of the final toxin. According to Perez Morales *et al.*, 2013, pro-SdpC is translocated across the membrane by the general secretory pathway (Sec) and the leader peptide thereby cleaved by the SipS/T peptidase (b). SdpAB further cleave SdpC* at the N- and C-termini to release the final SDP toxin to the environment. Similarly, pro-SkfA is hypothesized to be modified by SkfB to give pre-SkfA which is assumed to be further processed by SkfH to prepare for export and cyclization by SkfEF and SkfC, respectively (d). These assumptions are based on Liu *et al.*, 2010 and lack further evidence.

We tested both promoter activities over the whole time course and found P_{sdpA} to be the stronger promoter under our cultivation conditions (data not shown). Therefore, we assumed that P_{sdpA} is the crucial promoter driving also expression of *sdpC*. Thus, we studied the luminescence activity from P_{sdpA}- and P_{skfA}-*luxABCDE* reporter fusions throughout growth of the W168 wild type strain to test correlation between SDP/SKF production and P_{bceA} induction (Fig. 4.4). P_{sdpA} was induced about 10-fold, while P_{skfA} displayed a 100-fold induction. While both the *sdpA* and *skfA* promoters were induced 5-6 h after the beginning of the experiment, the *bceA* promoter became active approx. 2 h later. This indicates that the toxins first had to be produced, processed and likely also accumulated to a certain threshold concentration in order to activate the BceRS system.

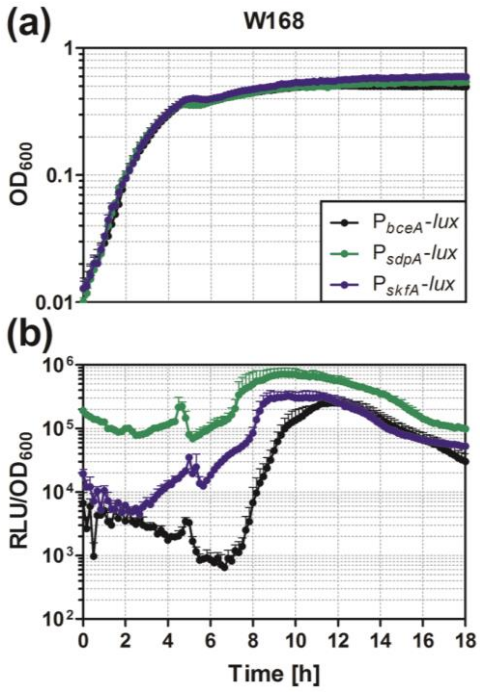

Fig. 4.4: Correlation of P_{sdpA} and P_{skfA} activities with P_{bceA} induction. Promoter activity was detected by following luminescence in a microplate reader (for details see legend Fig. 4.1). P_{sdpA} and P_{skfA} activity is shown over time (in green and blue, respectively). P_{bceA} induction is shown for comparison (black). P_{sdpA} revealed a higher basal activity compared to P_{skfA} and showed approx. 10-fold induction in stationary phase starting around 5h after beginning of the experiment. P_{skfA} exhibited a similar induction pattern starting slightly later (5-6 h) showing approx. 100-fold induction.

4.4.4 The BceRS system does not mediate resistance against cannibalism toxins

Based on its role in mediating resistance against the peptide antibiotic bacitracin, we reasoned that the BceRS system might also confer resistance against SDP. The immunity protein of the *sdpABC-sdpRI* operon is SdpI (Fig. 4.3). Both the toxin biosynthesis operon *sdpABC* and the immunity operon *sdpRI* are under control of the transition state repressor AbrB and the master regulator of sporulation Spo0A (Ellermeier *et al.*, 2006). SdpI reveals receptor/signal transducing properties, and its synthesis is induced by a combined interplay between SDP, SdpI and SdpR (Ellermeier *et al.*, 2006). In brief, SdpR constitutes an autorepressor blocking transcription of *sdpRI* in the absence of SDP. Upon SDP synthesis and export, SDP binds to SdpI at the membrane, which enables the latter to recruit SdpR into the SDP-SdpI membrane complex. This titration of SdpR away from the DNA induces transcription of *sdpRI*, which results in immunity against SDP (Ellermeier *et al.*, 2006). Accordingly, cannibalism-inactive cells are expected to neither produce and secrete SDP nor induce enhanced SdpI expression. Consequently, it is believed that these cells are highly sensitive to SDP and prone to lysis while toxin-producing cells are resistant against SDP (Ellermeier *et al.*, 2006).

In order to study the contribution of the BceRS system towards resistance against SDP, we first performed growth measurements of wild type and a mutant carrying unmarked deletions of all three Bce-like systems (Δ*bceRSAB* Δ*psdRSAB* Δ*yxdJKLM-yxeA*) of *B. subtilis* W168 (Gebhard *et al.*, 2014) (TMB1518, referred to as "3x*bce* mutant" hereafter) shown in Fig. 4.5(a).

Although this mutant strain lacks all important peptide antibiotic detoxification modules present in *B. subtilis*, this did not affect growth compared to wild type (Fig. 4.5a, blue and black curve, respectively). In contrast, comparison of wild type growth to an *sdpI* mutant revealed a severe growth defect upon entry into stationary phase (Fig. 4.5a, orange curve). Given that the 3x*bce* mutant seems to be unaffected in its growth behavior, we conclude that the BceRS system is not involved in mediating resistance against SDP. Furthermore, we observed no P_{bceA} induction in the 3x*bce* mutant, demonstrating that SDP/SKF cannot be sensed in the absence of the signal transduction system and resistance is not mediated by any of the Bce-like systems (data not shown).

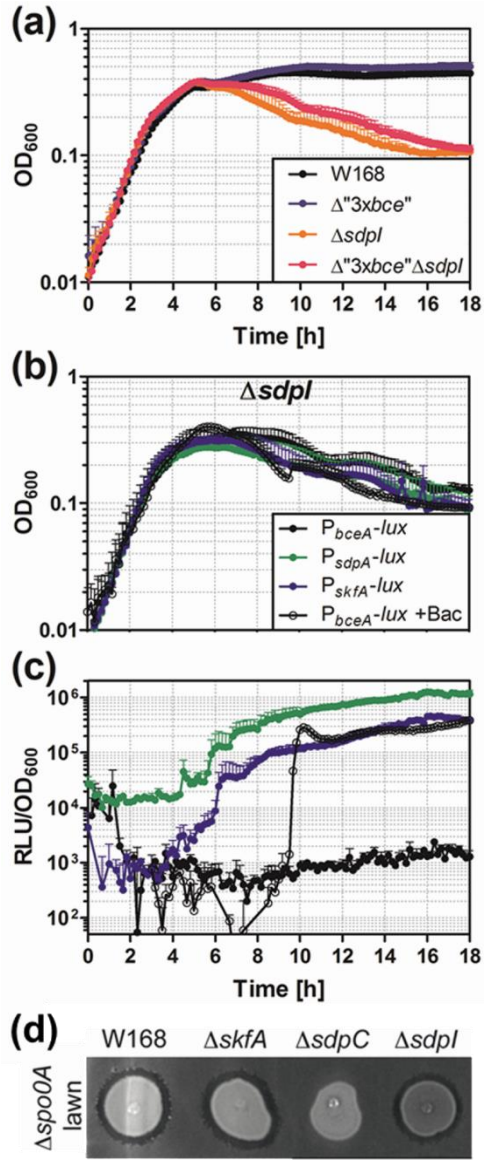

Fig. 4.5: Effect of an *sdpI* and triple *bceRSAB psdRSAB yxdJKML-yxeA* mutant on SDP sensitivity. (a) Growth in W168 (black) and Δ*bceRSAB* Δ*psdRSAB* Δ*yxdJKLM-yxeA* (referred to as Δ3x*bce* hereafter, blue) was similar whereas growth in Δ*sdpI* (orange) was impaired starting after entry into stationary phase. However, growth was not further impaired in Δ3x*bce* Δ*sdpI* (pink) indicating no additional role of the BceRS system in resistance against SDP. P_{bceA}, P_{sdpA} and P_{skfA} growth and induction (b, c) were detected by following luminescence in a plate reader (for details see legend Fig. 4.1). P_{bceA} is not intrinsically induced in Δ*sdpI* (black filled circles) whereas P_{sdpA} and P_{skfA} are activated after 5-6 h upon start of the experiment (green and blue, respectively) indicating correct expression of the respective loci. Upon induction with bacitracin (10 µg ml^{-1}) at t=9 h, P_{bceA} is fully activated (black open circles). Negative data points and values smaller than 50 RLU/OD_{600} are not depicted. Error bars smaller than symbols are not shown. In panel (d), stationary phase cells of W168 and mutants were applied to a plate containing a lawn of Δ*spo0A* cells. From left to right: W168, Δ*skfA* (SKF), Δ*sdpC* (SDP) and Δ*sdpI* (immunity protein against SDP). Halo indicates production of mature SDP. An *sdpC* mutant strain is unable to kill *spo0A* deficient cells. SDP seems to be the major cannibalism toxin on solid medium.

This is further supported by the finding that a mutant deficient in both the 3x*bce* resistance modules and the SdpI immunity protein (Fig. 4.5a, pink curve) did not show a stronger growth defect than the *sdpI* mutant alone. To further validate that the BceRS system is indeed not involved in resistance against SDP, we additionally tested the viability of stationary phase cultures (data not shown). We again observed no difference in susceptibility between the 3x*bce sdpI* mutant and the single *sdpI* deletion, underpinning the aforementioned result.

Next, we tested if the BceRS system instead might be involved in mediating resistance against SKF. Towards that end, we deleted *skfEF*, which encode the putative ABC transporter that is thought to be responsible for export and immunity of SKF and followed growth of a *skfEF* mutant over time (data not shown). In contrast to the *sdpI* deletion, there was no growth defect observable for the *skfEF* mutant. Next, we combined the 3x*bce* mutant with the *skfEF* deletion to see whether the additional 3x*bce* deletion affects growth. But again, the 3x*bce skfEF* mutant did not show any growth defect.

Taken together, we found no evidence for a role of Bce-like systems in mediating resistance against SDP and SKF despite its strong induction. We therefore next focused our attention on the specificity of this induction.

4.4.5 Mature SKF toxin strongly acts as inducer

Of the two cannibalism toxins, SKF was the stronger inducer of the *bceA* promoter. Given that the BceRS system did not confer resistance against SKF, we wondered about the physiological relevance of the intrinsic induction of the CESR systems in stationary phase. In order to approach this question, we first had to understand the true nature of the stimulus sensed by the BceRS system. Was it the mature toxin itself or could the unprocessed precursor also lead to its activation? SKF is a ribosomally synthesized AMP and requires posttranslational modification to be fully active (Gonzalez-Pastor *et al.*, 2003; Liu *et al.*, 2010). Our knowledge of this process is still limited and direct evidence for the functions described in the following sentences is still lacking. But it is assumed that the radical SAM (S-adenosyl-methionine) enzyme SkfB mediates the first step in SKF maturation by forming a thioether bond between the cysteine residue Cys4 and the α-carbon of the methionine residue Met12 resulting in pre-SkfA (Flühe *et al.*, 2013; Liu *et al.*, 2010) (Fig. 4.3). SkfH, a putative thioredoxin oxidoreductase-like protein and the last gene encoded in the *skfA-H* operon is presumed to mediate formation of a disulfide bond leading to SkfA* (Liu *et al.*, 2010) (Fig. 4.3). Export and immunity was postulated to be mediated by SkfEF, forming an ABC transporter in the membrane (Gonzalez-Pastor *et al.*, 2003). Likewise, SkfC was hypothesized to be responsible for the cyclization reaction prior to or during export of the SKF peptide (Liu *et al.*, 2010). SkfG is so far poorly understood and its function is unknown.

In order to gain deeper insight into the physiological properties of the genes encoded in the *skfA-H* operon, we next studied the intrinsic P_{bceA} induction in different *skf* mutants (Fig. 4.6a+b). In a *skfA* mutant lacking the structural gene of the SKF toxin, P_{bceA} induction is almost not detectable (Fig. 4.6b, dark grey curve). Similar results were obtained in a mutant deleted for *skfBC*, the products of which were hypothesized to be involved in maturation of the toxin precursor (Flühe *et al.*, 2013). This suggests that SkfBC perform critical steps in the maturation process of SKF. Likewise, P_{bceA} induction cannot be detected in a *skfEF* mutant, lacking the putative immunity transporter. In contrast, deletion strains lacking either *skfGH* or *skfH* alone were able to activate the BceRS system in stationary phase, albeit 10-fold reduced compared to the wild type reporter strain (see Fig. 4.1). SkfH is hypothesized to be responsible for one important disulfide bond formation in the maturation process of SKF (Liu *et al.*, 2010). Thus, it seems that SkfH performs a critical step in the maturation of SKF. Additionally, comparison of the *skfGH* mutant and the *skfBC* or *skfEF* deletion, respectively, revealed that potential modification of SKF by SkfBC and/or export via SkfEF seem to play more crucial roles in the SKF maturation pathway than SkfGH alone, since P_{bceA} induction is abolished in both the *skfBC* and *skfEF* mutant. In conclusion, SkfBC and SkfEF are necessary for production of a fully active SKF toxin, while SkfGH seem to play a minor role, at least as judged by the activation of the BceRS system in a *skfGH* mutant.

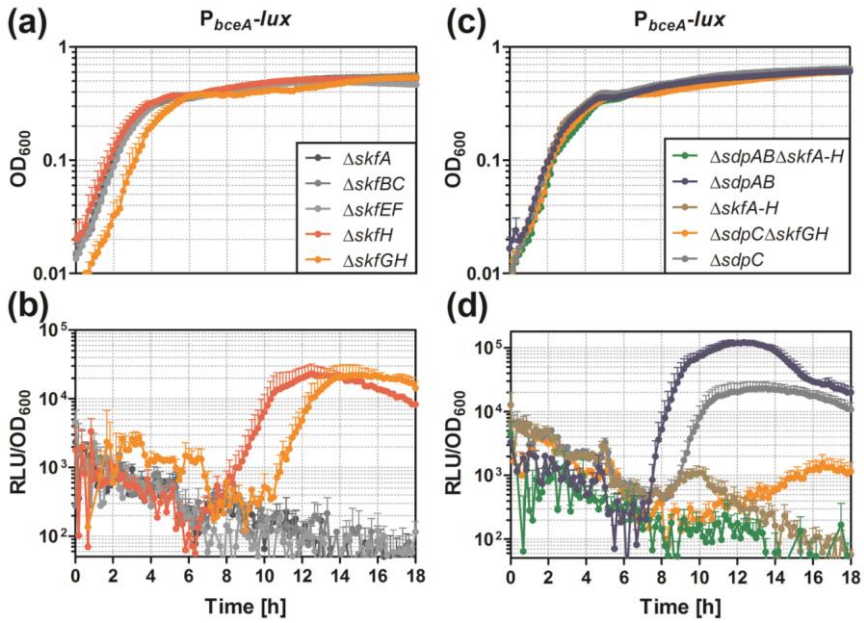

Fig. 4.6: P_{bceA} activity in different *sdp* and *skf* mutants. Promoter activity was detected by following luminescence in a microplate reader (for details see legend Fig. 4.1). P_{bceA} activity in Δ*skfA* (dark grey), Δ*skfBC* (middle grey) and Δ*skfEF* (light grey) is abolished (b). P_{bceA} response in Δ*skfGH* (orange) and Δ*skfH* (red) is about 10-fold reduced (b) compared to W168 (see Fig. 4.1). The time delay of promoter induction in Δ*skfGH* (orange) is due to an approx. 2 h prolonged lag phase but stays the same regarding stationary phase induction point. P_{bceA} induction in Δ*sdpAB*Δ*skfA-H* (d, green curve) as well as Δ*sdpC*Δ*skfGH* (d, orange curve) is lost indicating that posttranslational modification of SDP and SKF by SdpAB and SkfGH, each, is needed to trigger the BceRS system.

In order to elucidate if the mature SKF toxin or even its precursor acts as an inducer of the *bceA* promoter, we combined the *sdpC* deletion with the *skfGH* deletion (Fig. 4.6d, orange curve). The resulting double mutant is supposed to be deficient for SDP and lacks crucial steps of SKF maturation. Fig. 4.6d shows that the *sdpC skfGH* double mutant first displayed significantly decreased BceRS activation, when compared to the *sdpC* deletion mutant (orange vs. grey curve) but after some time (12-13 h), P_{bceA} becomes active although to a much lower extent. This observation might suggest that accumulation of immature SKF precursor could already act as a weak inducer since the time point of induction is much later and the dynamics considerably lower.

4.4.6 Mature SDP toxin acts as inducer

The absence of any role for the BceRS system in mediating resistance against SDP provokes the question why the BceRS system is triggered by this compound. In order to better understand this stimulus leading to P_{bceA} induction, we investigated BceRS activation in individual *sdp* mutants (Fig. 4.6).

SDP is encoded in the *sdpABC* operon and repressed by AbrB during exponential growth phase and in times of nutrient availability (Chen *et al.*, 2006; Fujita *et al.*, 2005). Upon entry into stationary phase, repression by AbrB is released by active Spo0A, and transcription of the corresponding genes is triggered. Like SKF, SDP is a ribosomally synthesized AMP that requires posttranslational modifications to mature into an active form (Gonzalez-Pastor *et al.*, 2003; Liu *et al.*, 2010; Perez Morales *et al.*, 2013), a process presumably mediated by SdpA and SdpB (Perez Morales *et al.*, 2013). SdpA is thought to be a soluble protein attached to the cytosolic face of the membrane, whereas SdpB is a transmembrane protein (Perez Morales *et al.*, 2013). Together, they are thought to mediate the final step of processing the SDP precursor peptide into active SDP by posttranslational cleavage of the N- and C-terminus (Fig. 4.3).

To better understand the stimulus leading to P_{bceA} induction by SDP, we first tested if the BceRS system is triggered by the mature SDP toxin or by its precursor. We initially monitored P_{bceA} induction in an *sdpAB* mutant (Fig. 4.6d, blue curve): Compared to the wild type reporter strain (Fig. 4.1) the induction was only slightly reduced. This is due to the fact that SKF is still present and acting as the main inducer. Consequently, we next compared P_{bceA} induction in a *skfA-H* mutant and a *skfA-H sdpAB* deletion. As a consequence, a deletion strain of Δ*skfA-H* Δ*sdpAB* would lack SKF and only produce immature, unprocessed SDP precursor that could potentially trigger the BceRS system. Fig. 4.6(d) shows that the *bceA* promoter induction was completely abolished in the double mutant (green curve), indicating that the SDP precursor is most likely not the inducer of the *bceA* promoter, but rather the mature SDP.

Next, we tested *bceA* promoter induction in an *sdpI* mutant, lacking the autoimmunity against SDP (Fig. 4.5b, c). Surprisingly, P_{bceA} induction was completely abolished in this strain. This unexpected finding provoked the question if the *sdpABC-sdpRI*/*skfA-H* operons are still expressed in an *sdpI* mutant since a loss of auto-immunity has previously been reported to sometimes abolish toxin production (Foulston & Bibb, 2010). Both P_{sdpA} and P_{skfA} showed a strong increase about 10-fold and 100-fold, respectively (Fig. 4.5c, green and blue curve, respectively), comparable to wild type results (see Fig. 4.4), demonstrating that the two toxin promoters are fully induced and the toxins are most likely also produced. Because of the severe growth defects of the *sdpI* mutant, we wondered whether the silence in the BceRS system is maybe a result of this growth defect. However, addition of bacitracin (10 µg ml^{-1}) to stationary phase cultures could still fully activate the BceRS system (Fig. 4.5c), demonstrating that the BceRS system itself is still functional in the *sdpI* mutant.

We next addressed the question if SDP itself is still produced as a potent toxin in the *sdpI* mutant. To this end, we performed a spot-on-lawn assay using a *spo0A* deletion strain as sensitive lawn (Fig. 4.5d). Since cannibalism toxin production and immunity is regulated in a Spo0A-dependent manner, a *spo0A* mutant is unable to produce both SDP and SKF and is therefore sensitive against both toxins. We spotted stationary phase cultures of wild type as well as *sdp* and *skf* mutants on a plate containing Δ*spo0A* lawn cells and compared zones of inhibition after incubation overnight. Wild type spots showed a clear zone of inhibition on the Δ*spo0A* lawn indicating production of functional cannibalism toxins. We then used a *skfA* deletion strain lacking SKF toxin but still expressing SDP. We found that the *skfA* mutant showed a clear inhibition zone just like wild type, indicating production of functional SDP toxin in the absence of SKF. Accordingly, we took an *sdpC* deletion strain lacking SDP but still producing SKF. However, Δ*sdpC* was unable to kill *spo0A* deficient cells, demonstrating that SDP rather than SKF is the major cannibalism toxin on solid medium, which is in agreement with a previous study (Liu *et al.*, 2010). Importantly, a significant zone of inhibition comparable in size to the wild type can be observed around spots of an *sdpI* deletion mutant. This result unequivocally demonstrates that functional SDP toxin is still produced in an *sdpI* mutant. Nevertheless, BceRS activation was abolished in this strain. This observation indicates a link between toxin sensing by the BceRS system and the presence of the immunity protein SdpI. While understanding the molecular mechanism behind this finding is beyond

the scope of this work and will require further investigations, it already points towards an indirect way of sensing as will be discussed below.

4.5 Conclusion

Our results demonstrate that the BceRS system is intrinsically activated in late stationary phase due to the production of two cannibalism toxins, SDP and SKF, with SKF being the stronger inducer. The *skfA-H* deletion resulted in a 100-fold reduced BceRS activity, whereas the *sdpC* deletion caused only a 10-fold reduced P_{bceA} induction (Fig. 4.2b). The exact physiological role of the BceRS system in the cannibalism stress response, however, remains unclear. Our data suggest that it provides no role in resistance against either SDP or SKF. However, it seems that the immunity determinants SdpI and SkfEF, respectively, are important for triggering the BceRS response since in corresponding deletion strains BceRS activation is abolished (Figs 4.5+4.6). For SkfEF, this finding is less surprising since this ABC transporter is thought to also export the SKF toxin. Hence, in its absence no mature inducer reaches the extracellular environment to trigger a BceRS response. But at present, this assumption is hard to investigate without a detectable SKF-dependent phenotype.

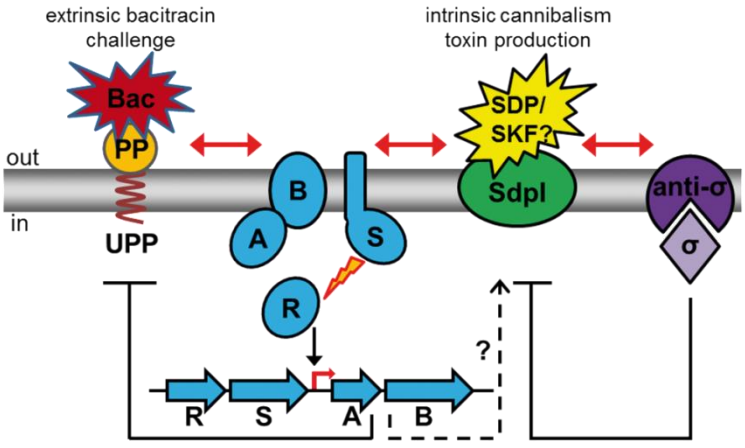

Fig. 4.7: Model of SDP/SKF sensing by the BceRS system. SdpI binding to SDP (and maybe SKF) is a prerequisite for sensing by the BceRS system. The BceRS system consists of an ABC transporter, BceAB (short: A, B) responsible for the detection of bacitracin (Bac) and is coupled to a TCS consisting of a histidine kinase BceS (short: S) and its cognate response regulator, BceR (short: R). Detection of Bac leads to an activation of P_{bceA} and subsequent transcription of AB to mediate resistance. Current research argues about Bac recognition by AB. One hypothesis is that it has to bind its target UPP (undecaprenol pyrophosphate) in the bacterial membrane in order to be sensed by AB. Taken this hypothesis for granted it could be that only the SdpI-SDP complex can be recognized by AB. ECF σ^W is induced by SDP (and SKF?) and provides a second layer of resistance. SdpAB and SkfGH, each, is needed to trigger the BceRS response.

SDP was shown to be the weaker inducer of the *bceA* promoter, displaying only a 10-fold reduced BceRS response in an *sdpC* mutant compared to the wild type (Fig. 4.2b). Remarkably, in an *sdpI* deletion, we observed a complete loss of the BceRS response despite the fact that both toxin loci are fully expressed (Figs 4.4+4.5c) and SDP is most likely functionally produced (Fig. 4.5d).

Taken together, these findings indicate that SdpI is required for SDP and potentially also SKF perception by the BceRS system (Fig. 4.7). This mode of an indirect sensing of SDP only in complex with SdpI resembles

the mode for bacitracin perception by the BceRS system that was suggested recently (Kingston *et al.*, 2014). Here, it has been proposed that only the complex of bacitracin to its membrane target, undecaprenol pyrophosphate, can act as a trigger of the BceRS response. Our findings on an SdpI-dependent sensing of SDP (and potentially also SKF) support this model of AMP perception by the BceRS system, in which the toxin/AMP has to be bound to a membrane target before it can be perceived by the BceRS system. Analyzing this novel mechanism will be the subject of further investigations.

Nevertheless, our results provide clear evidence for a tight link between signaling systems that mediate the CESR in *B. subtilis* and intrinsic AMP production as part of the stationary phase survival strategy of this organism.

4.6 Acknowledgements

This project was funded by the DFG priority program SPP1617 “Phenotypic Heterogeneity and Sociobiology of Bacterial Populations” (grant MA 2837/3-1 to TM).

4.7 References of CHAPTER IV

Albano, M., W. K. Smits, L. T. Ho, B. Kraigher, I. Mandic-Mulec, O. P. Kuipers & D. Dubnau, (2005) The Rok protein of *Bacillus subtilis* represses genes for cell surface and extracellular functions. *J Bacteriol* **187**: 2010-2019.

Breukink, E. & B. de Kruijff, (2006) Lipid II as a target for antibiotics. *Nat Rev Drug Discov* **5**: 321-332.

Butcher, B. G. & J. D. Helmann, (2006) Identification of *Bacillus subtilis* σ^W-dependent genes that provide intrinsic resistance to antimicrobial compounds produced by Bacilli. *Mol Microbiol* **60**: 765-782.

Butcher, B. G., Y.-P. Lin & J. D. Helmann, (2007) The *yydFGHIJ* operon of *Bacillus subtilis* encodes a peptide that induces the LiaRS two-component system. *J Bacteriol* **189**: 8616-8625.

Chen, G., A. Kumar, T. H. Wyman & C. P. Moran, Jr., (2006) Spo0A-dependent activation of an extended -10 region promoter in *Bacillus subtilis*. *J Bacteriol* **188**: 1411-1418.

Chung, J. D., G. Stephanopoulos, K. Ireton & A. D. Grossman, (1994) Gene expression in single cells of *Bacillus subtilis*: evidence that a threshold mechanism controls the initiation of sporulation. *J Bacteriol* **176**: 1977-1984.

Cutting, S. M. & P. B. Van der Horn, (1990) Genetic analysis. In: Molecular Biological Methods for *Bacillus.* C. R. Harwood & S. M. Cutting (eds). Chichester, United Kingdom: John Wiley & Sons, Ltd., pp. 27-74.

Dominguez-Escobar, J., D. Wolf, G. Fritz, C. Höfler, R. Wedlich-Söldner & T. Mascher, (2014) Subcellular localization, interactions and dynamics of the phage-shock protein-like Lia response in *Bacillus subtilis*. *Mol Microbiol* **92**: 716-732.

Dubois, J. Y., T. R. Kouwen, A. K. Schurich, C. R. Reis*, et al.*, (2009) Immunity to the bacteriocin sublancin 168 Is determined by the SunI (YolF) protein of *Bacillus subtilis*. *Antimicrob Agents Chemother* **53**: 651-661.

Ellermeier, C. D., E. C. Hobbs, J. E. Gonzalez-Pastor & R. Losick, (2006) A three-protein signaling pathway governing immunity to a bacterial cannibalism toxin. *Cell* **124**: 549-559.

Flühe, L., O. Burghaus, B. M. Wieckowski, T. W. Giessen, U. Linne & M. A. Marahiel, (2013) Two [4Fe-4S] clusters containing radical SAM enzyme SkfB catalyze thioether bond formation during the maturation of the sporulation killing factor. *J Am Chem Soc* **135**: 959-962.

Foulston, L. C. & M. J. Bibb, (2010) Microbisporicin gene cluster reveals unusual features of lantibiotic biosynthesis in actinomycetes. *Proc Natl Acad Sci U S A* **107**: 13461-13466.

Fujita, M., J. E. Gonzalez-Pastor & R. Losick, (2005) High- and low-threshold genes in the Spo0A regulon of *Bacillus subtilis*. *J Bacteriol* **187**: 1357-1368.

Gebhard, S., C. Fang, A. Shaaly, D. J. Leslie*, et al.*, (2014) Identification and characterization of a bacitracin resistance network in *Enterococcus faecalis*. *Antimicrob Agents Chemother* **58**: 1425-1433.

Gonzalez-Pastor, J. E., E. C. Hobbs & R. Losick, (2003) Cannibalism by sporulating bacteria. *Science* **301**: 510-513.

Harwood, C. R. & S. M. Cutting, (1990) *Molecular Biological Methods for Bacillus*. John Wiley & Sons, Chichester.

Helmann, J. D., (2002) The extracytoplasmic function (ECF) sigma factors. *Adv Microb Physiol* **46**: 47-110.

Huang, X., K. L. Fredrick & J. D. Helmann, (1998) Promoter recognition by *Bacillus subtilis* σ^W: autoregulation and partial overlap with the σ^X regulon. *J Bacteriol* **180**: 3765-3770.

Jordan, S., E. Rietkötter, M. A. Strauch, F. Kalamorz, B. G. Butcher, J. D. Helmann & T. Mascher, (2007) LiaRS-dependent gene expression is embedded in transition state regulation in *Bacillus subtilis*. *Microbiology* **153**: 2530-2540.

Kingston, A. W., X. Liao & J. D. Helmann, (2013) Contributions of the σ^W , σ^M and σ^X regulons to the lantibiotic resistome of *Bacillus subtilis*. *Mol Microbiol* **90**: 502-518.

Kingston, A. W., H. Zhao, G. M. Cook & J. D. Helmann, (2014) Accumulation of heptaprenyl diphosphate sensitizes Bacillus subtilis to bacitracin: implications for the mechanism of resistance mediated by the BceAB transporter. *Mol Microbiol* **93**: 37-49.

Liu, W. T., Y. L. Yang, Y. Xu, A. Lamsa*, et al.*, (2010) Imaging mass spectrometry of intraspecies metabolic exchange revealed the cannibalistic factors of *Bacillus subtilis*. *Proc Natl Acad Sci U S A* **107**: 16286-16290.

Mascher, T., A. B. Hachmann & J. D. Helmann, (2007) Regulatory overlap and functional redundancy among *Bacillus subtilis* extracytoplasmic function (ECF) σ factors. *J Bacteriol* **189**: 6919-6927.

Mascher, T., N. G. Margulis, T. Wang, R. W. Ye & J. D. Helmann, (2003) Cell wall stress responses in *Bacillus subtilis*: the regulatory network of the bacitracin stimulon. *Mol Microbiol* **50**: 1591-1604.

Missiakas, D. & S. Raina, (1998) The extracytoplasmic function sigma factors: role and regulation. *Mol Microbiol* **28**: 1059-1066.

Nakano, M. M., G. Zheng & P. Zuber, (2000) Dual control of *sbo-alb* operon expression by the Spo0 and ResDE systems of signal transduction under anaerobic conditions in *Bacillus subtilis*. *J Bacteriol* **182**: 3274-3277.

Nicolas, P., U. Mäder, E. Dervyn, T. Rochat*, et al.*, (2012) Condition-dependent transcriptome reveals high-level regulatory architecture in *Bacillus subtilis*. *Science* **335**: 1103-1106.

Oman, T. J., J. M. Boettcher, H. Wang, X. N. Okalibe & W. A. van der Donk, (2011) Sublancin is not a lantibiotic but an S-linked glycopeptide. *Nat Chem Biol* **7**: 78-80.

Perez Morales, T. G., T. D. Ho, W. T. Liu, P. C. Dorrestein & C. D. Ellermeier, (2013) Production of the cannibalism toxin SDP is a multistep process that requires SdpA and SdpB. *J Bacteriol* **195**: 3244-3251.

Radeck, J., K. Kraft, J. Bartels, T. Cikovic*, et al.*, (2013) The *Bacillus* BioBrick Box: generation and evaluation of essential genetic building blocks for standardized work with *Bacillus subtilis*. *J Biol Eng* **7**: 29.

Rietkötter, E., D. Hoyer & T. Mascher, (2008) Bacitracin sensing in *Bacillus subtilis*. *Mol Microbiol* **68**: 768-785.

Sambrook, J. & D. W. Russell, (2001) *Molecular Cloning - a laboratory manual*. Cold Spring Harbor Laboratory Press, Cold Spring Harbor, N.Y.

Schmalisch, M., E. Maiques, L. Nikolov, A. H. Camp*, et al.*, (2010) Small genes under sporulation control in the *Bacillus subtilis* genome. *J Bacteriol* **192**: 5402-5412.

Schrecke, K., A. Staroń & T. Mascher, (2012) Two-component signaling in the Gram-positive envelope stress response: intramembrane-sensing histidine kinases and accessory membrane proteins. In: Two component systems in bacteria. R. Gross & D. Beier (eds). Hethersett, Norwich, UK: Horizon Scientific Press, pp. 199-229.

Silver, L. L., (2003) Novel inhibitors of bacterial cell wall synthesis. *Curr Opin Microbiol* **6**: 431-438.

Silver, L. L., (2006) Does the cell wall of bacteria remain a viable source of targets for novel antibiotics? *Biochem Pharmacol* **71**: 996-1005.

Staroń, A., D. E. Finkeisen & T. Mascher, (2011) Peptide antibiotic sensing and detoxification modules of *Bacillus subtilis*. *Antimicrob Agents Chemother* **55**: 515-525.

Strauch, M. A., B. G. Bobay, J. Cavanagh, F. Yao, A. Wilson & Y. Le Breton, (2007) Abh and AbrB control of *Bacillus subtilis* antimicrobial gene expression. *J Bacteriol* **189**: 7720-7732.

Walsh, C., (2003) *Antibiotics - actions, origins, resistance*. ASM press, Washington, D.C.

CHAPTER V

Discussion

Future perspectives

5 Discussion

The cell envelope stress response network of *B. subtilis* involves a variety of 2CSs and ECF σ factors. The LiaSR system is a 2CS which responds to cell envelope targeting peptide antibiotics. Bacitracin has been shown to be one of the strongest inducers of the LiaSR system (Mascher *et al.*, 2003). Recently, it has been demonstrated that the LiaSR system provides a secondary resistance layer of resistance against bacitracin if the primary layer is missing (Georg Fritz, personal communication). Besides its strong induction by bacitracin, the LiaSR system is also intrinsically induced during transition from exponential to stationary growth phase. This induction was shown to be broadly heterogeneous occurring in only 5-10% of the cells and is considerably weaker (Jordan *et al.*, 2007, Dominguez-Escobar *et al.*, 2014).

In the first part of this thesis, we wanted to gain deeper insight into the underlying mechanisms responsible for the heterogeneity within the LiaSR system. First, we found that the LiaSR system is not only heterogeneously activated during transition phase but also upon addition of low bacitracin concentrations (Kesel *et al.*, 2013). Second, we could show that LiaI is a highly dynamic membrane protein under non-inducing conditions while it becomes static upon addition of bacitracin (Dominguez-Escobar *et al.*, 2014). Thereby, it recruits LiaH from the cytoplasm to the membrane forming a complex presumably to close the cell envelope damaged site and maintain cell envelope integrity (Dominguez-Escobar *et al.*, 2014). In the following section 5.1 and 5.2, I would like to discuss where heterogeneity in the LiaSR system might come from and the role of the LiaIH dynamics under bacitracin stress conditions.

In the course of investigating the transition phase induction of the LiaSR system, we observed that the BceRS, the PsdRS as well as the ECF σ factors σ^M, σ^X and σ^W also showed an intrinsic activation in stationary growth phase. Since these systems are known to respond to various cell envelope perturbing agents, we reasoned that they must be activated by one or several endogenously produced peptides.

In the second part of this thesis, we wanted to determine the stimuli responsible for this intrinsic induction of the different cell envelope stress response systems with our main focus on the BceRS system. First, we found that the cannibalism toxins SDP and SKF were the main inducers of this stationary phase activation (Höfler *et al.*, 2015). However, we found no evidence that the BceRS system is involved in mediating resistance although we could demonstrate that it only responds to the mature toxins. Second, we found a link between the presence of the immunity determinants of the cannibalism toxins (SdpI and SkfEF) and BceRS activation. They seemed to be needed for stimulus perception by the BceRS system. In the following section 5.2, I would like to discuss the physiological role and relevance of the BceRS activation by SDP and SKF and give some future perspectives.

5.1 Heterogeneous activation of the LiaSR system and its origins

Bacteria employ 2CSs to respond to different environmental stimuli via transfer of a phosphoryl group from the HK to its cognate RR. Subsequently, differential gene expression is induced to mount protective countermeasures. *B. subtilis* employs a number of 2CSs to respond to cell envelope stress, one of which is the LiaSR system. Besides the HK LiaS and the RR LiaR, it includes a third protein, LiaF, blocking LiaS activity under non-inducing conditions.

Signal transduction of 2CSs can lead to heterogeneous expression of genes regulated by these 2CSs although the cells of a population are genetically identical (Smits *et al.*, 2006, Botella *et al.*, 2011, Ghosh *et al.*, 2011). As a result, heterogeneous gene expression can lead to phenotypic heterogeneity. One example is the transition state and stationary phase differentiation cascade of *B. subtilis* with a fraction of cells already Spo0A-active and others still being Spo0A-inactive. Heterogeneous induction of the LiaSR system in response to low bacitracin concentrations during exponential growth phase on single cell level could be demonstrated in this thesis (Kesel *et al.*, 2013) (CHAPTER II). From this study, some open questions aroused: Where does heterogeneity in the LiaSR system come from? Does it derive from the LiaSR system itself? And if so, which proteins would be involved?

5.1.1 Heterogeneity might originate from the LiaSR system itself

Heterogeneous gene expression in bacteria is a common feature to adapt to fluctuating environmental conditions or in terms of cell differentiation. *B. subtilis* is a paradigm for studies on gene expression heterogeneity. Individual cells within a certain population are able to differentiate into different cell types, e.g. spores, matrix producers, cannibals, competent cells or peptide antibiotic producers (Lopez & Kolter, 2010). It is assumed that the regulation of gene expression by so-called 2CS connectors is critical for heterogeneity. Such connectors are thought to modulate the phosphorylation state and thereby the activity of HKs and RRs, thus affecting the output, i.e. gene expression. Connectors are present both in Gram-positive and Gram-negative bacteria and are critical for a variety of physiological functions, including sporulation and transition from exponential to stationary growth phase (Mitrophanov & Groisman, 2008). A well investigated example is the phosphorelay cascade of Spo0A in *B. subtilis*. The cascade leads to sporulation by starting with autophosphorylation of the sensor kinases KinA and KinB and a subsequent transfer of the phosphoryl group to Spo0F. Then, Spo0F~P transfers the phosphoryl group to Spo0B, which in turn, phosphorylates Spo0A. In cells that reach a certain threshold concentration of Spo0A~P, sporulation is triggered. Within that phosphorelay cascade, several connectors are present which directly inhibit the system (Fig. 5.1).

The first two connectors, Sda and KipI, inhibit the autophosphorylation step of KinA (Wang *et al.*, 1997, Burkholder *et al.*, 2001). A second step of regulation can take place at the level of Spo0F phosphorylation. Here, the proteins RapA, B, E and H promote dephosphorylation of Spo0F (Perego & Brannigan, 2001, Smits *et al.*, 2007). The last possible regulatory step can occur via

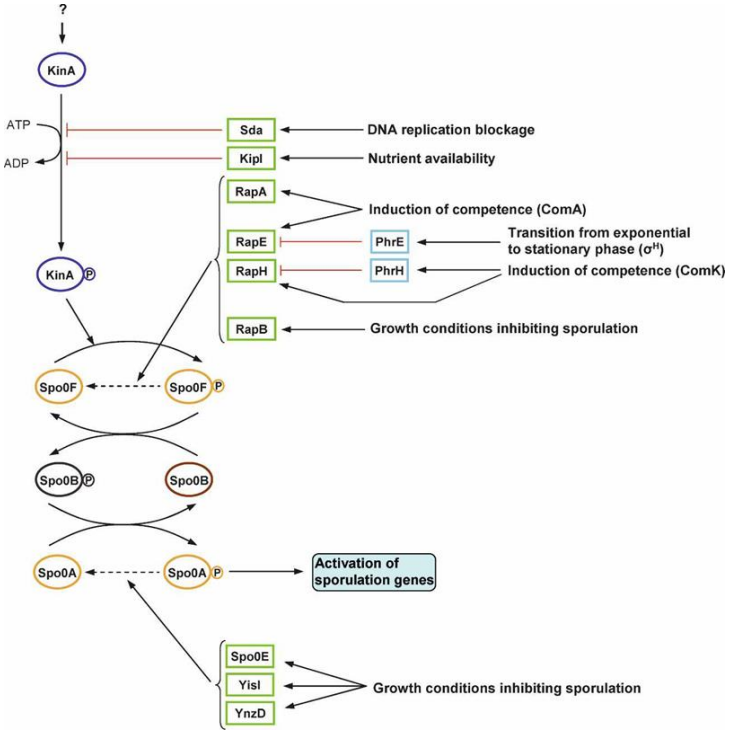

Fig. 5.1: Connectors of the Spo0A phosphorelay cascade. Connectors can inhibit phosphorylation of HKs or promote dephosphorylation of RRs. The kinase KinA undergoes autophosphorylation and transfers the phosphoryl group to the RR Spo0F. Spo0F~P phosphorylates Spo0B which then transfers the phosphoryl group to the terminal acceptor Spo0A. Above a certain threshold, Spo0A~P then activates sporulation genes. The connectors Sda and KipI block KinA phosphorylation whereas the connectors RapA, B, E and H induce dephosphorylation of Spo0F~P. The connector Spo0E acts similarly on Spo0A~P. This figure is taken from (Mitrophanov & Groisman, 2008).

dephosphorylation of Spo0A by the connector protein Spo0E. Both, Rap and Spo0E proteins are hypothesized to function by inducing the autodephosphorylation activity of Spo0F~P and Spo0A~P, respectively (Perego & Brannigan, 2001). All these connectors have in common that they are themselves induced by conditions that inhibit sporulation, either by nutrient availability (KipI) or induction of competence (e.g. RapA and RapE) (Wang *et al.*, 1997). In fact, this is important for the fine-tuning of Spo0A (de)phosphorylation and thereby tight regulation. There are two subpopulations of sporulating (high Spo0A~P levels) and non-sporulating cells (low Spo0A~P levels). If environmental conditions change and nutrients become available again, the non-sporulating cells are able to resume growth, thus having an advantage over the sporulating cells. Indeed, heterogeneity is assumed to be an advantageous characteristic giving the population the opportunity to avoid commitment to the timely and costly developmental sporulation pathway (Dubnau & Losick, 2006). Strikingly, the two connector proteins RapA and Spo0E have been shown to directly affect Spo0A-associated heterogeneity. Deletions of *rapA* and *spo0E* abolish heterogeneity by inducing the activity of Spo0A in almost all cells of the population (Veening *et al.*, 2005).

Such connector proteins show many similarities with LiaF, modulating the phosphorylation state of LiaS and thereby regulating the kinase activity. It is known that LiaF is an inhibitor protein of LiaS under non-inducing conditions and maybe even promoting dephosphorylation of LiaS (Jordan *et al.*, 2006, Schrecke *et al.*, 2013). Therefore, LiaF would constitute and function as such a connector protein modulating the phosphorylation state of LiaS and thus affecting gene expression of the *liaIH-GFSR* operon. Recently, it has been demonstrated that the ratio of LiaF:LiaS:LiaR under native conditions is 18:4:1 (Schrecke *et al.*, 2013). This shows that LiaF needs to be in excess over LiaS in order to maintain the phosphatase activity of LiaS and to keep the system silent in the

absence of a stimulus (Schrecke *et al.*, 2013). Upon addition of bacitracin, LiaF releases its inhibitory effect on LiaS which undergoes autophosphorylation resulting in activation of the LiaSR system. Heterogeneous activation of the LiaSR system was shown to occur only upon the addition of low antibiotic concentrations (Kesel *et al.*, 2013). This could be explained as follows: If there are only few bacitracin molecules in the environment, not all cells perceive the bacitracin stimulus. Also the ratio of LiaF:LiaS:LiaR is not a fixed ratio and it changes upon bacitracin addition. There are possibly cell-to-cell variations (or noise) in the number of proteins relative to each other. Therefore, low concentrations of bacitracin could presumably only induce the LiaSR system in cells with a slightly lower amount of LiaF molecules.

During the intrinsic transition phase induction of the LiaSR system, again LiaF releases LiaS inhibition only in a certain subpopulation of cells. Here, the stimulus for activation of the LiaSR system was shown to be the endogenously produced YydF peptide (Butcher *et al.*, 2007). Since the expression of *yydF* was shown to be dependent on AbrB and Spo0A (Butcher *et al.*, 2007), again cell-to-cell variations in the number of peptide producing cells might occur due to the heterogeneous activation of Spo0A. This means that not all cells produce and secrete YydF and therefore, not all cells do respond. Furthermore, it has been shown that under native conditions the detection of LiaR molecules was challenging despite the presence of the constitutive promoter P_{liaG} (Schrecke *et al.*, 2013). One the one hand, this could be explained by the presence of two stem-loop structures at the end of *liaS* (Schrecke *et al.*, 2013). These could lead to premature termination of transcription. On the other hand, the reason for the little amount of LiaR molecules under non-inducing conditions might be the instability of the 3'end of the *liaFSR* transcript which could be subject to RNase degradation (Schrecke *et al.*, 2013). Thus, the number of LiaR molecules per cell controlling expression from P_{lial} depends on the external bacitracin concentration. At low antibiotic concentrations, the low number of LiaR proteins might explain the variations in gene expression leading to heterogeneity (Kesel *et al.*, 2013, Schrecke *et al.*, 2013). Cell-to-cell differences in the exact number of LiaR molecules therefore directly affect gene expression from P_{lial}.

Taken together, heterogeneous gene expression is frequently used by bacteria to adapt to changing environmental conditions. This can be achieved by precisely controlled signaling pathways which modulate the transcription of individual genes. Heterogeneity in the expression levels of individual genes or the occurrence of bistability where some genes are only expressed in a subpopulation of cells have been observed. Heterogeneous activation of the LiaSR system at low antibiotic concentrations or during transition phase might derive from LiaF and its relative amount to LiaS modulating its activity or the little amount of LiaR proteins regulating expression from P_{lial}.

5.2 LiaIH dynamics vary under stress and non-stress conditions

Bacteria respond to cell envelope stress by mounting protective countermeasures. The most common signal transduction pathways are 2CSs and ECF σ factors (Jordan *et al.*, 2008). Additionally, another protective layer is provided by the phage-shock protein (PSP) response. The PSP response has been thoroughly studied in *E. coli* and more recently in *Yersinia enterocolitica* (Model *et al.*, 1997, Darwin, 2005, Joly *et al.*, 2010, Yamaguchi *et al.*, 2013, Flores-Kim & Darwin, 2015). It is mainly induced by phage infection, high osmolarity, heat shock and changes in lipid biosynthesis (Brissette *et al.*, 1990, Bergler *et al.*, 1994, Model *et al.*, 1997). In this thesis, the dynamics of LiaI and the PspA homolog LiaH was investigated in the presence and absence of bacitracin (CHAPTER III). We found that LiaI is highly dynamic under non-inducing conditions possibly scanning the membrane for damaged sites. Upon stress conditions, LiaI recruits LiaH from the cytoplasm to the membrane forming a complex. However, LiaH was still detected at the membrane in the absence of LiaI. Therefore, we assume that LiaH has more than one interaction partner. Since the PSP response is well-understood in *E. coli*, but only little is known for *B. subtilis*, first I would like to compare both systems and highlight some similarities in the following section. Furthermore, I would like to provide some future perspectives for other potential interaction partners of LiaH and draw some conclusions.

5.2.1 The PSP response of *E. coli* – similarities in *B. subtilis*

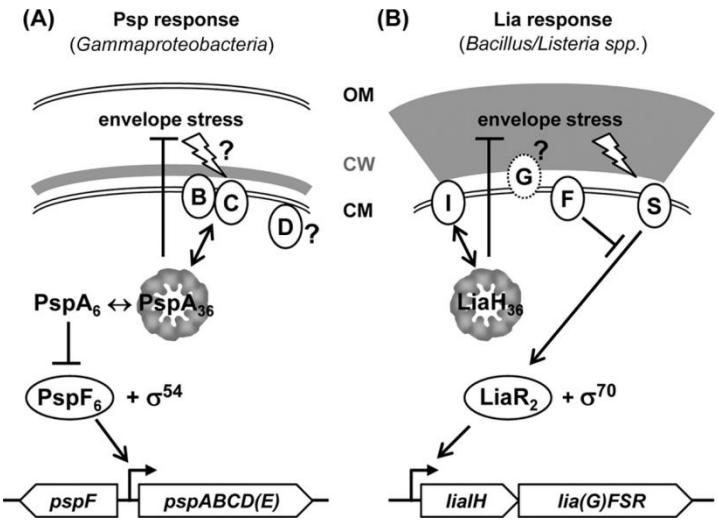

Fig. 5.2: Comparison of the PSP response in γ-proteobacteria (A) and Firmicutes bacilli (B). Proteins are depicted as circles at their known or predicted cellular location, with the letters corresponding to the respective genes, indicated below. The phage shock proteins PspA and LiaH are depicted in their oligomeric ring form structure. LiaG is depicted as a dotted circle because homologs are only present in *B. subtilis* and its closest relatives. Double-ended arrows indicate protein-protein interactions, regular arrows activation and T-shaped lines inhibition. CM, cytoplasmic membrane; CW, cell wall; OM, outer membrane. This figure is taken and modified from (Wolf *et al.*, 2010).

The PSP regulon in *E. coli* consists of the *pspABCDE* operon and the two distinct genes *pspF* and *pspG* (Joly *et al.*, 2010). Under non-inducing conditions, the transcriptional activator protein PspF is kept inactive by the cytosolic PspA protein. In the presence of stress signals, PspA is recruited to the membrane proteins PspB and PspC in order to counteract membrane damage. PspF is released and acts as an activator for *pspABCDE* transcription (Fig. 5.2).

Despite this detailed knowledge about the molecular mechanisms, the physiological role of the PSP response remains unclear. However, studies on the PSP response suggest a role in stabilizing and

protecting the membrane against proton leakage and loss of membrane potential (Kobayashi *et al.*, 2007, Vrancken *et al.*, 2008, Horstman & Darwin, 2012). It is hypothesized that PspA binds to phosphatidyl-glycerol (PG) and phosphatidyl-serine (PS) within the lipid bilayer (Kobayashi *et al.*, 2007). This is thought to cause a change in rigidity of the inner membrane which is suggested to facilitate proton motive force (PMF) maintenance (Kobayashi *et al.*, 2007). Another role for PspA, potentially including PspG, was suggested by Engl *et al.*, 2009. It was found that PspA and PspG formed static complexes at the cell poles and rather mobile foci along the cell. They hypothesized that the polar complexes modulate PMF-consuming processes such as chemotaxis (Engl *et al.*, 2009). Additionally, they proposed a role for PspA in cell wall biogenesis since lateral movement of PspA seems to involve cytoskeletal proteins such as MreB. Therefore, the PSP response is hypothesized to play a role in the repair of stress-induced membrane damage and PMF maintenance (Engl *et al.*, 2009, Joly *et al.*, 2010).

In *B. subtilis*, there are two PspA homologs, PspA and LiaH. Here, expression of *pspA* is mediated by the ECF σ factor σ^W under envelope stress conditions. However, its physiological role remains elusive. In contrast, the LiaSR system has been studied extensively over the last decade and the function of many proteins of the *liaIH-GFSR* operon has been elucidated. The 2CS consisting of LiaSR included an accessory inhibitory protein LiaF. Transcription and expression of the last four genes of the operon is ensured by the constitutive promoter P_{liaG}. Expression of *liaIH* is strictly dependent on the LiaR-regulated promoter P_{liaI}. LiaH is a PspA homolog and was shown to form large oligomeric ring structures similar to those observed for other PspA-like proteins (Aseeva *et al.*, 2004, Hankamer *et al.*, 2004, Standar *et al.*, 2008, Wolf *et al.*, 2010, Otters *et al.*, 2013).

In this thesis, we were able to show that LiaI and LiaH were shown to interact upon cell envelope stress, i.e. addition of bacitracin, thereby LiaI being a membrane anchor for LiaH (see CHAPTER III, Fig. 2). LiaH was predominantly found to localize in the cytoplasm under non-inducing conditions and seemed to be recruited to the membrane upon cell envelope stress (see CHAPTER III, Fig. 3), where LiaI and LiaH co-localize in distinct foci. This is a first link to the PSP response in *E. coli*. $PspA_{E.c.}$ and LiaH both localize in the cytoplasm under native conditions which changes upon envelope stress: Both proteins get recruited into (a) complex(es) at the membrane. In *E. coli*, PspA gets recruited into the PspB-PspC complex while, in *B. subtilis*, LiaH forms a complex with LiaI. Both events finally lead to the initiation of gene transcription in a direct or indirect manner. In *E. coli*, the release of PspF by PspA leads to the transcription of the *pspABCDE* operon whose gene products are thought to counteract membrane damage. Within the LiaSR system of *B. subtilis*, other phage-shock protein homologs are missing. Here, the release of LiaF inhibition of LiaS ultimately results in transcription initiation by LiaR binding to P_{liaI}. From our knowledge gained during this study, we hypothesize that LiaIH serve as a “patch” from the inside at the sites of membrane damage to shield against AMP-induced membrane damage.

Interestingly, we found that LiaH was still able to associate with the cytoplasmic membrane in a *liaI* mutant, pointing towards the fact that LiaH might have more than one interaction partner (see CHAPTER III, Fig. 2). So far unpublished data gained over the last years also indicated a link of

LiaH and the σ^W-regulated proteins encoded in the *yvlABCD* operon (Fig. 5.3), which will be discussed below.

5.2.2 LiaH and its connection to the YvlABCD interaction network

In order to search for other LiaH interaction partners besides LiaI, a genome-wide analysis was performed to determine other phage-shock protein homologs in *B. subtilis*. YvlC, a member of the *yvlABCD* operon was discovered to be a homolog to PspC from *E. coli* (PhD thesis, Diana Wolf). Remarkably, YvlB was identified to be a paralog to LiaG of *B. subtilis*. Little is known about the function and localization of the Yvl proteins but preliminary data obtained from bacterial two-hybrid analyses revealed interactions between some Lia proteins, PspA and Yvl proteins giving rise to the following scheme (PhD thesis, Diana Wolf; Master thesis, Marion Kirchner) (Fig. 5.3).

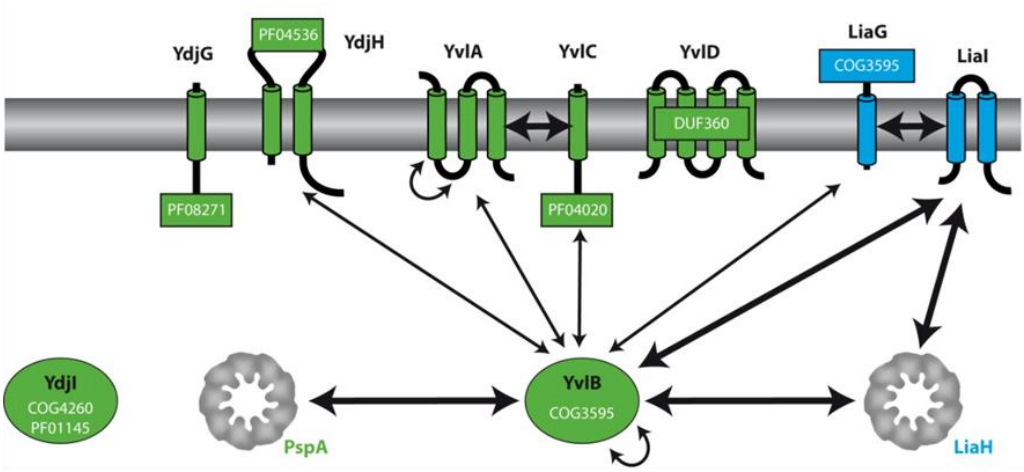

Fig. 5.3: Interconnection of proteins involved in cell envelope protection. Proteins encoded in ECF σ^W-dependent operons are shown in green. Proteins encoded in the *lia* locus are marked in blue. Thin arrows indicate weak interactions; thick arrows illustrate strong interactions as judged from bacterial two-hybrid analyses. Based on sequence analyses, the location of each protein is displayed. Final evidence for the above indicated interactions and potential protein localization is lacking. This figure is based on Diana Wolf, PhD thesis, 2012 and adapted from Marion Kirchner, Master thesis, 2013.

As indicated in Fig. 5.3, YvlB is a key player in this interaction network. It seems to comprise the central hub connecting the LiaSR response and PspA as part of the PSP response. Indeed, preliminary data from bacterial two-hybrid analyses already showed that YvlB interacts with LiaH and LiaI. It is conceivable that YvlB guides LiaH to the membrane where it interacts with LiaI under stress conditions. Together, they might form a complex at the membrane under inducing conditions. This would be in agreement with the observation that YvlB localizes both to the membrane and to the cytoplasm in a growth phase-dependent manner (Master thesis, Korinna Kraft). YvlB was predominantly found in the cytoplasm during middle sporulation stages and at the membrane during exponential and early sporulation stages. As mentioned, YvlB is a LiaG paralog harboring a COG3595 domain consisting of β-sheets forming a β-propeller motif. This domain is assumed to be responsible for protein-protein interactions or signal transduction (Fülöp & Jones,

1999, Menke *et al.*, 2010). In this respect, the signal that leads to the halt of LiaI scanning in the membrane, might also serve as a signal for YvlB which could help LiaI to recruit LiaH.

The bacterial two-hybrid analyses already pointed towards some interaction between YvlB and PspA. Since PspA in *E. coli* is recruited to the membrane under stress conditions it would be interesting to test this finding in *B. subtilis* as well and additionally look for co-localization with LiaH. A preliminary study from a Master student (Annika Sprenger) already revealed that PspA in *B. subtilis* localizes to the membrane in few distinct foci under non-inducing conditions. However, PspA localization upon induction has not been tested. Although the results of the bacterial two-hybrid analyses depicted in Fig. 5.3 let us to assume that there is no direct interaction between PspA and LiaH, it would be conceivable that these two proteins may interact directly upon inducing conditions or that interaction is mediated by their common interaction partner YvlB. Therefore, it would be interesting to test, if LiaH and PspA co-localize at the membrane under envelope stress conditions.

Other possible LiaH interaction partners at the membrane could be YvlA, YvlC or YvlD assuming their predicted localization is correct. In a preliminary study about the localization of YvlA, YvlB and YvlC from the Master student Korinna Kraft, it was shown that all three proteins exhibit distinct localization patterns. YvlA and YvlC were predominantly found at the membrane throughout the different stages of growth (from exponential until late stationary phase including spore formation). Here, YvlC localization is in agreement with the localization pattern of its homolog PspC in *E. coli*. Remarkably, YvlB was found both in the cytoplasm (during middle sporulation stages) and at the membrane (during exponential and early sporulation stages). This, indeed, suggests a central role for YvlB potentially mediating interaction of two or more proteins in a growth phase-dependent manner. Therefore, one could assume some level of interaction between LiaH and YvlA or YvlC via YvlB, which potentially helps to recruit LiaH to the membrane. Hence, all these very preliminary and highly speculative data suggest that there are, in fact, a number of possible candidates which might be involved in LiaH recruitment to the membrane upon inducing conditions.

In this study, we were also able to show that LiaI foci display fast and random movement in the membrane in unstressed cells (see CHAPTER III, Fig. 3). Under inducing conditions, most of these foci become static (see CHAPTER III, Fig. 3). LiaH reveals disperse cytoplasmic localization under non-inducing conditions and only gets recruited to the membrane upon addition of stressors. In the following section, I would like to compare this finding to the PSP response in *Yersinia enterocolitica* and highlight some similarities and differences between the two systems.

5.2.3 The PSP response of *Y. enterocolitica* – similarities and differences in *B. subtilis*

The *Y. enterocolitica* PSP response is reminiscent to the Lia response in *B. subtilis* (Fig. 5.4). In *Y. enterocolitica*, the cytosolic phage-shock protein PspA, the enhancer protein PspF and the two membrane proteins PspB and PspC exhibit high dynamics under non-inducing conditions (Yamaguchi *et al.*, 2013). This is reminiscent of the membrane protein LiaI in *B. subtilis* scanning the membrane in the absence of a stimulus. Also LiaH appears to be located diffusely in the

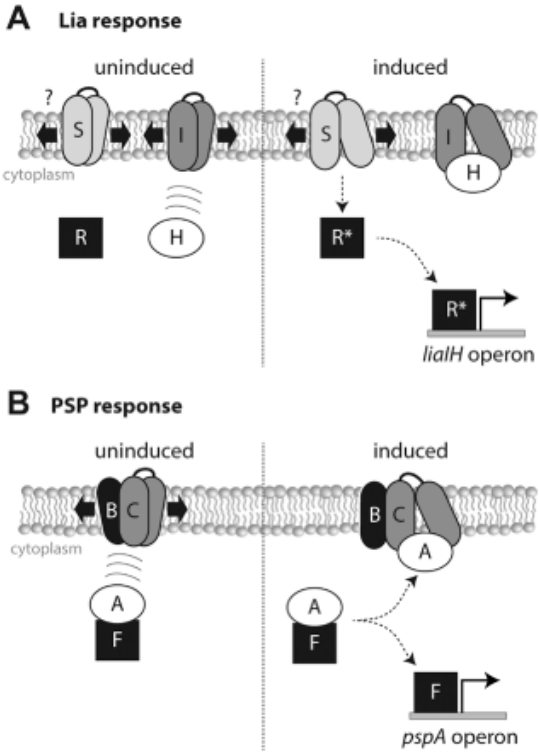

Fig. 5.4: Graphical illustration of the Lia response in *B. subtilis* (A) and the PSP response in *Y. enterocolitica* (B). This scheme illustrates the protein dynamics of LiaI and the recruitment of LiaH during the Lia stress response of *B. subtilis* (A) and the protein dynamics of PspBC and relocalization of PspA in the PSP response of *Y. enterocolitica* (B). The arrows indicate the mobility of the proteins within the cytoplasmic membrane or within the cytoplasm. This figure is taken from (Dominguez-Escobar *et al.*, 2014).

cytoplasm as judged from our fluorescence microscopy data. In *Y. enterocolitica*, upon stress, PspA is recruited to PspC at the membrane which then forms large stationary foci together with PspB (Yamaguchi *et al.*, 2013). These findings indeed match (at least to a certain point) with the dynamics of the LiaSR system where LiaH is recruited to LiaI at the membrane when cells encounter stress. They appear to co-localize into static foci potentially with other, so far unknown proteins to counteract the specific stress signal. One difference between the PSP response in *Y. enterocolitica* and the Lia response in *B. subtilis* is that $PspA_{Y.e.}$ has an interaction partner in the cytoplasm while for LiaH in *B. subtilis* no interaction partners have been found so far. As already discussed in the previous section (see Fig. 5.3), LiaH after all might have interaction partners. The bacterial two-hybrid analyses already pointed towards an interaction between LiaH and YvlB and potentially other Yvl proteins within that network. These preliminary observations need further investigation in the future.

5.3 A novel mode of BceRS activation by the cannibalism toxins SDP and SKF

In addition to the LiaSR system, this thesis also addressed the question about the intrinsic stimuli responsible for the stationary phase induction of the BceRS and PsdRS 2CSs as well as the ECF σ factors σ^M, σ^X and σ^W. We found that all systems responded to the two cannibalism toxins SDP and SKF. Since the effect was most prominent for the BceRS 2CS, we focused on that system to gain deeper insight into the physiological relevance of this process.

We found that only the mature toxins are able to fully trigger the BceRS response and that the toxin precursors only play minor roles in activation of the BceRS system (see CHAPTER IV, Fig. 4.6). P_{bceA} induction was further shown to correlate with toxin production (see CHAPTER IV, Fig. 4.4). The toxin promoters, P_{sdpA} and P_{skfA}, revealed increased activity about two hours before the BceRS system started to respond (see CHAPTER IV, Fig. 4.4). We assumed that this time delay is needed in order to produce a fully functional toxin with all the posttranslational modifications needed. Given the fact that the BceRS system mediates resistance against the AMP

bacitracin, it stood to reason that it would also confer resistance against SDP and SKF. But our comprehensive study let us to conclude that it does not mediate resistance against the toxins.

Remarkably, the BceRS system was not activated in an *sdpI* mutant although functional SDP and SKF are produced (see CHAPTER IV, Fig. 4.5c+d). In conclusion, the BceRS system seems to require SdpI in order to be activated by the two toxins.

The outstanding questions arising from this study are: (i) Why is P_{bceA} induction completely abolished in an *sdpI* or *skfEF* mutant? (ii) How do the BceRS system and the resistance determinants interact or rely on each other so that induction is lost in the absence of the latter?

In the case of SkfEF, loss of BceRS activation can be explained as follows: Since SkfEF is hypothesized to constitute an exporter of the toxin (Gonzalez-Pastor *et al.*, 2003, Liu *et al.*, 2010), translocation of the toxin to the outer surface of the membrane will presumably not occur if SkfEF are missing. Hence, the BceRS system will not be activated. Additionally, we did not observe any growth defect in a *skfEF* mutant, indicating that SKF is not active in the intracellular environment.

In contrast, an *sdpI* mutant exhibited a severe growth defect starting from entry into stationary phase where SDP and SKF are supposed to be produced. SdpI is proposed to be a membrane and signal transduction protein (Ellermeier *et al.*, 2006). Ellermeier and colleagues suggested a model in which SdpI binds to SDP at the membrane and that this complex then sequesters SdpR away from the DNA to the membrane thereby inducing transcription of the two-gene operon *sdpRI* (Ellermeier *et al.*, 2006). This leads to increasing amounts of SdpI protein in the membrane needed for resistance and survival. If this protein is missing, cells lose their ability to induce appropriate countermeasures in response to the lethal toxin damage. Since we were not able to observe any BceRS response in the absence of SdpI, we conclude that the BceRS system somehow requires SdpI in order to sense both SDP and SKF (Fig. 5.5).

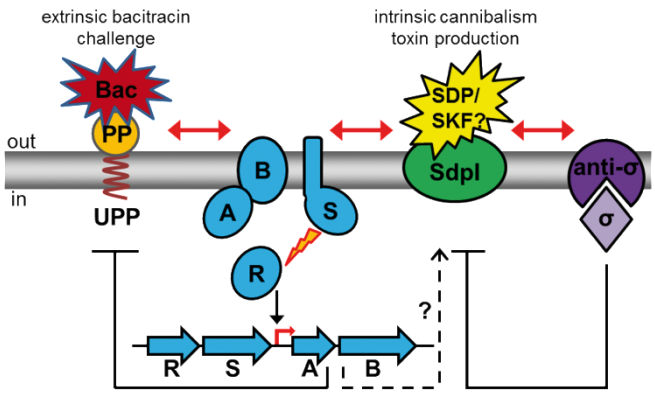

Fig. 5.5: Model of BceRS activation via SDP/SKF-SdpI complex formation. The BceRS system is shown in blue. Circles indicate proteins and their location in the membrane or cytoplasm. The flash indicates activation (transfer of phosphoryl group). Double arrows indicate potential interaction. Genomic context of the BceRS system is shown as big blue arrows. Red bent arrow indicates P_{bceA}. R, BceR; S, BceS; A, BceA; B, BceB; UPP, undecaprenol pyrophosphate; PP, pyrophosphate group; Bac, bacitracin; σ, ECF σ factor. This figure is taken from (Höfler *et al.*, 2015).

Notably, this model of BceRS activation is reminiscent of the P_{bceA} induction by bacitracin when bound to its target UPP. Recently, bacitracin was hypothesized to be sensed either directly or indirectly (Dintner *et al.*, 2014, Kingston *et al.*, 2014). Dintner and colleagues were able to demonstrate a direct binding of bacitracin to the ABC transporter BceAB *in vitro*. This finding is in good agreement with a recent study by Fritz and colleagues who demonstrated that BceAB is a bacitracin flux sensor which monitors its detoxification capacity in order to precisely adjust the

protein levels needed for protection (Fritz *et al.*, 2015). These two studies demonstrated a direct bacitracin binding to BceAB. In contrast, Kingston and colleagues rather postulated that bacitracin first has to be bound to its membrane target UPP in order to be recognized by the BceRS system (Kingston *et al.*, 2014). Such an indirect sensing mechanism including a membrane target protein could be also conceivable for SDP/SKF recognition. Only the presence of SdpI, the membrane target of SDP, enables the BceRS system to respond to the two cannibalism toxins. Binding of SdpI to SDP/SKF could alter membrane rigidity or integrity which could be the trigger for activation of the BceRS system. This would describe a novel mode of AMP perception in which the toxin has to be bound to a membrane target which somehow "presents" the AMP to the BceRS system prior to detection.

5.4 Future perspectives and concluding remarks

In this study, we identified two novel inducers of the BceRS system. SDP and SKF are two cannibalism toxins produced at the onset of stationary phase and under nutrient-limiting conditions in order to kill sensitive siblings. The lysed cells then provide nutrients for the cannibalistic subpopulation and enable them to maintain vegetative growth and delay entry into the sporulation cycle. Besides, we were also able to demonstrate that SDP and SKF induction is not solely Bce-specific but rather a common phenomenon of the different 2CSs and ECF σ factors tested, which are involved in the cell envelope stress response. However, the mechanism behind the BceRS activation by the toxins remains unclear. At this point, I would like to mention a few open questions and provide some future perspectives. The main outstanding question is, as already mentioned, the mechanism of BceRS activation by SDP and SKF. In order to address this question, it would be interesting to isolate and purify the two toxins and induce growing wild type and *sdpI* mutant cultures with certain concentrations of SDP and SKF. It would be possible to test whether the BceRS system only responds to the toxins in the presence of SdpI as expected from our results. Furthermore, it would be interesting to perform *in vitro* binding studies in order to determine if SDP/SKF molecules are able to bind to BceAB or whether SdpI is, in fact, needed for a successful interaction.

All data gained and presented in CHAPTER IV were performed on population level and so far, detailed single cell studies have been neglected. To further investigate and correlate P_{bceA} induction with toxin production, it would be tempting to perform time-lapse microscopy with double labeled promoters. In growing microcolonies, it would be exciting to observe whether the BceRS system responds in cells lying next to a toxin producer or not. Another question would be, if the BceRS system is also activated in a toxin producer or whether only sensitive cells trigger the BceRS response. Labeling proteins (BceAB, BceS, SdpI, SkfEF) and peptides (SDP, SKF) instead of their promoters would provide further insights into the localization pattern of these proteins and peptides. Co-localization studies would give a hint on potential interaction partners in or at the membrane. By using TIRFM (total internal reflection microscopy) it would be also possible to reveal protein dynamics, if any, upon addition of SDP or SKF. Since SdpI is proposed to be an integral

membrane protein and signal transduction protein, a scanning mechanism reminiscent of LiaI scanning the membrane in the absence of an inducer would be possible. The presence of SDP (and also potentially SKF) might lead to a complex formation with SdpI possibly resulting in stalling of SdpI and a change in membrane rigidity or integrity which could, in turn, trigger the BceRS response.

In conclusion, during this study, many novel and interesting insights have been gained about the activation of the BceRS system in stationary growth phase. Novel AMPs, such as SDP and SKF, have been identified to be inducers of the BceRS system. So far, we have no evidence that the BceRS system is involved in resistance against these peptides and induction seems to rely on the presence of the immunity protein SdpI. The whole mechanism behind this is still unclear and needs further investigation in the future.

References of CHAPTER I and CHAPTER V

Albano, M., W. K. Smits, L. T. Ho, B. Kraigher, I. Mandic-Mulec, O. P. Kuipers & D. Dubnau, (2005) The Rok protein of *Bacillus subtilis* represses genes for cell surface and extracellular functions. *J Bacteriol* **187**: 2010-2019.

Arnison, P. G., M. J. Bibb, G. Bierbaum, A. A. Bowers*, et al.*, (2013) Ribosomally synthesized and post-translationally modified peptide natural products: overview and recommendations for a universal nomenclature. *Nat Prod Rep* **30**: 108-160.

Aseeva, E., F. Ossenbuhl, L. A. Eichacker, G. Wanner, J. Soll & U. C. Vothknecht, (2004) Complex formation of Vipp1 depends on its α-helical PspA-like domain. *J Biol Chem* **279**: 35535-35541.

Barrett, D., T. S. Wang, Y. Yuan, Y. Zhang, D. Kahne & S. Walker, (2007) Analysis of glycan polymers produced by peptidoglycan glycosyltransferases. *J Biol Chem* **282**: 31964-31971.

Bergler, H., D. Abraham, H. Aschauer & F. Turnowsky, (1994) Inhibition of lipid biosynthesis induces the expression of the *pspA* gene. *Microbiology* **140 (Pt 8)**: 1937-1944.

Bernard, R., M. El Ghachi, D. Mengin-Lecreulx, M. Chippaux & F. Denizot, (2005) BcrC from *Bacillus subtilis* acts as an undecaprenyl pyrophosphate phosphatase in bacitracin resistance. *J Biol Chem* **280**: 28852-28857.

Bernard, R., A. Guiseppi, M. Chippaux, M. Foglino & F. Denizot, (2007) Resistance to bacitracin in *Bacillus subtilis*: Unexpected requirement of the BceAB ABC transporter in the control of expression of its own structural genes. *J Bacteriol* **189**: 8636-8642.

Bierbaum, G. & H. G. Sahl, (2009) Lantibiotics: mode of action, biosynthesis and bioengineering. *Curr Pharm Biotechnol* **10**: 2-18.

Boguslawski, K. M., P. A. Hill & K. L. Griffith, (2015) Novel mechanisms of controlling the activities of the transcription factors Spo0A and ComA by the plasmid-encoded quorum sensing regulators Rap60-Phr60 in *Bacillus subtilis*. *Mol Microbiol* **96**: 325-348.

Botella, E., S. Hubner, K. Hokamp, A. Hansen*, et al.*, (2011) Cell envelope gene expression in phosphate-limited *Bacillus subtilis* cells. *Microbiology* **157**: 2470-2484.

Bouhss, A., A. E. Trunkfield, T. D. Bugg & D. Mengin-Lecreulx, (2008) The biosynthesis of peptidoglycan lipid-linked intermediates. *FEMS Microbiol Rev* **32**: 208-233.

Breukink, E. & B. de Kruijff, (2006) Lipid II as a target for antibiotics. *Nat Rev Drug Discov* **5**: 321-332.

Brissette, J. L., M. Russel, L. Weiner & P. Model, (1990) Phage shock protein, a stress protein of *Escherichia coli*. *Proc Natl Acad Sci U S A* **87**: 862-866.

Brown, K. L. & K. T. Hughes, (1995) The role of anti-sigma factors in gene regulation. *Mol Microbiol* **16**: 397-404.

Burbulys, D., K. A. Trach & J. A. Hoch, (1991) Initiation of sporulation in *B. subtilis* is controlled by a multicomponent phosphorelay. *Cell* **64**: 545-552.

Burkholder, W. F., I. Kurtser & A. D. Grossman, (2001) Replication initiation proteins regulate a developmental checkpoint in *Bacillus subtilis*. *Cell* **104**: 269-279.

Butcher, B. G. & J. D. Helmann, (2006) Identification of *Bacillus subtilis* σ^W-dependent genes that provide intrinsic resistance to antimicrobial compounds produced by Bacilli. *Mol Microbiol* **60**: 765-782.

Butcher, B. G., Y.-P. Lin & J. D. Helmann, (2007) The *yydFGHIJ* operon of *Bacillus subtilis* encodes a peptide that induces the LiaRS two-component system. *J Bacteriol* **189**: 8616-8625.

Cao, M., B. A. Bernat, Z. Wang, R. N. Armstrong & J. D. Helmann, (2001) FosB, a cysteine-dependent fosfomycin resistance protein under the control of σ^W, an extracytoplasmic-function σ factor in *Bacillus subtilis*. *J Bacteriol* **183**: 2380-2383.

Cao, M. & J. D. Helmann, (2002) Regulation of the *Bacillus subtilis bcrC* bacitracin resistance gene by two extracytoplasmic function σ factors. *J Bacteriol* **184**: 6123-6129.

Cao, M. & J. D. Helmann, (2004) The *Bacillus subtilis* extracytoplasmic-function σ^X factor regulates modification of the cell envelope and resistance to cationic antimicrobial peptides. *J Bacteriol* **186**: 1136-1146.

Cao, M., T. Wang, R. Ye & J. D. Helmann, (2002) Antibiotics that inhibit cell wall biosynthesis induce expression of the *Bacillus subtilis* σ^W and σ^M regulons. *Mol Microbiol* **45**: 1267-1276.

Chang, H. Y., C. C. Chou, M. F. Hsu & A. H. Wang, (2014) Proposed carrier lipid-binding site of undecaprenyl pyrophosphate phosphatase from *Escherichia coli*. *J Biol Chem* **289**: 18719-18735.

Chastanet, A., D. Vitkup, G. C. Yuan, T. M. Norman, J. S. Liu & R. M. Losick, (2010) Broadly heterogeneous activation of the master regulator for sporulation in *Bacillus subtilis*. *Proc Natl Acad Sci U S A* **107**: 8486-8491.

Chen, G., A. Kumar, T. H. Wyman & C. P. Moran, Jr., (2006) Spo0A-dependent activation of an extended -10 region promoter in *Bacillus subtilis*. *J Bacteriol* **188**: 1411-1418.

Chung, J. D., G. Stephanopoulos, K. Ireton & A. D. Grossman, (1994) Gene expression in single cells of *Bacillus subtilis*: evidence that a threshold mechanism controls the initiation of sporulation. *J Bacteriol* **176**: 1977-1984.

Cotter, P. D., C. Hill & R. P. Ross, (2005) Bacteriocins: developing innate immunity for food. *Nat Rev Micro* **3**: 777-788.

Crandall, A. D. & T. J. Montville, (1998) Nisin resistance in *Listeria monocytogenes* ATCC 700302 is a complex phenotype. *Appl Environ Microbiol* **64**: 231-237.

Darwin, A. J., (2005) The phage-shock-protein response. *Mol Microbiol* **57**: 621-628.

Davies, E. A., M. B. Falahee & M. R. Adams, (1996) Involvement of the cell envelope of *Listeria monocytogenes* in the acquisition of nisin resistance. *J Appl Bacteriol* **81**: 139-146.

Delcour, J., T. Ferain, M. Deghorain, E. Palumbo & P. Hols, (1999) The biosynthesis and functionality of the cell-wall of lactic acid bacteria. *Antonie Van Leeuwenhoek* **76**: 159-184.

Devi, S. N., M. Vishnoi, B. Kiehler, L. Haggett & M. Fujita, (2015) *In vivo* functional characterization of the transmembrane histidine kinase KinC in *Bacillus subtilis*. *Microbiology* **161**: 1092-1104.

Dintner, S., R. Heermann, C. Fang, K. Jung & S. Gebhard, (2014) A sensory complex consisting of an ATP-binding cassette transporter and a two-component regulatory system controls bacitracin resistance in *Bacillus subtilis*. *J Biol Chem* **289**: 27899-27910.

Dintner, S., A. Staron, E. Berchtold, T. Petri, T. Mascher & S. Gebhard, (2011) Co-evolution of ABC-transporters and two-component regulatory systems as resistance modules against antimicrobial peptides in Firmicutes bacteria. *J Bacteriol* **193**: 3851-3862.

Dominguez-Escobar, J., D. Wolf, G. Fritz, C. Höfler, R. Wedlich-Söldner & T. Mascher, (2014) Subcellular localization, interactions and dynamics of the phage-shock protein-like Lia response in *Bacillus subtilis*. *Mol Microbiol* **92**: 716-732.

Dubnau, D. & R. Losick, (2006) Bistability in bacteria. *Mol Microbiol* **61**: 564-572.

Dubois, J. Y., T. R. Kouwen, A. K. Schurich, C. R. Reis*, et al.*, (2009) Immunity to the bacteriocin sublancin 168 Is determined by the SunI (YolF) protein of *Bacillus subtilis*. *Antimicrob Agents Chemother* **53**: 651-661.

Economou, N. J., S. Cocklin & P. J. Loll, (2013) High-resolution crystal structure reveals molecular details of target recognition by bacitracin. *Proc Natl Acad Sci U S A* **110**: 14207-14212.

Eiamphungporn, W. & J. D. Helmann, (2008) The *Bacillus subtilis* σ^M regulon and its contribution to cell envelope stress responses. *Mol Microbiol* **67**: 830-848.

Ellermeier, C. D., E. C. Hobbs, J. E. Gonzalez-Pastor & R. Losick, (2006) A three-protein signaling pathway governing immunity to a bacterial cannibalism toxin. *Cell* **124**: 549-559.

Engelberg-Kulka, H., S. Amitai, I. Kolodkin-Gal & R. Hazan, (2006) Bacterial programmed cell death and multicellular behavior in bacteria. *PLoS Genet* **2**: e135.

Engl, C., G. Jovanovic, L. J. Lloyd, H. Murray*, et al.*, (2009) In vivo localizations of membrane stress controllers PspA and PspG in *Escherichia coli*. *Mol Microbiol* **73**: 382-396.

Errington, J., (2003) Regulation of endospore formation in *Bacillus subtilis*. *Nat Rev Microbiol* **1**: 117-126.

Eswaramoorthy, P., D. Duan, J. Dinh, A. Dravis, S. N. Devi & M. Fujita, (2010) The threshold level of the sensor histidine kinase KinA governs entry into sporulation in *Bacillus subtilis*. *J Bacteriol* **192**: 3870-3882.

Flores-Kim, J. & A. J. Darwin, (2015) Activity of a bacterial cell envelope stress response is controlled by the interaction of a protein binding domain with different partners. *J Biol Chem* **290**: 11417-11430.

Flühe, L., T. A. Knappe, M. J. Gattner, A. Schäfer, O. Burghaus, U. Linne & M. A. Marahiel, (2012) The radical SAM enzyme AlbA catalyzes thioether bond formation in subtilosin A. *Nat Chem Biol* **8**: 350-357.

Foster, S. J. & D. L. Popham, (2002) Structure and synthesis of cell wall, spore cortex, teichoic acid, S-layers and capsules. In: *Bacillus subtilis* and Its Closest Relatives From Genes to Cells. A. L. Sonenshein, J. A. Hoch & R. Losick (eds). Washigton D.C.: ASM Press, pp. 21-41.

Fritz, G., S. Dintner, N. S. Treichel, J. Radeck, U. Gerland, T. Mascher & S. Gebhard, (2015) A New Way of Sensing: Need-Based Activation of Antibiotic Resistance by a Flux-Sensing Mechanism. *MBio* **6**.

Fujita, M., J. E. Gonzalez-Pastor & R. Losick, (2005) High- and low-threshold genes in the Spo0A regulon of *Bacillus subtilis*. *J Bacteriol* **187**: 1357-1368.

Fülöp, V. & D. T. Jones, (1999) Beta propellers: structural rigidity and functional diversity. *Curr Opin Struct Biol* **9**: 715-721.

Ghosh, S., K. Sureka, B. Ghosh, I. Bose, J. Basu & M. Kundu, (2011) Phenotypic heterogeneity in mycobacterial stringent response. *BMC Syst Biol* **5**: 18.

Ghuysen, J. M., (1991) Serine beta-lactamases and penicillin-binding proteins. *Annu Rev Microbiol* **45**: 37-67.

Gonzalez-Pastor, J. E., (2011) Cannibalism: a social behavior in sporulating *Bacillus subtilis*. *FEMS Microbiol Rev* **35**: 415-424.

Gonzalez-Pastor, J. E., E. C. Hobbs & R. Losick, (2003) Cannibalism by sporulating bacteria. *Science* **301**: 510-513.

Hankamer, B. D., S. L. Elderkin, M. Buck & J. Nield, (2004) Organization of the AAA(+) adaptor protein PspA is an oligomeric ring. *J Biol Chem* **279**: 8862-8866.

Helmann, J. D., (2002) The extracytoplasmic function (ECF) sigma factors. *Adv Microb Physiol* **46**: 47-110.

Higgins, D. & J. Dworkin, (2012) Recent progress in *Bacillus subtilis* sporulation. *FEMS Microbiol Rev* **36**: 131-148.

Höfler, C., J. Heckmann, A. Fritsch, P. Popp, S. Gebhard, G. Fritz & T. Mascher, (2015) Cannibalism Stress Response in *Bacillus subtilis*. *Microbiology*.

Höltje, J. V., (1998) Growth of the stress-bearing and shape-maintaining murein sacculus of *Escherichia coli*. *Microbiol Mol Biol Rev* **62**: 181-203.

Horstman, N. K. & A. J. Darwin, (2012) Phage shock proteins B and C prevent lethal cytoplasmic membrane permeability in *Yersinia enterocolitica*. *Mol Microbiol* **85**: 445-460.

Huang, X., K. L. Fredrick & J. D. Helmann, (1998) Promoter recognition by *Bacillus subtilis* σ^W: autoregulation and partial overlap with the σ^X regulon. *J Bacteriol* **180**: 3765-3770.

Hulko, M., F. Berndt, M. Gruber, J. U. Linder*, et al.*, (2006) The HAMP domain structure implies helix rotation in transmembrane signaling. *Cell* **126**: 929-940.

Joly, N., C. Engl, G. Jovanovic, M. Huvet*, et al.*, (2010) Managing membrane stress: the phage shock protein (Psp) response, from molecular mechanisms to physiology. *FEMS Microbiology Reviews* **34**: 797-827.

Jordan, S., M. I. Hutchings & T. Mascher, (2008) Cell envelope stress response in Gram-positive bacteria. *FEMS Microbiol Rev* **32**: 107-146.

Jordan, S., A. Junker, J. D. Helmann & T. Mascher, (2006) Regulation of LiaRS-dependent gene expression in *Bacillus subtilis*: Identification of inhibitor proteins, regulator binding sites and target genes of a conserved cell envelope stress-sensing two-component system. *J Bacteriol* **188**: 5153-5166.

Jordan, S., E. Rietkötter, M. A. Strauch, F. Kalamorz, B. G. Butcher, J. D. Helmann & T. Mascher, (2007) LiaRS-dependent gene expression is embedded in transition state regulation in *Bacillus subtilis*. *Microbiology* **153**: 2530-2540.

Joseph, P., A. Guiseppi, A. Sorokin & F. Denizot, (2004) Characterization of the *Bacillus subtilis* YxdJ response regulator as the inducer of expression for the cognate ABC transporter YxdLM. *Microbiology* **150**: 2609-2617.

Kesel, S., A. Mader, C. Höfler, T. Mascher & M. Leisner, (2013) Immediate and heterogeneous response of the LiaFSR two-component system of *Bacillus subtilis* to the peptide antibiotic bacitracin. *PloS one* **8**: e53457.

Kingston, A. W., X. Liao & J. D. Helmann, (2013) Contributions of the σ^W , σ^M and σ^X regulons to the lantibiotic resistome of *Bacillus subtilis*. *Mol Microbiol* **90**: 502-518.

Kingston, A. W., H. Zhao, G. M. Cook & J. D. Helmann, (2014) Accumulation of heptaprenyl diphosphate sensitizes Bacillus subtilis to bacitracin: implications for the mechanism of resistance mediated by the BceAB transporter. *Mol Microbiol* **93**: 37-49.

Kobayashi, R., T. Suzuki & M. Yoshida, (2007) *Escherichia coli* phage-shock protein A (PspA) binds to membrane phospholipids and repairs proton leakage of the damaged membranes. *Mol Microbiol* **66**: 100-109.

Kramer, N. E., E. J. Smid, J. Kok, B. De Kruijff, O. P. Kuipers & E. Breukink, (2004) Resistance of Gram-positive bacteria to nisin is not determined by Lipid II levels. *FEMS Microbiol Lett* **239**: 157-161.

Lamsa, A., W. T. Liu, P. C. Dorrestein & K. Pogliano, (2012) The *Bacillus subtilis* cannibalism toxin SDP collapses the proton motive force and induces autolysis. *Mol Microbiol* **84**: 486-500.

LeDeaux, J. R., N. Yu & A. D. Grossman, (1995) Different roles for KinA, KinB, and KinC in the initiation of sporulation in *Bacillus subtilis*. *J Bacteriol* **177**: 861-863.

Levin, P. A. & R. Losick, (1994) Characterization of a cell division gene from *Bacillus subtilis* that is required for vegetative and sporulation septum formation. *J Bacteriol* **176**: 1451-1459.

Lin, D., L. J. Qu, H. Gu & Z. Chen, (2001) A 3.1-kb genomic fragment of *Bacillus subtilis* encodes the protein inhibiting growth of *Xanthomonas oryzae pv. oryzae*. *J Appl Microbiol* **91**: 1044-1050.

Linde, D., L. Marischen & J. P. Muller, (2003) Characterisation of preYvaY export reveals differences in the substrate specificities of *Bacillus subtilis* and *Escherichia coli* leader peptidases. *FEMS Microbiol Lett* **227**: 149-156.

Liu, W. T., Y. L. Yang, Y. Xu, A. Lamsa*, et al.*, (2010) Imaging mass spectrometry of intraspecies metabolic exchange revealed the cannibalistic factors of *Bacillus subtilis*. *Proc Natl Acad Sci U S A* **107**: 16286-16290.

Lopez, D. & R. Kolter, (2010) Extracellular signals that define distinct and coexisting cell fates in *Bacillus subtilis*. *FEMS Microbiol Rev* **34**: 134-149.

Maisnier-Patin, S. & J. Richard, (1996) Cell wall changes in nisin-resistant variants of *Listeria innocua* grown in the presence of high nisin concentrations. *FEMS Microbiol Lett* **140**: 29-35.

Mantovani, H. C. & J. B. Russell, (2001) Nisin resistance of *Streptococcus bovis*. *Appl Environ Microbiol* **67**: 808-813.

Mascher, T., (2006) Intramembrane-sensing histidine kinases: a new family of cell envelope stress sensors in Firmicutes bacteria. *FEMS Microbiol Lett* **264**: 133-144.

Mascher, T., (2014) Bacterial (intramembrane-sensing) histidine kinases: signal transfer rather than stimulus perception. *Trends Microbiol* **22**: 559-565.

Mascher, T., A. B. Hachmann & J. D. Helmann, (2007) Regulatory overlap and functional redundancy among *Bacillus subtilis* extracytoplasmic function (ECF) σ factors. *J Bacteriol* **189**: 6919-6927.

Mascher, T., J. D. Helmann & G. Unden, (2006) Stimulus perception in bacterial signal-transducing histidine kinases. *Microbiol Mol Biol Rev* **90**: 910-938.

Mascher, T., N. G. Margulis, T. Wang, R. W. Ye & J. D. Helmann, (2003) Cell wall stress responses in *Bacillus subtilis*: the regulatory network of the bacitracin stimulon. *Mol Microbiol* **50**: 1591-1604.

Mascher, T., S. L. Zimmer, T. A. Smith & J. D. Helmann, (2004) Antibiotic-inducible promoter regulated by the cell envelope stress-sensing two-component system LiaRS of *Bacillus subtilis*. *Antimicrob Agents Chemother* **48**: 2888-2896.

McKenney, P. T., A. Driks & P. Eichenberger, (2013) The *Bacillus subtilis* endospore: assembly and functions of the multilayered coat. *Nat Rev Microbiol* **11**: 33-44.

Menke, M., B. Berger & L. Cowen, (2010) Markov random fields reveal an N-terminal double beta-propeller motif as part of a bacterial hybrid two-component sensor system. *Proc Natl Acad Sci U S A* **107**: 4069-4074.

Ming, L.-J. & J. D. Epperson, (2002) Metal binding and structure-activity relationship of the metalloantibiotic peptide bacitracin. *Journal of Inorganic Biochemistry* **91**: 46-58.

Missiakas, D. & S. Raina, (1998) The extracytoplasmic function sigma factors: role and regulation. *Mol Microbiol* **28**: 1059-1066.

Mitrophanov, A. Y. & E. A. Groisman, (2008) Signal integration in bacterial two-component regulatory systems. *Genes Dev* **22**: 2601-2611.

Model, P., G. Jovanovic & J. Dworkin, (1997) The *Escherichia coli* phage-shock-protein (*psp*) operon. *Mol Microbiol* **24**: 255-261.

Molle, V., M. Fujita, S. T. Jensen, P. Eichenberger, J. E. Gonzalez-Pastor, J. S. Liu & R. Losick, (2003) The Spo0A regulon of *Bacillus subtilis*. *Mol Microbiol* **50**: 1683-1701.

Msadek, T., (1999) When the going gets tough: survival strategies and environmental signaling networks in *Bacillus subtilis*. *Trends Microbiol* **7**: 201-207.

Nakano, M. M., G. Zheng & P. Zuber, (2000) Dual control of *sbo-alb* operon expression by the Spo0 and ResDE systems of signal transduction under anaerobic conditions in *Bacillus subtilis*. *J Bacteriol* **182**: 3274-3277.

Neuhaus, F. C. & J. Baddiley, (2003) A continuum of anionic charge: structures and functions of D-alanyl-teichoic acids in Gram-positive bacteria. *Microbiol Mol Biol Rev* **67**: 686-723.

Nicolas, P., U. Mäder, E. Dervyn, T. Rochat*, et al.*, (2012) Condition-dependent transcriptome reveals high-level regulatory architecture in *Bacillus subtilis*. *Science* **335**: 1103-1106.

Ohki, R., Giyanto, K. Tateno, W. Masuyama, S. Moriya, K. Kobayashi & N. Ogasawara, (2003) The BceRS two-component regulatory system induces expression of the bacitracin transporter, BceAB, in *Bacillus subtilis*. *Mol Microbiol* **49**: 1135-1144.

Oman, T. J., J. M. Boettcher, H. Wang, X. N. Okalibe & W. A. van der Donk, (2011) Sublancin is not a lantibiotic but an S-linked glycopeptide. *Nat Chem Biol* **7**: 78-80.

Otters, S., P. Braun, J. Hubner, G. Wanner, U. C. Vothknecht & F. Chigri, (2013) The first alpha-helical domain of the vesicle-inducing protein in plastids 1 promotes oligomerization and lipid binding. *Planta* **237**: 529-540.

Paik, S. H., A. Chakicherla & J. N. Hansen, (1998) Identification and characterization of the structural and transporter genes for, and the chemical and biological properties of, sublancin 168, a novel lantibiotic produced by *Bacillus subtilis* 168. *J Biol Chem* **273**: 23134-23142.

Papagianni, M., (2003) Ribosomally synthesized peptides with antimicrobial properties: biosynthesis, structure, function, and applications. *Biotechnol Adv* **21**: 465-499.

Parker, G. F., R. A. Daniel & J. Errington, (1996) Timing and genetic regulation of commitment to sporulation in *Bacillus subtilis*. *Microbiology* **142 (Pt 12)**: 3445-3452.

Perego, M. & J. A. Brannigan, (2001) Pentapeptide regulation of aspartyl-phosphate phosphatases. *Peptides* **22**: 1541-1547.

Perego, M., P. Glaser, A. Minutello, M. A. Strauch, K. Leopold & W. Fischer, (1995) Incorporation of D-alanine into lipoteichoic acid and wall teichoic acid in *Bacillus subtilis*. Identification of genes and regulation. *J Biol Chem* **270**: 15598-15606.

Perego, M., G. B. Spiegelman & J. A. Hoch, (1988) Structure of the gene for the transition state regulator, *abrB*: regulator synthesis is controlled by the *spo0A* sporulation gene in *Bacillus subtilis*. *Mol Microbiol* **2**: 689-699.

Perez Morales, T. G., T. D. Ho, W. T. Liu, P. C. Dorrestein & C. D. Ellermeier, (2013) Production of the cannibalism toxin SDP is a multistep process that requires SdpA and SdpB. *J Bacteriol* **195**: 3244-3251.

Peschel, A. & H. G. Sahl, (2006) The co-evolution of host cationic antimicrobial peptides and microbial resistance. *Nat Rev Microbiol* **4**: 529-536.

Petersohn, A., M. Brigulla, S. Haas, J. D. Hoheisel, U. Völker & M. Hecker, (2001) Global analysis of the general stress response of *Bacillus subtilis*. *J Bacteriol* **183**: 5617-5631.

Phillips, Z. E. & M. A. Strauch, (2002) *Bacillus subtilis* sporulation and stationary phase gene expression. *Cell Mol Life Sci* **59**: 392-402.

Pietiäinen, M., M. Gardemeister, M. Mecklin, S. Leskela, M. Sarvas & V. P. Kontinen, (2005) Cationic antimicrobial peptides elicit a complex stress response in *Bacillus subtilis* that involves ECF-type sigma factors and two-component signal transduction systems. *Microbiology* **151**: 1577-1592.

Reichmann, N. T., C. P. Cassona & A. Gründling, (2013) Revised mechanism of D-alanine incorporation into cell wall polymers in Gram-positive bacteria. *Microbiology* **159**: 1868-1877.

Revilla-Guarinos, A., S. Gebhard, T. Mascher & M. Zuniga, (2014) Defence against antimicrobial peptides: different strategies in Firmicutes. *Environ Microbiol*.

Rietkötter, E., D. Hoyer & T. Mascher, (2008) Bacitracin sensing in *Bacillus subtilis*. *Mol Microbiol* **68**: 768-785.

Sahl, H. G., R. W. Jack & G. Bierbaum, (1995) Biosynthesis and biological activities of lantibiotics with unique post-translational modifications. *Eur J Biochem* **230**: 827-853.

Sauvage, E., F. Kerff, M. Terrak, J. A. Ayala & P. Charlier, (2008) The penicillin-binding proteins: structure and role in peptidoglycan biosynthesis. *FEMS Microbiol Rev* **32**: 234-258.

Schneider, T. & H.-G. Sahl, (2010) An oldie but a goodie - cell wall biosynthesis as antibiotic target pathway. *International Journal of Medical Microbiology* **300**: 161-169.

Schrecke, K., S. Jordan & T. Mascher, (2013) Stoichiometry and perturbation studies of the LiaFSR system of *Bacillus subtilis*. *Mol Microbiol* **87**: 769-788.

Silhavy, T. J., D. Kahne & S. Walker, (2010) The Bacterial Cell Envelope. *Cold Spring Harbor Perspectives in Biology* **2**.

Smits, W. K., C. Bongiorni, J. W. Veening, L. W. Hamoen, O. P. Kuipers & M. Perego, (2007) Temporal separation of distinct differentiation pathways by a dual specificity Rap-Phr system in *Bacillus subtilis*. *Mol Microbiol* **65**: 103-120.

Smits, W. K., O. P. Kuipers & J. W. Veening, (2006) Phenotypic variation in bacteria: the role of feedback regulation. *Nat Rev Microbiol* **4**: 259-271.

Standar, K., D. Mehner, H. Osadnik, F. Berthelmann, G. Hause, H. Lunsdorf & T. Bruser, (2008) PspA can form large scaffolds in *Escherichia coli*. *FEBS Lett* **582**: 3585-3589.

Staroń, A., D. E. Finkeisen & T. Mascher, (2011) Peptide antibiotic sensing and detoxification modules of *Bacillus subtilis*. *Antimicrob Agents Chemother* **55**: 515-525.

Staroń, A. & T. Mascher, (2010) Extracytoplasmic function σ factors come of age. *Microbe* **5**: 164-170.

Staroń, A., H. J. Sofia, S. Dietrich, L. E. Ulrich, H. Liesegang & T. Mascher, (2009) The third pillar of bacterial signal transduction: classification of the extracytoplasmic function (ECF) σ factor protein family. *Mol Microbiol* **74**: 557-581.

Stein, T., (2005) *Bacillus subtilis* antibiotics: structures, syntheses and specific functions. *Mol Microbiol* **56**: 845-857.

Stock, A. M., V. L. Robinson & P. N. Goudreau, (2000) Two-component signal transduction. *Annu Rev Biochem* **69**: 183-215.

Stone, K. J. & J. L. Strominger, (1971) Mechanism of action of bacitracin: complexation with metal ion and C 55 -isoprenyl pyrophosphate. *Proc Natl Acad Sci U S A* **68**: 3223-3227.

Storm, D. R. & J. L. Strominger, (1973) Complex formation between bacitracin peptides and isoprenyl pyrophosphates. The specificity of lipid-peptide interactions. *J Biol Chem* **248**: 3940-3945.

Strauch, M., V. Webb, G. Spiegelman & J. A. Hoch, (1990) The Spo0A protein of *Bacillus subtilis* is a repressor of the *abrB* gene. *Proc Natl Acad Sci U S A* **87**: 1801-1805.

Strauch, M. A., B. G. Bobay, J. Cavanagh, F. Yao, A. Wilson & Y. Le Breton, (2007) Abh and AbrB control of *Bacillus subtilis* antimicrobial gene expression. *J Bacteriol* **189**: 7720-7732.

Strauch, M. A., G. B. Spiegelman, M. Perego, W. C. Johnson, D. Burbulys & J. A. Hoch, (1989) The transition state transcription regulator *abrB* of *Bacillus subtilis* is a DNA binding protein. *Embo J* **8**: 1615-1621.

Strominger, J. L. & D. J. Tipper, (1965) Bacterial cell wall synthesis and structure in relation to the mechanism of action of penicillins and other antibacterial agents. *Am J Med* **39**: 708-721.

Tam le, T., C. Eymann, D. Albrecht, R. Sietmann, F. Schauer, M. Hecker & H. Antelmann, (2006) Differential gene expression in response to phenol and catechol reveals different metabolic activities for the degradation of aromatic compounds in *Bacillus subtilis*. *Environ Microbiol* **8**: 1408-1427.

Tan, I. S. & K. S. Ramamurthi, (2014) Spore formation in *Bacillus subtilis*. *Environ Microbiol Rep* **6**: 212-225.

Thackray, P. D. & A. Moir, (2003) SigM, an extracytoplasmic function sigma factor of *Bacillus subtilis*, is activated in response to cell wall antibiotics, ethanol, heat, acid, and superoxide stress. *J Bacteriol* **185**: 3491-3498.

Trach, K., D. Burbulys, M. Strauch, J. J. Wu*, et al.*, (1991) Control of the initiation of sporulation in *Bacillus subtilis* by a phosphorelay. *Res Microbiol* **142**: 815-823.

Ulrich, L. E., E. V. Koonin & I. B. Zhulin, (2005) One-component systems dominate signal transduction in prokaryotes. *Trends Microbiol* **13**: 52-56.

van Heusden, H. E., B. de Kruijff & E. Breukink, (2002) Lipid II induces a transmembrane orientation of the pore-forming peptide lantibiotic nisin. *Biochemistry* **41**: 12171-12178.

Veening, J.-W., L. W. Hamoen & O. P. Kuipers, (2005) Phosphatases modulate the bistable sporulation gene expression pattern in *Bacillus subtilis*. *Mol Microbiol* **56**: 1481-1494.

Verheul, A., N. J. Russell, T. H. R. Van, F. M. Rombouts & T. Abee, (1997) Modifications of membrane phospholipid composition in nisin-resistant *Listeria monocytogenes* Scott A. *Appl Environ Microbiol* **63**: 3451-3457.

Vollmer, W., D. Blanot & M. A. de Pedro, (2008) Peptidoglycan structure and architecture. *FEMS Microbiol Rev* **32**: 149-167.

Vrancken, K., L. Van Mellaert & J. Anne, (2008) Characterization of the *Streptomyces lividans* PspA response. *J Bacteriol* **190**: 3475-3481.

Wang, L., R. Grau, M. Perego & J. A. Hoch, (1997) A novel histidine kinase inhibitor regulating development in *Bacillus subtilis*. *Genes Dev* **11**: 2569-2579.

Wecke, T. & T. Mascher, (2011) Antibiotic research in the age of omics: from expression profiles to interspecies communication. *J Antimicrob Chemother* **66**: 2689-2704.

Wiegert, T., G. Homuth, S. Versteeg & W. Schumann, (2001) Alkaline shock induces the *Bacillus subtilis* σ^W regulon. *Mol Microbiol* **41**: 59-71.

Willey, J. M. & W. A. van der Donk, (2007) Lantibiotics: peptides of diverse structure and function. *Annu Rev Microbiol* **61**: 477-501.

Wolf, D., P. Dominguez-Cuevas, R. A. Daniel & T. Mascher, (2012) Cell envelope stress response in cell wall-deficient L-forms of *Bacillus subtilis*. *Antimicrob Agents Chemother* **56**: 5907-5915.

Wolf, D., F. Kalamorz, T. Wecke, A. Juszczak*, et al.*, (2010) In-depth profiling of the LiaR response of *Bacillus subtilis*. *J Bacteriol* **192**: 4680-4693.

Yamaguchi, S., D. A. Reid, E. Rothenberg & A. J. Darwin, (2013) Changes in Psp protein binding partners, localization and behaviour upon activation of the *Yersinia enterocolitica* phage shock protein response. *Mol Microbiol* **87**: 656-671.

Zheng, G., R. Hehn & P. Zuber, (2000) Mutational analysis of the *sbo-alb* locus of *Bacillus subtilis*: identification of genes required for subtilosin production and immunity. *J Bacteriol* **182**: 3266-3273.

Acknowledgements

An dieser Stelle möchte ich ein paar Menschen nennen, ohne deren Unterstützung die letzten Jahre nicht möglich gewesen wären.

Zunächst geht mein Dank an Thorsten. Von Anfang an hatte ich das Gefühl bei Dir willkommen zu sein und ich fühlte mich durch Deine stete Unterstützung, Motivation und aufmunternden Worte immer gut betreut. Deinen grenzenlosen Optimismus bewundere ich sehr und ich wünsche Dir und Deiner Familie einen guten Start in Dresden!

Weiterhin möchte ich allen Gutachtern meiner Dissertation danken, ganz besonders Prof. Dr. Marc Bramkamp für die Übernahme des Zweitgutachtens. Aber auch dem restlichen Prüfungskomitee, bestehend aus Prof. Dr. Angelika Böttger und Dr. Caroline Gutjahr, möchte ich meinen Dank aussprechen.

Natürlich vergesse ich nicht, an dieser Stelle alle derzeitigen und ehemaligen AG Mascher Mitglieder zu nennen, allen voran Susanne Gebhard. Ich habe unglaublich viel von Dir gelernt, nicht nur experimentell sondern auch menschlich! Danke Susanne, dass ich Dich kennen lernen durfte. Weiterhin geht mein Dank natürlich auch an Georg „Schorsch“ Fritz. Ich durfte mit Dir gerade in der Anfangszeit sehr viel zusammenarbeiten und auch viel von Dir lernen. Danke für die schöne Zeit!
Eine weitere Person, die ich hier nennen muss, ist Ainhoa. Du hast mir immer Mut gemacht und mich angespornt durchzuhalten. Danke, dass Du immer für mich da warst. Ich danke Dir außerdem für die Korrektur meiner Arbeit! Viel Erfolg in Dresden! Wir bleiben in Kontakt!
Außerdem geht mein Dank auch an alle derzeitigen AG Mascher Studis/PhDs. Danke, Dayane, Chong und Xiaoluo für die lustige Zeit im Büro ;-) Dann natürlich auch Danke an Jara, Julia, Franzi, Mona, Daniela, Niko, Qiang und Daniel für die tolle Atmosphäre im Labor.
An dieser Stelle möchte ich auch noch meine großartigen Studenten nennen, ohne die ein Großteil dieser Arbeit nicht möglich gewesen wäre. Zunächst geht mein Dank an meine allererste Studentin, Judith. Danke für die tollen Ergebnisse und Wochen im Labor mit Dir! Weiterhin auch ganz lieben Dank an Anne, Philipp und Donna für die tollen Ergebnisse! Besonders danken möchte ich Annika, Korinna und Nadja. Ich hatte mit Euch die mit Abstand lustigsten Kaffeepausen. Ich werde Euch nie vergessen! Korinna, Du warst meine beste „persönliche Assistentin“ im letzten Jahr. Ohne Deine gute Laune und stete Motivation hätten wir die Mikroskopie nicht so weit gebracht. Behalte Dir Deine gute Laune und den Glauben an das Gute im Menschen. Und immer ACTION ;-)

Zu guter Letzt möchte ich natürlich auch meinen Freunden und meiner Familie danken. Emi, Martha und Sarah: Ihr seid die besten! Ihr wart immer da, wenn ich Euch gebraucht habe und ich konnte mich immer auf Eure Unterstützung verlassen. Danke!

Mein letzter Dank geht an Ben. Du bist das Beste, was mir in meinem Leben passiert ist und ich danke Dir für die unzähligen aufmunternden Worte in den letzten 3,5 Jahren. Ohne Deine Unterstützung und Liebe hätte ich schon längst aufgegeben. Aber Du hast immer an mich geglaubt und das hat mir die Kraft gegeben weiter zu machen und siehe da, ich habe es geschafft! Danke für Deine Geduld und Deine ununterbrochene Motivation. Ich bin wahnsinnig glücklich Dich an meiner Seite zu haben.

Curriculum vitae

Personal Data

Name	Carolin Höfler
Date and place of birth	16.08.1985, Heidelberg
Nationality	German
Profession	Biologist (M.Sc.)

Education

07/2014 – 08/2015	Distance study „Business economics“ (Betriebswirtschaftslehre) at ILS, Hamburg
since 04/2012	PhD student in the group of Prof. Dr. Thorsten Mascher at the Department Biology I, Microbiology, at the Ludwig-Maximilians-University, Munich Thesis title: “Response of *Bacillus subtilis* to Antimicrobial Peptide Stress”
10/2009 – 11/2011	Master studies „Molecular Biosciences“ at the Ruprecht-Karls-University, Heidelberg Thesis title: “Investigating the *Bacillus subtilis* Chemotaxis Pathway via FRET”
10/2005 – 06/2008	Bachelor studies „Biology“ at the Ruprecht-Karls-University, Heidelberg Thesis title: “Lokalisation und Interaktion von Zuckertransportern in *Escherichia coli*“
06/2005	A-levels (Abitur) at the Ottheinrich-Gymnasium, Wiesloch

Publications

Kesel, S., Mader, A., Höfler, C., Mascher, T., Leisner, M. (2013). Immediate and Heterogeneous Response of the LiaFSR Two-Component System of *Bacillus subtilis* to the Peptide Antibiotic Bacitracin. PLoS ONE 8(1): e53457. doi:10.1371/journal.pone.0053457

Domínguez-Escobar, J., Wolf, D., Fritz, G., Höfler, C., Wedlich-Söldner, R., Mascher, T. (2014). Subcellular localization, interactions and dynamics of the phage-shock protein-like Lia response in *Bacillus subtilis*. Molecular Microbiology, 92: 716–732. doi: 10.1111/mmi.12586

Yang, Y., Pollard, A., Höfler, C., Poschet, G., Wirtz, M., Hell, R., Sourjik, V. (2015). Relation between chemotaxis and consumption of amino acids in bacteria. Molecular Microbiology. doi: 10.1111/mmi.13006

Höfler, C., Heckmann, J., Popp, P., Fritsch, A., Gebhard, S., Fritz, G., Mascher, T. (2015). Cannibalism Stress Response in *Bacillus subtilis*. Microbiology. doi: 10.1099/mic.0.000176

Conferences – Posters

Höfler, C., Heckmann, J., Fritz, G., Mascher, T. (2015). Cannibalism and its connection to the cell envelope stress response network of *Bacillus subtilis*. Annual Conference of the Association for General and Applied Microbiology (VAAM), Marburg, Germany.

Höfler, C., Heckmann, J., Fritz, G., Mascher, T. (2014). Cannibalism and its connection to the cell envelope stress response network of *Bacillus subtilis*. SPP1617 International Conference "Phenotypic Heterogeneity and Sociobiology of Bacterial Populations", Kloster Irsee, Germany.

Höfler, C., Bauer, T., Kesel, S., Leisner, M., Fritz, G., Mascher, T. (2012). Transition phase induction of the stress response switch P_{lial} of *B. subtilis*: Heterogeneity of the Lia- and AbrB-modules. 29th Symposium "Mechanisms of Gene Regulation", Herrsching am Ammersee, Germany.

Conferences - Talks

Höfler, C., Heckmann, J., Fritz, G., Mascher, T. (2014). Cannibalism and its connection to the cell envelope stress response network of *Bacillus subtilis*. 30th Symposium "Mechanisms of Gene Regulation", Düsseldorf, Germany.

Höfler, C., Heckmann, J., Fritz, G., Mascher, T. (2013). Cannibalism Stress Response in *Bacillus subtilis*. Progress-Meeting of the DFG-Priority Program SPP1617 "Phenotypic Heterogeneity and Sociobiology of Bacterial Populations", Kloster Banz, Germany.

Höfler, C., Fritz, G., Schrecke, K., Mascher, T. (2012). Heterogeneous induction of the LiaFSR-dependent stress response system of *Bacillus subtilis*. Kick-off Meeting of the DFG-Priority Program SPP1617 "Phenotypic Heterogeneity and Sociobiology of Bacterial Populations", Munich, Germany.

Prizes

Short-talk award for the best scientific talk at the 30th Symposium "Mechanisms of Gene Regulation", Düsseldorf, Germany, 2014.